



THE UNIVERSITY OF
WAIKATO
Te Whare Wānanga o Waikato

Research Commons

<http://waikato.researchgateway.ac.nz/>

Research Commons at the University of Waikato

Copyright Statement:

The digital copy of this thesis is protected by the Copyright Act 1994 (New Zealand).

The thesis may be consulted by you, provided you comply with the provisions of the Act and the following conditions of use:

- Any use you make of these documents or images must be for research or private study purposes only, and you may not make them available to any other person.
- Authors control the copyright of their thesis. You will recognise the author's right to be identified as the author of the thesis, and due acknowledgement will be made to the author where appropriate.
- You will obtain the author's permission before publishing any material from the thesis.

Analysis of bonded joints for small craft and marine applications

A thesis
submitted in partial fulfilment
of the requirements for the Degree
of
Master of Engineering
at the
University of Waikato
by
Liviu Eduard Armeanu



THE UNIVERSITY OF
WAIKATO
Te Whare Wānanga o Waikato

University of Waikato

2010

Abstract

This Thesis investigates the possibility of replacing, in small craft and recreational boats, some of the more traditionally made joints (using tabbing) with ones made using structural adhesives (adhesive used where the load applied may cause the separation of the adherends [2]), which have the potential to be quicker to produce and have good fatigue resistance.

It also focuses on methods that are available to a small and medium size boatbuilding or boat design company in order to design and produce a general safe, light weight adhesive joint.

Several static tests were conducted in order to identify the characteristics of the materials to be joined and the properties of the adhesives investigated. A summary of the analytical theories available in order to determine the characteristics of the joints are presented and compared, and several finite element models have been investigated in order to determine the suitability of this method when using adhesive materials.

This Thesis focuses first on Single-Lap joints, not only as a joint, but also as a way to compare the characteristics of the adhesives to be used. Three types of adhesives have been tested, two commercially available (Plexus MA550 and Sikaflex 252) and one commonly found on boatbuilding yards, a mixture of vinyl ester and Epiglass HT120 (a silica based filler). It was found that the Plexus MA550 adhesive performed well across different substrates (aluminium and composites) followed closely in performance by the vinyl ester/filler mixture. Very promising results were obtained when a carrier fabric was used inside the adhesive layer.

Secondly, a very common type of joint, the T-joint, has been anti - symmetrically tested. A comparison has been made between a more traditionally produced joint (using a small fillet made from vinyl ester and microballoons based filler and EU-glass tabbing) with a joint produced using a fillet made from the above adhesives. It was found that the results from samples with the fillet using the vinyl ester/filler mixture are the closest to the benchmark samples and it seems to be the best candidate to replace the traditional joint, given the strength, failure mode, price and the availability. The joint using a Sikaflex 252 fillet has shown the most interesting results such that none of

the materials forming the joint suffered any visible damage after deformation. The joint using a R20mm Plexus MA550 fillet has benefited from the stiffness and the good adhesion characteristics of the adhesive but in all the tests the panels joined were damaged earlier than for the benchmark samples.

Acknowledgements

The author wishes to thank his supervisor, Dr. Kim Pickering, for her patience, guidance and assistance during the preparation of the thesis.

I would like to add a special thank to Derek Kelsall for mentoring me in boat design for the last ten years, to Paula Hesterman who graciously allowed me to use her workshop. All the materials used during the tests were provided by Kelsall Catamarans Ltd.

A very special thank to Johanna Jopie Heusevelt for all the help received from her and, in general, just for being our guardian angel in New Zealand.

Contents

1	Introduction	1
1.1	Background	1
1.2	Thesis objective	3
2	Adhesive Joints	5
2.1	Literature review	5
2.1.1	The BONDSHIP project	6
2.1.2	The ISO Standards	6
2.1.3	The Rules and Regulations of Germanischer Lloyd (GL)	7
2.2	Definition of terms	8
2.3	Classification of adhesives	8
2.4	Advantages and Limitations	9
2.5	Joint Configurations	10
2.5.1	Classification of joints	10
2.6	Failure modes for bonded joints	11
2.7	Temperature, Moisture and other Environmental Effects . . .	13
2.8	Fatigue and Creep in bonded joints	14
2.9	End Effects in Bonded Joints	14
2.9.1	The Effect of Adherend Shape and Ply Sequence in Bonded Joints	15
2.10	Surface Preparation in Bonded Joints	15
2.11	Glue-Line Thickness	16
2.11.1	Characteristics Required of Matrix Resins and Adhesives	16
2.12	Characterization Tests for Materials and Joints	17
2.13	Materials	20
2.13.1	Laminate Resin and Catalist	20
2.13.1.1	Vinyl ester Polyplex 4000 VE	20
2.13.1.2	Norox 925H MEKP catalyst	21
2.13.2	Glass reinforced plastic	21
2.13.3	Foam	23
2.13.4	Fillers	23
2.13.5	Adhesives	25

2.13.5.1	Plexus MA550	25
2.13.5.2	Sikaflex 252	26
2.13.5.3	In-shop made adhesives	26
2.13.6	Aluminium	26
2.14	Experimental tests	27
2.14.1	Sikaflex 252	27
2.14.2	Vinyl ester and Epiglass mixture	27
2.14.3	Vinyl ester and QCel mixture	29
2.14.4	Laminate Properties	30
3	Single lap joints	33
3.1	Analytical Models of Single Lap joints	33
3.1.1	Average Shear Stress Analysis	33
3.1.2	Volkersen Analysis	34
3.1.3	Goland and Reissner Analysis	36
3.1.4	Cooper and Sawyer Model	40
3.1.5	Bigwood and Crocombe Analysis	43
3.1.6	L.J. Hart-Smith Model - Elastic Analysis	46
3.1.7	Wiedemann Analysis	50
3.1.8	Chamis-Murthy Preliminary Analysis	52
3.1.9	Failure Criteria	54
3.1.9.1	Adhesive Failure	54
3.1.9.2	Adherend Failure	56
3.1.10	Summary of analytical models	57
3.2	Finite Element Analysis	60
3.2.1	FE Models	61
3.2.2	FE Model A	62
3.2.3	FE Model B	63
3.2.4	FE Model C	64
3.2.5	FE Model D	67
3.3	FE Analysis Summary	68
3.4	Single Lap Tests	68
3.4.0.1	Single Lap with Aluminium Adherends	71
3.4.0.2	Single Lap Joint with Composite Adherends	74
3.4.0.3	Single Lap Joint with Hybrid (Aluminium and Composite) Adherends	76
3.4.0.4	Single Lap Joint with Composite Adherends and Carrier Fabric	78
3.4.0.5	Single Lap Joint with Hybrid (Composite and Aluminium) Adherends and Carrier Fabric	79

3.5	Summary of single lap tests (ASTM D1002)	80
3.6	Computer Code	81
4	T-joints	82
4.1	Quasi-Static Analysis of T-joints	82
4.1.1	Design Rules for joints	82
4.1.2	R.A. Sheno and F.L.M. Violette Study of T-joint . . .	87
4.1.3	Burchardt Analysis	88
4.2	Experimental Conditions	91
4.2.1	Specimen Construction and Experimental Details . . .	95
4.2.2	Static Tests	97
4.2.2.1	T-joint with Tabbing	98
4.2.2.2	T-joint with vinyl ester/Epiglass HT120 fillet R40mm	99
4.2.2.3	T-joint with SikaFlex 252 Fillet R40mm . . .	100
4.2.2.4	T-joint with Plexus MA550 fillet R20mm . . .	100
4.3	Finite Element Analysis of T-joints	102
5	Conclusions and future work	105
5.1	Conclusions from Chapter 2 - Adhesive Joints	105
5.2	Conclusions from Chapter 3 - Single lap joints	106
5.2.0.5	Future Work	107
5.3	Conclusions from Chapter 4 - T joints	108
5.3.0.6	Future Work	109
A	Scilab Program for Adhesive Stress Calculation	111
B	T-Joint Experimental settings	117

Chapter 1

Introduction

1.1 Background

The building of small craft is a notoriously time-consuming activity, and nowadays builders are facing considerable pressure to remain competitive for orders on a world-wide basis. The rise of economies in countries like China and South America with cheap labour put much pressure on the yacht market. So there is a need to reduce production costs while introducing novel materials, structural designs and reducing labour hours.

A ship (and a small craft for that matter) is a heavily loaded dynamic structure and structural failures are typically caused by abnormal overloading or fatigue. More often than not, these failures occur at connections and interfaces, and very rarely in the bulk material sections.

Although the use of adhesive bonding as a structural joining method has been successful in high performance applications such as aerospace, automotive and rail, the adoption of this building method in the marine environment has been slow. Most designers and builders are not aware of the possibilities (and limitations) of the structural adhesive bonding. In modern small crafts, there are not many practical applications where adhesives are used, and they are mostly non-structural, like bonding and sealing of window panes, tanks or deck hardware. Where the stresses are anticipated to be large, the bond has

been doubled by bolts or by tabbing with fibreglass.

Traditionally, glues have been used extensively in the construction of wooden or plywood boats, as structural and non-structural material. Over time, they partly replaced the innumerable fastenings used to hold parts together in heavily built old boats, so the new wooden craft resulted, could be considered as lightly built. The best glues for wood were the resorcinol resin types (like Elmer's Glue marketed by the Borden Co.), and later, epoxy based ones gained ground. The first are waterproof, easy to mix and to work with, but have a relative short work time. The latter are generally stronger but, unless bought in bulk, the price is usually excessive. Both have to be prepared on site, mixing the two parts (a liquid resin and a catalyst powder or a hardener) requires a fair amount of attention.

In recent years several companies have developed products that can be used as load-carrying adhesives, specific for the use in a marine environment. There are potentially many interesting areas where bonded joints can be used, including:

- replacement of bimetallic joints between aluminium and steel, to compensate for large relative movements due to differences in thermal coefficients.
- where complex shaped surfaces are necessary and cannot or are expensive to manufacture from metals. Applications like complex shaped bow or stern sections for metallic structures, foils or water-jet ducts attached to shells, composite skins for wing masts with aluminium frames.
- in places where welding is not practical such as places with thinner plating, where electrical cables are adjacent to the joint, or metal.
- hybrid structures such as craft with aluminium hulls and composite superstructures - either new designs or refit.
- hybrid structures such as craft with composite hulls and metallic skeleton/framework - for military applications where the craft is required to

absorb radar energy, to be quieter and non-magnetic for mines and torpedoes etc.

- modular designs where because of boat-building constraints (space or cleanliness) the boat is to be built in multiple prefabricated parts. In catamarans for example, hulls (very narrow places) are built separately to allow free access at the machinery, then joined later with the superstructure.

Today, an independent design office or a small or mid-sized boatbuilding company has the choice to decide between a myriad of materials that are available on the market. Annually several new materials are developed, many combinations between them have to be taken into account and the data sheets with the materials' characteristics are hard to find, assess or are incomplete. On top of this, the actual process of gluing is a complex process with many variables, the interaction of which is not fully understood.

1.2 Thesis objective

This Thesis is focused on the methods available to a small and medium size boatbuilding or boat design company in order to design and produce safe, light weight adhesive joints.

It provides a comparative study between the traditional way of joining used by the small craft industry, and a proposed improved method using adhesives. Several tests are conducted in order to identify the characteristics of the materials to be joined and the properties of the adhesives investigated. A summary of the analytical theories available in order to determine the characteristic of the joints are presented and compared, and several finite element models have been investigated to determine the suitability of this method in a design office.

The two kinds of joints most commonly found in marine small crafts are assessed: the single-lap joint and the T-joint. Foundation tests for both these

joints using quasi static tests have been carried out. Other test methods are proposed in order to fully characterize the system between adhesive and adherend.

Chapter 2

Adhesive Joints

2.1 Literature review

An important source of information for the design of bonded joints with application in a marine environment are the classification societies' Rules or Guidelines. The responsibility of the Classification Society (like Germanischer Lloyd, American Bureau of Shipping, Det Norske Veritas etc) as an independent body, is to verify that merchant ships or marine structures comply with the rules that the society has established for design, construction and periodic survey.

Research results are also published by local initiatives (governmental or regional), in order to boost the competitiveness of the local industry. For example, the U.S. Navy initiated in 2000 a programme named "The Advanced Hull form Inshore Demonstrator" (AHFID), with the goal of installing an advanced drive system by attaching it to the ship using composite struts. In conjunction with this, another programme "Modular Advanced Composite Hullform" (MACH) has the goal of installing composite panels to underwater lifting bodies. In both of these programmes adhesives were employed as a method of joining.

A summary of the literature regarding the use of adhesives in the boating industry is presented below.

2.1.1 The BONDSHIP project

”BONDSHIP - *bonding of lightweight materials for cost effective production of high speed craft and passenger ships*” is a major project (approx. 5mil. Euro) funded by the European Commission, in order to introduce adhesive bonding into ship building (and small craft building) as an industrial process for joining materials and structures.

The result of this programme was a set of guidelines (a collection of recommended practices) for selecting adhesives, for design and analysis of joints.

The guidelines [32] have been based on the following assumptions:

1. for a bonded joint design, a numerical analysis cannot reliably predict joint failure, but can give useful information about the behaviour of the bonded joint. It is indicated to utilize additional large scale tests.
2. for a bonded joint design the long-term performance cannot be reliably predicted from the results of accelerated ageing tests. It is indicated that the design must limit the consequences of failure of the joint
3. joining parts with adhesives is a complex process with many variables. No non-destructive tests (NTD) have been found, so far, to be able to measure the quality of the finished joint reliably. It is indicated to establish a rigorous quality control system at every production step.

2.1.2 The ISO Standards

Since 1998, in the EU, all recreational craft, with few exceptions, between 2.5 metres and 24 metres in length, must comply with the essential requirements of the Recreational Craft Directive which introduced improved standards in safety, stability and buoyancy to the existing standards enforced.

There is one ISO standard - ISO 12215 - published in eight parts, that deals with small craft construction and scantlings. Part 6 [16] deals with

structural arrangements and details. It recognizes that the stress distribution in glued bonds are complex and higher safety factors are required than in other structural materials. For example the design shear stress in a bond (τ_{dbond}) is recommended to be taken as :

$$\tau_{dbond} = 0.2 \cdot \tau_{ubond}$$

(unless specific tested values are available), where τ_{ubond} is the ultimate shear strength of the bond.

2.1.3 The Rules and Regulations of Germanischer Lloyd (GL)

Germanischer Lloyd's Rules for Classification and Construction 2003 - Ship Technology [12] advises that the connection between the various parts of the hull, as well as connection of reinforcing members to the hull, when made by adhesives, are subject to special examination by the Society using a procedure test to be agreed on for each individual case. For cold-moulded wood construction only, the mixed adhesives (phenolic and epoxy resins) are recommended and only those who passed GL approved tests are to be used.

This states that when bonding FRP (fibre reinforced plastic) to itself, or to other materials, only solvent-free adhesives can be used. Preference should be given to two component reaction adhesives, if possible with the same basis as the laminating resin. It is specified that the laminates shall only be bonded in the cured state. Hot-setting adhesives generally attain a higher strength; however, the maximum allowable temperature of the materials to be bonded shall not be exceeded. This applies especially when using single component hot-melt adhesive. The temperature range to be used is -20° to $+60^{\circ}C$.

GL advises (from a design point of view) that a bonding-suitable design shall be used which, as far as possible, avoids peeling moments and forces. The thickness of the adhesive layer shall be kept as thin as possible. The joining surfaces shall be kept as large as possible, and forces shall be applied over a

large area.

2.2 Definition of terms

The following terms are used in this study:

Adhesive: R.D. Adams [2] defines an adhesive as a polymeric material used to join surfaces and resist separation when load is applied. The same author defines a structural adhesive as an adhesive used where the load applied may cause the separation of the adherends.

Adherend: An adherend (substrate) is a body held to another body by an adhesive [19].

Bonded Joint (adhesive bonded): A bonded joint is a joint where adherends are bonded by placing a layer of adhesive or resin material between the substrates with the primary role of transmitting the loads (this distinguishes the adhesive from a sealant) [32]. The bond strength is defined [19] as the unit load applied in tension, compression, flexure, peel, impact, cleavage, or shear, required to break an adhesive assembly with failure occurring in or near the plane of the bond.

Small Craft: ISO defines a small craft as a boat with the hull length of maximum 24m.

Secondary Bonding and Co-curing: A Secondary Bonding is a joint which is fabricated by laying up and curing FRP onto FRP. Co-curing is where both adherends and the joint are created in a single cure (FRP only).

2.3 Classification of adhesives

There is a huge array of adhesives available for general use. There are several major classification systems based on factors such as chemical composition, structure or curing method.

From a chemical composition perspective there are synthetic adhesives and natural adhesives. Typical synthetic adhesives include epoxies, polyurethanes, cyanoacrylates, silicones, acrylics, polyvinyl acetate (PVA or hot melts) and urethanes. Typical natural adhesives include animal-base glues (like casein and fish glue), vegetable-based glues (like starch glue) and natural rubber (latex) glue.

From a structural point of view there are three major types of adhesives: thermosetting, thermoplastic and elastomeric. Thermoset molecules are cross-linked (an irreversible process and therefore cannot be melted) by strong covalent intermolecular bonds, forming one giant molecule. This process is initiated by heat, chemical agents and/or radiation with a result of increased strength and stiffness; epoxies and polyesters are typical examples.

Thermoplastics consist of polymer molecules where no new cross-links form (no chemical curing) when cooled and hardened and may be reprocessed by heating or by applying a solvent. Cyanoacrylates and polyvinyl acetate (PVA) are typical thermoplastic adhesives. Elastomeric adhesives are polymers with long cross-linked molecules with high failure strain. Heat or solvent evaporation are used to set the adhesive. Natural rubbers, silicones and polyurethanes are typical elastomeric adhesives.

From a curing method perspective some adhesives are heat, light/UV or moisture activated (mostly one-part adhesives), others are cured when two or more components are mixed and chemical reaction takes place forming cross-links of the polymer molecules. The latter are mostly two-part adhesives like epoxies, urethane, acrylics and silicones.

Mechanically, adhesives can be described as flexible or rigid.

2.4 Advantages and Limitations

Generally the main advantages of adhesives are:

- From a structural perspective, the adhesive bond is continuous, so lo-

cal stress concentrations can be avoided and provide a good vibration damping;

- From a manufacturing perspective, the adhesive bond can join dissimilar materials, reduces weight and part counts and can be easily combined with other fastening methods. Adhesive bonds join and seal in the same process.

There are several important disadvantages that need to be taken into account:

- Environmental resistance depends on the integrity and the type of the adhesive. Temperature usually negatively affects the bond strength;
- A lack of reliable inspection methods;
- The bonded structures are hard to dismantle for service or inspection.

2.5 Joint Configurations

2.5.1 Classification of joints

Adhesive joints can generally be classified into several types of joints (see Fig. 2.1):

- single lap joints - have two straight adherends joined by adhesive where they overlap. The single lap joint is the simplest and the most studied type of adhesive joint.
- double lap joints - including here joints with a doubler - have two adhesive joints;
- single (or double) sided stepped and scarfed joints;

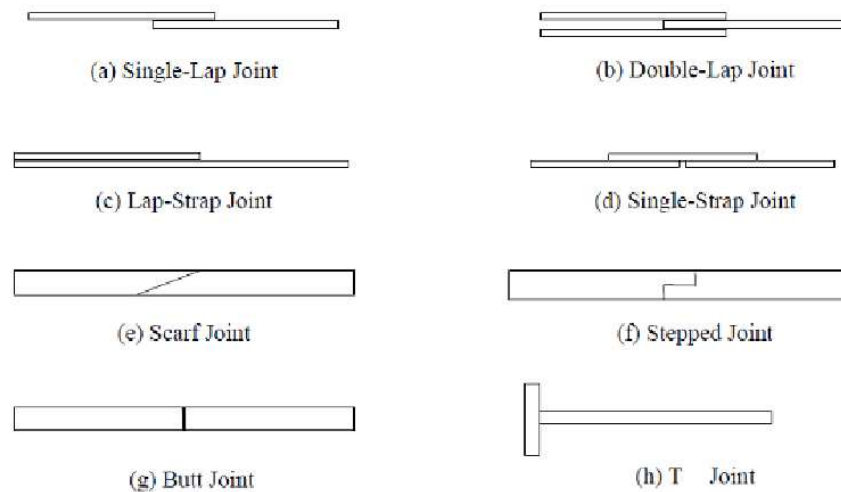


Figure 2.1: Basic Joint Geometries (from [34]).

- t-joints - including here L-type joints (corner joints, as used for example in hull to deck joints). T-joints are extensively used in boat structures; bulkhead to hull joint are the main structural joint in a craft, several hundreds of metres of this joint can be found in a mid-sized yacht. Being a more complex configuration than the lap joint it is more difficult to analyse. In the same category can be included the L-joints, which are used, for example, in hull to deck joints;
- butt joints;
- other joints types (like strap or tubular joints).

Most of these joints are designed to transmit shear or compressive loads. However T-type joints transmit a complex set of loads. In all cases excessive peel stresses should be avoided.

2.6 Failure modes for bonded joints

Understanding the failure modes of adhesive bonds creates the possibility to implement designs that can minimize the likelihood of these failures. There are four main types of adhesive failure modes: adherend, adherend interlaminar tension, cohesive and adhesive [4] as presented in Fig. 2.2.

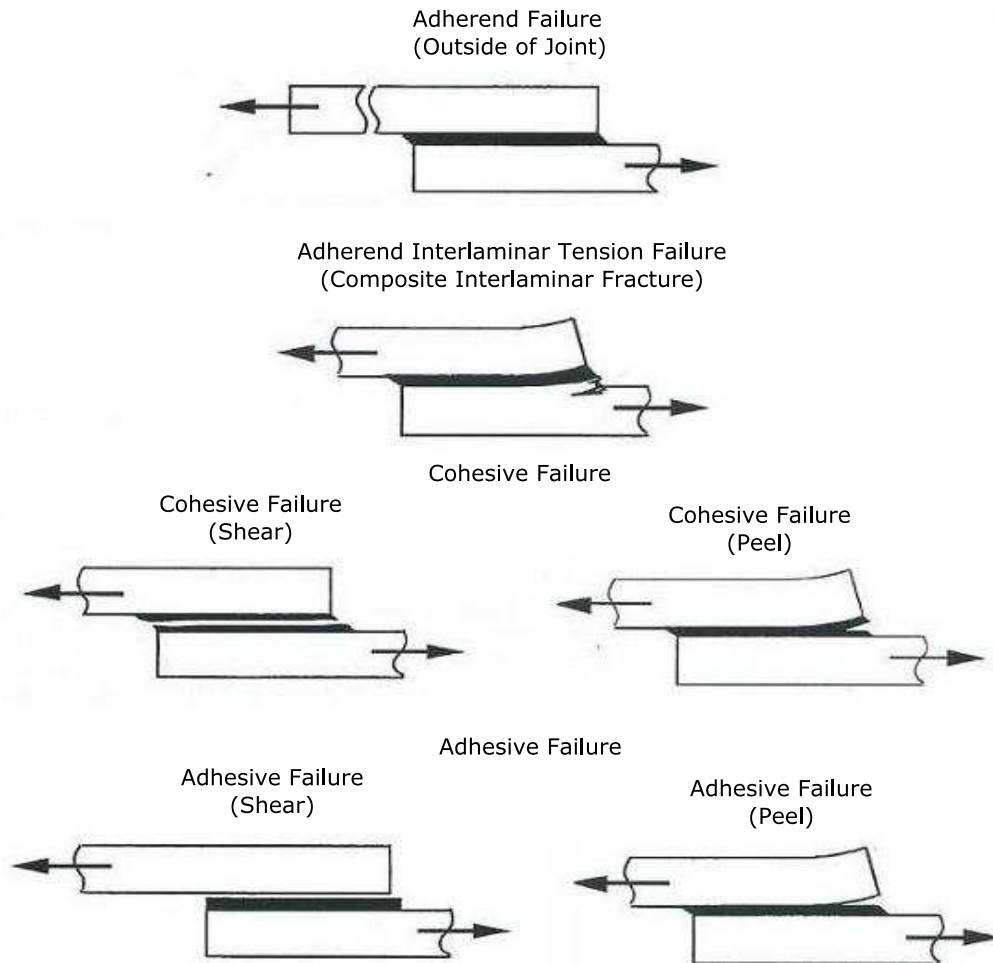


Figure 2.2: Failure Modes in Single-Lap joint (from [30]).

- Adherend Failure - it is the most preferable joint failure. It indicates that the adhesive was correctly chosen and it is necessary to increase the stiffness or the strength of the adherends in the joint area;
- Adherend Interlaminar Tension Failure - this mode of failure is found in composite joints only. It occurs when peel forces (which act out of plane) cause the plies of the composite adherend to fracture or pull apart. It indicates that changes are required to reduce the peel forces. It can also indicate that the resin matrix used in composite adherend is too brittle for the application.
- Cohesive Failure: - it is the failure mode that occurs inside the adhesive layer and it is an indication that an alternative adhesive is required.

- Adhesive Failure: - this failure mode occurs between the adhesive and the adherend and indicates an unacceptable surface preparation or an incompatibility between adherend and adhesive.

2.7 Temperature, Moisture and other Environmental Effects

The mechanical properties of polymeric materials depend on temperature. The normal design of a joint under static load requires that the service temperature is lower than the glass transition temperature (T_g) of the adhesive. For components working at a temperature close to T_g , creep is expected to occur. T_g is usually a figure found in the data sheet provided with the adhesive by the manufacturer, or it can be obtained using a standard test (see Table 2.1).

One major problem which limits the use of structural adhesives is their susceptibility to environmental water, which in the case of boats, is commonly salt water. This can seriously weaken and degrade the joints due to swelling (resulting in internal stresses) and plasticization. When metal is one of the adherends, the effect of the water on the surface is of particular concern. Some companies have formulated special adhesives to be used in these harsh conditions. Accelerated ageing tests may allow screening of the suitable adhesives. It is recommended [2] to make large joints (to increase the diffusion path), to select a suitable surface pre-treatment or primer or to isolate the structural adhesive by means of using special formulated sealants.

Resistance to ultraviolet radiation is also an important factor that may affect the selection of the adhesive system.

2.8 Fatigue and Creep in bonded joints

Despite 50 years of composite use in the marine environment, data regarding the fatigue history of recreational boats is sparse. Miller [24] has estimated that the hours sailed by a J type boat vary in service between 11,300 hours for a charter boat with coefficient of variation of 12%, to 740 hours for a regular sailing boat translated into 10.2 million wave encounters and respectively 600,000 wave encounters with frequencies ranging from 0 to 0.71Hz.

A different picture than the one obtained from wave-structure interaction is obtained when rotating machinery is taken into account (mostly repeated stress cycles). The sailing gear (the stays) is another source of fatigue related stresses (similar in profile with hull shocks from waves where stress and frequency vary randomly).

It has been observed ([2]) that joint durability of bonded metals is low at low frequencies similar with those found in boats, so special attention is needed when the service of the joint is established. It has been found ([2]) that, for a lap joint with aluminium adherends under fatigue stresses, the joint strength starts to degrade quickly from about 40% of the ultimate tensile strength (as determined by the static tensile test).

For joints bonded with elastic adhesives, creep normally governs the life expectancy of the joints, whereas for joints with brittle adhesives, extreme load events govern the life expectancy of the joint [32] (like loads caused by - for military craft - underwater explosions, hitting floating obstacles or shock loads caused by deck machinery).

2.9 End Effects in Bonded Joints

In real life, structural adhesive joints do not have a square end. A fillet (or spew) is developed at the end of the lap joint due to the pressure on the adherends during the manufacture. Several studies [2] have shown that this fillet actually helps reduce the maximum shear stress in the adhesive (a 30%

reduction was noted in some examples). The cracks are formed approximately at right-angles to the direction of the maximum principal stresses starting close from the corner of the adherend and ending at the surface of the fillet.

It is worth noting that the complete removal of the adhesive fillet (eg. for cosmetic reasons) is sometimes difficult. Machining the fillet can damage the adherend or can introduce cracks in the adhesive, especially in the case of brittle ones.

2.9.1 The Effect of Adherend Shape and Ply Sequence in Bonded Joints

It has been observed [2] that an important increase of the joint strength can be obtained by machining the sharp corner of the adherend, especially rounding the corner. This method is easy to apply to metallic adherends, however, it is difficult to apply to composite materials like GRP (glass reinforced plastics) without damaging the edge. The tendency to fail in peel is reduced by tapering the adherends. A further improvement of the strength of the joint is gained by thickening the end of the lap joint [8].

For GRP adherends, the performance of the joint is improved if the stacking sequence is changed, placing the 0° plies on the surface of the laminate.

2.10 Surface Preparation in Bonded Joints

Surface preparation is a critical factor in adhesive bonding. The surfaces of the materials to be bonded should be dry and free of grease, dust and solvents. Particularly when degreasing, attention should be paid to compatibility between the solvent and the adherend material [12].

General methods of surface treatment include: abrasive methods (the use of abrasive papers or cloths, or grit- and shot-blasting), the use of solvents and detergents, the use of chemical etching solutions. From these, the use of ace-

tone for cleaning after the treatment with abrasive papers is the boatbuilders' choice. This is mainly due to the nature of the boatyard environment (dust present from other manufacturing processes like cutting or sanding), and due to the scale of operation (the length of the joints where these treatments need to be applied).

In general, an increase of the adhesive strength is obtained by the application of specially matched primers (which are subsequently subjected to negative environmental influences [12]).

For GRP, the use of peel ply helps protect the surface being joined and improve the roughness of the surface but does not remove the need to abrade.

2.11 Glue-Line Thickness

The importance of the thickness of the glue line varies from one adhesive to another. For a single lap joint, the constant thickness of adhesive layer can be achieved using shims placed between substrates or using a carrier fabric. Carrier fabrics may be woven nylon or random mat polyester fabrics, but for a boat building yard, tapes of fibreglass are more convenient to use.

2.11.1 Characteristics Required of Matrix Resins and Adhesives

In boat building, the desirable common characteristic required of matrix resins and adhesives are [4]:

- must have a good wettability.
- should have a simple cure cycle process.
- must be tolerant of imperfect processing.
- should be tolerant of small inaccuracies in mix ratio (for two-part systems).

- should not shrink during cure.
- must have a low water absorption rate.

Researchers such as Armstrong ([3], [4]) suggest that the mechanical properties required of the matrix resins and adhesives are somewhat different. It was shown that, for ASTM-D-1002 test and aluminium adherends, the strength of single-lap joint depends on the fracture energy of the adhesive and a high joint strength could not be achieved with the high-modulus resins because adequate toughness could not be produced at the same time. The tensile modulus value required was higher for matrix resins.

2.12 Characterization Tests for Materials and Joints

As mentioned in the first chapter, for a bonded joint design, numerical analysis cannot reliably predict joint failure or long-term performance and it was recommended to utilize additional large scale tests. BONDSHIP guidelines [32] recommend a series of tests to be conducted in order to select the right adhesive for the application. In order to reduce the number of possible combinations of adhesives, primers and other surface preparations, first a list of requirements has to be compiled. This should include: materials and surfaces to join, geometry and the load of joint, curing conditions, environment etc. After selection, according to adhesive type (rigid or flexible), a testing programme is developed. A list of ASTM and ISO standard tests is presented in the Table 2.1.

Table 2.1: ASTM & ISO Testing standards for Adhesives and Bonded Joints [34]

ASTM & ISO Testing standards for Adhesives and Bonded Joints	
Property to Measure	ASTM Standard & ISO Standard
Tests used for adhesive characterization	
Standard Terminology	D907-05, D4800-94
Physical & Mechanical Properties	D1084-97, D7149-05, D2556-93A, D638, ISO37
Strength and Shear Modulus	D3983-98, D4027-98, D905-03, D4896-01
Bonding Characteristics	D5868-01
Environmental Aging	D1183-03
Tests used for joint characterization	
Laminate Surface Preparation	D2093-03
Failure Mode Classification	D5573-99
Tensile Shear Loading	D5868-01, D3163-01, D3164-03, D3165-00, D897-01, D2095-96, ISO6922, ISO4587
Tensile Loading (Butt-Joint)	D1784-98, D1876-01, D3167-03a
Flexural, Cleavage and Peel Loading	D5041-98, D950-03, D1062-02, D3433-99, D1780-05, D2293-96, D2294-96(2002), D1184-98
Creep, Fatigue and Durability	D3166-99, D1151-00, D1828-01e1, D2918-99

The commonly used tests are:

- Lap-shear test for strength. The applicable test is ASTM D 1002 (DIN ED 1465, ISO 4587). This is the most used test for all types of adhesives, and it is the simplest to execute. The test gives the apparent average shear strength and it is not intended for designing the bond, but it allows to compare the adhesives. It should be conducted before and after ageing. This test was used in this study to compare some most commonly used adhesives in the boatbuilding companies in New Zealand.
- Boeing wedge test. The applicable test is ASTM D 3762-98 [32]. This is used to characterize the entire bonding system (adhesive, coating and surface preparation).
- Bead test. The applicable test is SIKA SQP033-0, SIKA SQP034-0 [32]. This is used to assess the bonding system only for flexible adhesives.
- Determination of tensile properties. Reference is made to the standard DIN 530504, ASTM D638 and DIN EN ISO 527-2. It is a test carried out in order to describe the non-linear behaviour of the adhesive in a one-dimensional state of stress. The results cannot characterize the ultimate fracture of a bonded joint because the state of stress is quite different from that in a bonded joint. This test was used in this study to characterize the chosen adhesive and the test results are used in finite element analysis.

There is also a multitude of other tests for various purposes that can provide information about the adhesives and the bonding system. These include: measurement of glass transition temperature (T_g - not applicable to flexible adhesives), measurement of pH value, measurement of electrical resistance of the adhesive and tests to measure the thick adherend shear strength, adhesive simple shear strength test of the adhesive, compression strength (Raghava equivalent), the creep strength and ageing performance.

Where possible, a full scale test is recommended [32]. The samples used for testing should as far as possible be geometrically identical to the real joint; the loading shall reflect the critical events that the structure (component or part) experiences during the life span of the product; the resulting failure mode, mechanism and location should be fully understood; the environmental conditions (temperature and humidity) that may influence the failure mechanism should be considered during the tests.

2.13 Materials

2.13.1 Laminate Resin and Catalyst

Polyesters, epoxies and vinyl esters are three most common types of resins used to fabricate marine laminates. Of these, polyesters are the most common; they account for 95% of all resins used in FRP boat building [25]. Epoxies are very strong and are usually used in high tech crafts. In recent years, vinyl ester has become the resin of choice for design offices and boat building companies. They provide good impact, fatigue and blistering resistance.

Vinyl ester resin Polyplex 4000 VE was used as matrix for laminate throughout this thesis and Norox 925H MEKP (a organic peroxide) was used as catalyst.

2.13.1.1 Vinyl ester Polyplex 4000 VE

The vinyl ester used was Polyplex 4000 VE (marketed by Nuplex Industries Limited). It is a fully promoted, low-viscosity, thixotropic, unwaxed vinyl ester resin containing styrene. The published mechanical properties are: tensile strength 84MPa (ASTM D638), tensile elongation 5.5% (ASTM D638) and flexural strength 134MPa (ASTM D790).

2.13.1.2 Norox 925H MEKP catalyst

The catalyst used was Norox 925H MEKP which is a liquid organic peroxide type D. In all applications in this thesis, a 2% by volume of catalyst was mixed with the resin. All the samples were prepared at $20^{\circ} - 25^{\circ}C$.

2.13.2 Glass reinforced plastic

The end properties of the composite materials are not only a function of materials themselves but also the way they are processed. There are several manufacturing processes used in boat building, each one with advantages or disadvantages [29]: spray lay-up, wet or hand lay-up, resin transfer moulding RTM, SCRIMP, resin infusion. Between these, the hand lay-up is the most widely used, but the laminate quality is very dependent on the skills of the laminators.

ISO standard 12215-5(2008) [15] advice boat manufacturers to determine the materials properties by testing experimentally according with international or national standards. The fibre content by mass shall be obtained by ignition, ingestion of the resin or by direct measurement of the laminate from the known fibre mass. Where no explicit measurements are made, the nominal fibre content by mass ψ can be estimated for unidirectional fabric of E-glass as 0.55 for open mould process and application on simple surfaces, as 0.41 for open mould process and application on complex surfaces, and as 0.66 for vacuum bag process.

The mechanical properties of the E-glass with polyester matrix can be estimated using the fibre content by mass as shown in figure 2.3:

The above values are intended to be lower-bound estimates that are achievable using high-end industry standard quality material control and fabrication procedures and can be used as benchmark. The standard also advice to apply a 0.8 multiplying factor on this data if there are no occasional spot checks of the samples representative of the product are made according recognized standards.

Uni-directional (UD) reinforcement		
Property	Parallel to the fibres	Perpendicular to the fibres
Ultimate tensile strength, σ_{ut}	$880 \psi^2 + 140 \psi + 140$	42
Ultimate compressive strength, σ_{uc}	$250 \psi + 190$	105
In-plane modulus, E	$46\,600 \psi^2 + 7\,200 \psi + 7\,250$	$48\,600 \psi^2 - 39\,000 \psi + 12\,500$
In-plane shear modulus, G	$14\,380 \psi^2 - 10\,560 \psi + 3\,840$	
In-plane shear strength, τ_u	50	
Major Poisson's ratio, ν_{12}	0,3	
Interlaminar (out of plane) shear strength $\tau_{u\ inter}$		22,5 – 17,5 ψ

Figure 2.3: E-glass fibre mechanical properties function of fibre content by mass ψ according with ISO 12215-5.

A suite of six tests is necessary to fully characterize an unidirectional laminate for failure analysis. These tests are used to determine the independent composite elastic constants ($E_{11}, E_{22}, G_{12}, G_{23}, \nu_{12}$) and the ultimate composite strengths ($\sigma_{tension11}, \sigma_{tension22}, \sigma_{compression11}, \sigma_{compression22}, \sigma_{12}, \sigma_{23}$).

The relevant ASTM standards used to determine the above characteristics are presented in the Table 2.2:

ASTM standards for unidirectional laminate		
ASTM Standard	Type of Test	Constants Determined
D3039	Tension (Longitudinal)	$E_{t11}, \sigma_{t11}, \nu_{12}$
D3039	Tension (Transversal)	$E_{t22}, \sigma_{t22}, \nu_{21}$
D3410	Compression (Longitudinal)	$E_{c11}, \sigma_{c11}, \nu_{12}$
D3410	Compression (Transversal)	$E_{c22}, \sigma_{c22}, \nu_{21}$
D3518	Shear (Longitudinal)	G_{12}, σ_{12}
D5379	Shear (Transversal)	G_{23}, σ_{23}

Table 2.2: Relevant ASTM standards for characterize the unidirectional laminate.

For this study E-glass (which currently accounts for about 90% of all glass fibres made boats) was used as a substrate in testing the mechanical properties of chosen adhesives, and as tabbing reinforcement for T-joints.

2.13.3 Foam

Several types of foam core are used in boat building. End grain balsa wood is used extensively as a core material. Also honeycomb cores, which are made, among others materials, of FRP, aramid paper or aluminium. The foam plastics are the most common of the core materials and PVC foam is used the most. These are available as cross linked and linear grades and in different densities which makes them suitable in a wide range of applications.

The Airex C70.75 core (used in the tests conducted for T-joints) is a PVC cross linked foam at $80\text{kg}/\text{m}^3$. It has the following characteristics (as published by the manufacturer): compressive strength perpendicular to the plane (ISO844) = 1.3MPa, compressive modulus perpendicular to the plane (DIN53421) = 83MPa, tensile strength in plane (DIN53455) = 2.0MPa, tensile modulus in plane (DIN53457) = 63MPa, shear strength (ISO1922) = 1.2MPa, shear modulus (ASTM C393) = 30MPa, shear elongation at break (ISO1922) = 23%.

2.13.4 Fillers

The effect of fillers is a study in itself. The majority of studies are focused on the influence of fillers on the epoxies in aircraft industries and the author is not aware about studies regarding their use in boat building together with polyesters or vinyl esters.

The mixture resulted between fillers and the matrix is called a syntactic foam [23]. There are two types of syntactic foams: the particulate reinforced polymers (commonly known as filled polymers) and the short fibre reinforced polymers. Common fillers used across the plastic industries are calcium carbonate, kaolin, talc, mica, wollastonite, silica, alumina trihydrate and hollow glass microsphere. Common short fibres are the E-glass, Aramid fibres, carbon fibres or metal fibres and metal coated glass fibres. Unless there is a preferred orientation due to the processing, both particulate reinforced polymers and the short fibre reinforced polymers can be considered isotropic materials.

In boatbuilding industry there are three most used types of filler/short fibres materials [4]:

- Milled fibres - are used to improve toughness, compressive and tensile strength. Aramid fibres are the first candidate. For a mid-size boat building company, the fibres which are normally used in composite (the E-glass) can be used in milled form. They are the cheapest solution as they can be obtained in site by cutting them out of the E-glass roll or by hammer milling into lengths of 3.2, 6.4, 12.7, or 25.4mm.
- Silica - used a thixotrope (nonsag) and has little effect on resin tensile strength [4].
- Microballoons or Microspheres - are small polymeric hollow spheres (50-150 microns) which contain a small amount of hydrocarbon gas (usually pentane or butane). They are used to improve the viscosity of resin matrix and being compressible and elastic, also the tensile and compressive strength of the mix is slightly increased. Also they are expected to reduce the styrene emissions, to reduce the weight of the finished product and to improve the dimensional stability.

A fairly common filler used in the small craft boat building industry is "Epiglass HT120", a high strength glue powder based on silica, produced by the West System Industries. For this thesis, the filler was mixed with vinyl ester in a 1.5:1 filler/resin ratio by volume. The mixture resulted has a viscosity like a grease, which is easy to work and easy to apply in corners or on the overhead joints. The working time is estimated at 5-10 minutes. Experimental tests have been conducted in order to determine its mechanical properties, the results are presented in section 2.14.2.

QCelTM 5019 - a product supplied by Potters Industries Inc. - are hollow microspheres (or microballoons) often used in boatbuilding as fillers and are expected to improve mainly the impact resistance of the mix. The producer published the following properties: bulk density $0.11g/cm^3$, effective

density $0.190g/cm^3$, with the mean particle size of $75\mu m$ and $3.45MPa$ maximum working pressure (compressive strength). These particles have sufficient pressure and shear resistance to withstand a typical mixing and pumping process. For the purpose of this thesis, a 2.3:1 mixture by volume with vinyl ester has been used as a radiused fillet for the T-joint. Experimental tests have been conducted in order to determine its mechanical properties, the results are presented in section 2.14.3.

2.13.5 Adhesives

Adhesives for boat building are generally available as liquid and paste adhesives, foaming adhesives and film adhesives, with the first ones being the most commonly used adhesives in boat yards. These are available in one-part or two-part liquids or pastes. Many epoxies are available both as adhesives and as matrix resins.

Plexus MA550, Sikaflex 252 and a vinyl ester mixed with filler were assessed as adhesives in T and single-lap joints. Sikaflex and Plexus are two of the most commonly used adhesives in boatbuilding. The first one is classified as flexible and the second one (MA550) as intermediate ([32]). The vinyl ester and filler mixture is expected to behave as a rigid adhesive.

2.13.5.1 Plexus MA550

The adhesive Plexus MA550 (supplied by ITW Plexus) is a two component methacrylate, mixed with 10:1 ratio, working time 40-45min., with 75% of ultimate strength in 70-75min. It is primerless, requires no sanding or grinding and virtually no surface preparation. The adhesive has received from the main classification societies, Lloyds of London, DNV (Det Norske Veritas) and ABS (American Bureau of Shipping) approval for the use in marine structure. The manufacturer advertise the product as environmentally friendly with less than 1% VOC emissions.

ITW Plexus published the following characteristics: $G = 21MPa$, Poisson's

ratio = 0.3, Tensile Strength ASTM D638 = $12.1 - 13.8N/mm^2$, Modulus = $275.8 - 344.7N/mm^2$, Strain to failure = 35-45%, Lap Shear ASTM D1002 (Cohesive Strength) = $9.0 - 12.4N/mm^2$.

2.13.5.2 Sikaflex 252

The adhesive Sikaflex-252 (supplied by Sika Group Switzerland) is a non-sag 1-component polyurethane adhesive of stiff, paste-like consistency that cures on exposure to atmospheric moisture. The product is recommended as a general use structural adhesive and not strictly as a marine grade one. The manufacturer published the following characteristics: Tensile strength (ISO 37) = $4MN/m^2$ approx., Elongation at break (ISO 37) > 300%, Tensile-shear strength (ISO 4587) = $2,5MN/m^2$ approx. In order to complete the existing data experimental tests have been conducted and the test results are presented in section 2.14.1.

2.13.5.3 In-shop made adhesives

Mixtures between epoxy, vinyl ester or polyester with microballoons or milled fibres are the most common in-shop made adhesives used in boatbuilding. For this thesis (and for comparison with the above mentioned industrial made adhesives), a mixture between vinyl ester and Epiglass HT120 (a silica based glue powder) was chosen as adhesive to test, its bulk material properties have been determined (see section 2.14.2) according to ASTM D638 and single lap joint using the mixture have been tested according to ASTM D1002.

2.13.6 Aluminium

Aluminium is widely used as a boatbuilding material. During this study, Aluminium - 5083-H32 was used as a substrate for single-lap joints. This aluminium is a marine grade material, non-heat treatable and is mainly used for metal plating.

For sheet and plates the published properties are: ultimate tensile stress

$\sigma_u = 305\text{MPa}$, yield tensile stress $\sigma_y = 215\text{MPa}$, elongation = 17%, Young's modulus of elasticity $E = 68918\text{MPa}$.

2.14 Experimental tests

2.14.1 Sikaflex 252

In order to approximate the elastic modulus of the material, several dog-bone samples (Fig. 2.4) were tested according to ASTM D638 (or ISO527 equivalent) on a Instron-4204 universal testing machine with a crosshead speed of 1 mm/min. No extensometer was used; the displacement of the machine's crosshead was considered accurate enough for the purpose of this test. The value found for Young modulus is $= 9.7\text{MN}/\text{m}^2$. It is to be recognized that the result of this test is to be used as qualitative value only. It is also realized that the mechanical properties of polymeric materials are highly dependent on rate of strain, temperature and moisture.

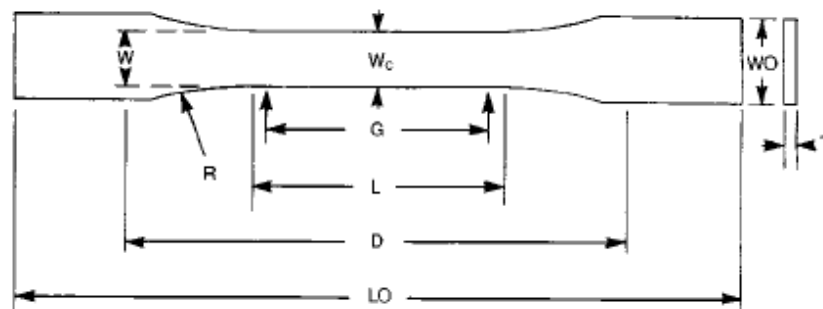


Figure 2.4: ASTM D638-3 - Test Specimen form and dimensions.

2.14.2 Vinyl ester and Epiglass mixture

A series of 5 samples were prepared according with the ASTM D638-03 - *Standard Test Method for Tensile Properties of Plastics*. The filler was thoroughly mixed with the resin for 3 minutes in order to eliminate any dry lumps of un-dispersed powder that might occur, then it was placed in a mould and left to cure for 24 hours. These samples were tested on an Instron-4204 universal

testing machine with a crosshead speed of 1 mm/min and extensometers were placed on the samples in order to record the extensions. No strain gauges were used. The results for the 1.5:1 ratio mixture are presented in the graph 2.5.

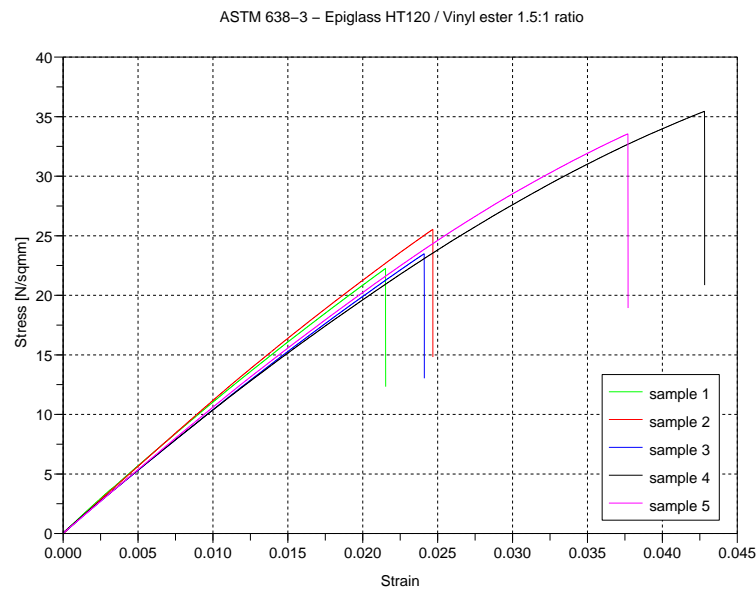


Figure 2.5: ASTM 638-3 - Tensile properties of Epiglass HT120/Vinyl ester ratio 1.5:1.

The 1.5:1 mixture exhibits the characteristics of a rigid adhesive. It can be noted that the plastic region is almost non-existent. In these conditions, the Young's modulus of the adhesive, based on the average value, is found to be 1176MPa. The ultimate strength of the mixture varies between a value of 22.25MPa and 35.44MPa with an average value of 28.05MPa. In the absence of a compressive test, the material will be considered isotropic and the Poisson's ratio will be considered equal to 0.3.

An inspection of the rupture zone of the samples shows a fair amount of voids, which reduces the strength of the material itself and they are presumed to appear due to the curing process. These imperfections are almost impossible to eliminate in a normal (on the yard and by-hand) application of the mixture.

It is expected that the material will behave differently in compression than in tension and the mechanical properties will be influenced by the rate of cure. The mixture in the samples will cure differently in the moulds than the mixture

used in the joints - the exothermic reactions will produce different amounts of energy (due to the thickness of the adhesive layer) hence the cure temperature will be different (eg. for the T-joints it is expected that the cure temperature be higher than for the Lap-joints).

2.14.3 Vinyl ester and QCel mixture

A series of 5 samples were prepared according with the ASTM D638-03 - *Standard Test Method for Tensile Properties of Plastics* in the same conditions as the previous material. The results for the mixture are presented in the graph 2.6.

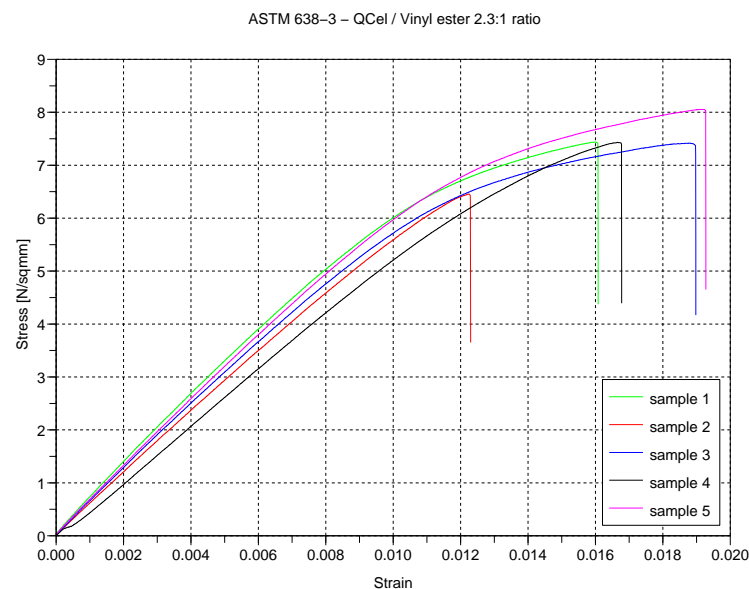


Figure 2.6: ASTM 638-3 - Tensile properties of QCel/Vinyl ester ratio 2.3:1.

The Young's modulus of the mixture, based on the average value, is found to be 642.4MPa. The ultimate strength of the mixture varies between a value of 6.46MPa and 8.05MPa with an average value of 7.36MPa. In the absence of a compressive test, the material will be considered isotropic and the Poisson's ratio will be considered equal to 0.3.

The notes regarding the voids and mechanical properties made for the previous material are valid for the QCel/Vinyl ester mixture also.

2.14.4 Laminate Properties

The material used as reinforcement for the composites is EU460 (unidirectional E-glass 460g/sqm) and the matrix is Polyplex 4000 vinyl ester. A series of 5 samples (see Fig. 2.7) for each of the orientations (0° , 45° and 90°) were prepared according to ASTM standard D3039/D 3039M-00 - *Standard Test Method for Tensile Properties of Polymer Matrix Composite Materials*. The tests were executed on a Instron-4204 universal testing machine with a crosshead speed of 1 mm/min.

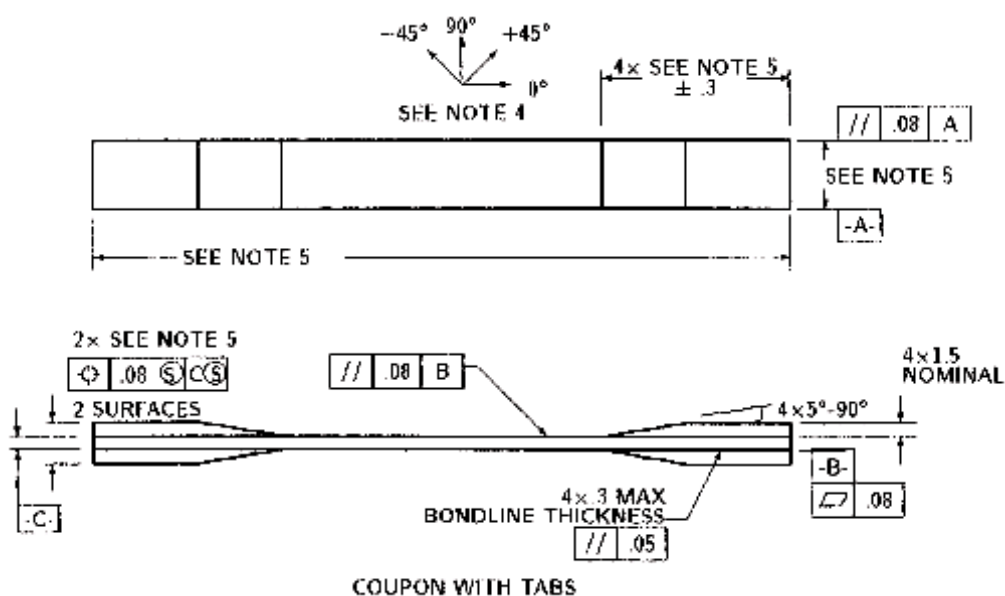


Figure 2.7: ASTM D3039/D 3039M-00 - Specimen form and dimensions.

In order to avoid notches or local delaminations, the specimens were carefully cut from a plate made from 3 layers of glass at the above orientation. The plates were prepared by hand lamination, using 2% volume of MEKP as catalyst at 20°C ambient temperature and left to cure overnight.

Tabs prepared from the same material (E-glass 460g/sqm and vinyl ester) have been attached to all samples, glued onto the ends of the samples using a thin layer of commercial grade SuperGlue. All tabs have been beveled at one end at an angle of around 30° . However, these tabs are required only for the unidirectional samples with 0° orientation, where the shear strength is typically at least an order of magnitude lower than its axial strength (the

load must be transmitted from the testing machine through the grips to the specimen via shear). An extensometer has been used in order to record the extensions. No strain gauges were used.

The values obtained are presented in the Table 2.3:

EU460/Vinyl ester mechanical properties		
Tension (0°)	$E_{t11} = 20760MN/m^2$	$\sigma_{t11} = 411MN/m^2$
Tension (45°)	$E_{txx} = 7445MN/m^2$	$\sigma_{txx} = 51.2MN/m^2$
Tension (90°)	$E_{t22} = 7082MN/m^2$	$\sigma_{t22} = 39.07MN/m^2$

Table 2.3: EU460/Vinyl ester mechanical properties.

Presuming that the Poisson's ratio for this laminate is $\nu_{12} = 0.3$, the shear modulus was calculated to be $G_{12} = 1663MN/m^2$ and $\nu_{21} = 0.1$. The fibre content by mass ψ of the specimens was determined by ignition of the resin and was found to be in average $\psi = 0.5$, which is close to the value recommended by ISO 12215 [15] for unidirectional fabric in an open mould ($\psi = 0.55$). The thickness of one layer was found to be in average 0.78mm.

Throughout this study, two kind laminates have been used: a $0^\circ, 90^\circ$ and a $0^\circ, 90^\circ, 90^\circ, 0^\circ$ arrangement. The laminate properties have been calculated according to Classical Lamination Theory (CLT) and the results are presented for $0^\circ, 90^\circ$ laminate in the Table 2.4 and for $0^\circ, 90^\circ, 90^\circ, 0^\circ$ laminate in the Table 2.5 respectively.

EU460/Vinyl ester effective laminate properties.	
Extensional in-plane properties.	
E_{xx}	$11400MN/m^2$
E_{yy}	$11400MN/m^2$
G_{xy}	$1660MN/m^2$
ν_{xy}	0.153
Flexural properties	
E_{xxf}	$11400MN/m^2$
E_{yyf}	$11400MN/m^2$
ν_{xyf}	0.153
ν_{yxf}	0.153

Table 2.4: EU460/Vinyl ester $0^\circ, 90^\circ$ laminate properties.

EU460/Vinyl ester effective laminate properties	
Extensional in-plane properties	
E_{xx}	$14000MN/m^2$
E_{yy}	$14000MN/m^2$
G_{xy}	$1660MN/m^2$
ν_{xy}	0.153
Flexural properties	
E_{xxf}	$19100MN/m^2$
E_{yyf}	$8830MN/m^2$
ν_{xyf}	0.242
ν_{yxf}	0.112

Table 2.5: EU460/Vinyl ester $0^\circ, 90^\circ, 90^\circ, 0^\circ$ laminate properties.

Chapter 3

Single lap joints

The single-lap joint is a common method of joining two plates in-plane. It is easy to produce and inspect. Its geometry seems simple enough, but the state of stress developed in the joint makes it one of the weakest ones.

3.1 Analytical Models of Single Lap joints

A typical single-lap joint configuration is represented in Fig. 3.1 where P represents the load per unit width (w), T is the load.

$$P = \frac{T}{w} \quad (3.1)$$

The adherends are identified by the numerical subscripts 1 and 2, while the adhesive is identified by the subscript a. Here t represents the thickness and E , G , ν are the Young's modulus, shear modulus and Poisson's ratio of the adherends and of the adhesive layer.

3.1.1 Average Shear Stress Analysis

Average Shear Stress Analysis is the simplest analysis and considers the adherends to be rigid and the adhesive to deform only in shear. If the width and the length of the bondline are w and L respectively, then the average shear stress in the adhesive is [2]:

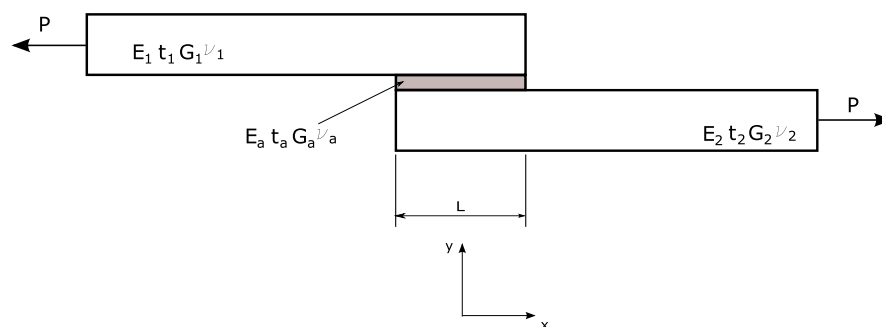


Figure 3.1: Single-Lap Geometry and Notations.

$$\tau = \frac{T}{wL} \quad (3.2)$$

It can be seen that increasing any of the two parameters - width and length - decreases the shear stress. From the ultimate shear strength of the adhesive τ_u (e.g. through tests) one can calculate the bondline length:

$$L = \frac{P}{\tau_u} \quad (3.3)$$

However, this analysis is too simplistic in the way that it does not take into account the out-of plane deformation associated with eccentricity of the load path and the characteristics of the adhesive and adherends.

3.1.2 Volkersen Analysis

In his study published in 1938 [31], Volkersen assumed that the adhesive deforms only in shear, while the adherends deform only in tension. Also, he considered the adhesive and the adherends as perfectly elastic and isotropic. He obtained the following closed-form solution for the adhesive shear stress distribution:

$$\tau = \frac{P\lambda \cdot \cosh(\lambda x)}{2 \cdot \sinh(\lambda \frac{L}{2})} + \frac{P\lambda \cdot \sinh(\lambda x)}{2 \cdot \cosh(\lambda \frac{L}{2})} \cdot \frac{E_2 \cdot t_2 - E_1 \cdot t_1}{E_2 \cdot t_2 \cdot E_1 \cdot t_1}. \quad (3.4)$$

where

$$\lambda = \sqrt{\frac{G_a}{t_a} \cdot \frac{E_2 \cdot t_2 + E_1 \cdot t_1}{E_2 \cdot t_2 \cdot E_1 \cdot t_1}}.$$

This analysis does not take into account the fact that the two forces involved are not collinear, hence a bending moment is developed in addition to the in-plane tension. As a result of this bending moment, the adherends bend which results in the joint rotating. The development of normal (peel) stresses is also ignored.

The λ value plays an important role in Volkersen analysis: $1/\lambda$ is the characteristic "lag" distance where the shear stress is decreased at 37% of its maximum value. In other words, "shear lag" is a finite distance required to transfer (equilibrate) the load from one adherend to another.

In Fig. 3.2 the shear stress has been plotted against the bondline length. For the same configuration the constant shear stress represents the stress obtained using Average Shear Stress Analysis. The third line represents the shear stress using aluminium and composite adherends (with the characteristics defined later in section 3.1). It should be noted that the case of single-lap joints with dissimilar adherends is the worst one.

At the end of overlaps $x = L/2$ and in the case of identical adherends, the maximum shear stress is:

$$\tau_{max} = \frac{P\lambda}{2} \coth\left(\lambda \frac{L}{2}\right). \quad (3.5)$$

Considering τ_{max} as the ultimate shear strength of the adhesive τ_u , the predicted joint failure strength became:

$$P_{max} = \frac{2\tau_u}{\lambda} \tanh\left(\lambda \frac{L}{2}\right). \quad (3.6)$$

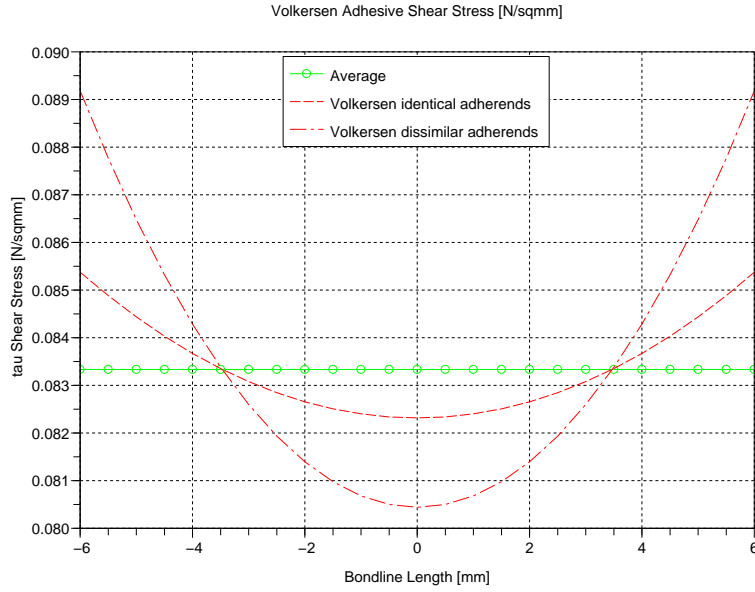


Figure 3.2: Shear Stress along bondline according to Volkersen

In Fig. 3.3 joint strength has been plotted against the adhesive thickness. As the graph shows, P_{max} grows with t_a , which means that the thicker the adhesive layer, the higher the strength of the joint. This fact is not supported by experiments [2].

3.1.3 Goland and Reissner Analysis

Goland and Reissner in their study in 1944 [17], took rotation into account by using a bending moment factor k which relates the bending moment at the adherend end M_0 with the in-plane loading, as follows:

$$M_0 = k \cdot P \cdot \frac{t}{2} \quad (3.7)$$

where t is the adherend thickness ($t = t_1 = t_2$), but the thickness of adhesive layer is neglected. The bending moment factor k is approaches 1 if the load is small or for (infinitely) stiff adherends, while k is < 1 when the load increases and the adherends are subject to bending. Using the following notation:

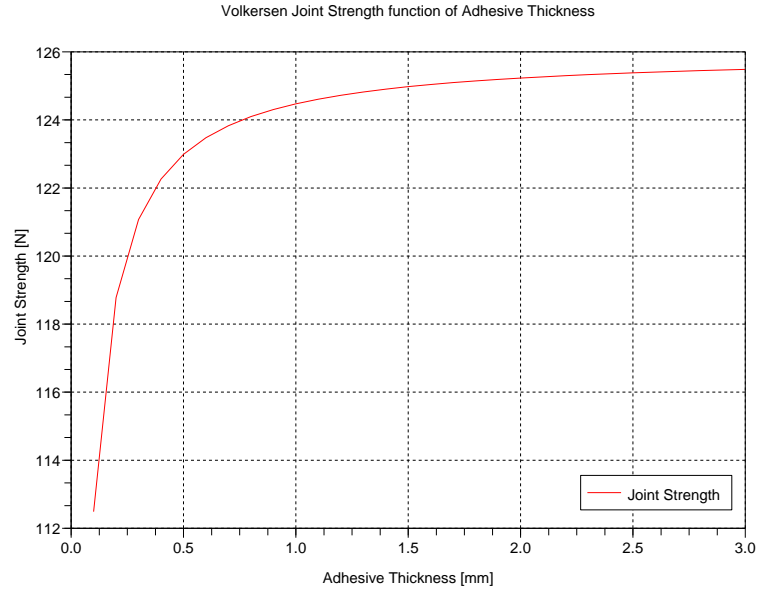


Figure 3.3: Joint Strength as function of the adhesive thickness according to Volkersen.

$$\beta = \sqrt{\frac{8G_a t_1}{E_1 t_a}}$$

$$\lambda_s = \frac{\beta L}{2t}$$

$$\phi = \frac{L}{2t} \cdot \sqrt{\frac{P 3(1-\nu^2)}{E 2}}$$

with ν the Poisson's ratio of the adherend, the bending moment factor may be expressed as:

$$k = k_{GR} = \frac{\cosh(\phi)}{\cosh(\phi) + 2\sqrt{2} \cdot \sinh(\phi)} = \frac{1}{1 + 2\sqrt{2} \cdot \tanh(\phi)} \quad (3.8)$$

The shear stress in this case is (as obtained by Goland and Reissner):

$$\tau(x) = \frac{1}{4} \cdot \frac{P}{L} \cdot \left(\lambda_s (1 + 3k) \cdot \frac{\cosh(\lambda_s \cdot 2x/L)}{\sinh(\lambda_s)} + 3(1 - k) \right). \quad (3.9)$$

or, using a non-dimensional expression:

$$\frac{\tau(x)}{\tau_{av}} = \frac{1}{4} \cdot \left(\lambda_s (1 + 3k) \cdot \frac{\cosh(\lambda_s \cdot 2x/L)}{\sinh(\lambda_s)} + 3(1 - k) \right). \quad (3.10)$$

Several expressions for k exist in literature [2]: Hart-Smith [18] considered the bending factor as:

$$k_{HS} = \frac{1}{1 + \phi + \frac{(\phi)^2}{6}} \quad (3.11)$$

where Zhao, Adams and Pavier developed a simpler equation:

$$k_{ZAP} = \frac{1}{1 + \phi}$$

Plotting the shear stress along the bondline (Fig. 3.4), more variable stress profile is predicted compared with the one resulting from Volkersen analysis, for the same conditions. Also, another aspect of the analysis is that it predicts far bigger adhesive shear stresses at the edge of the joint.

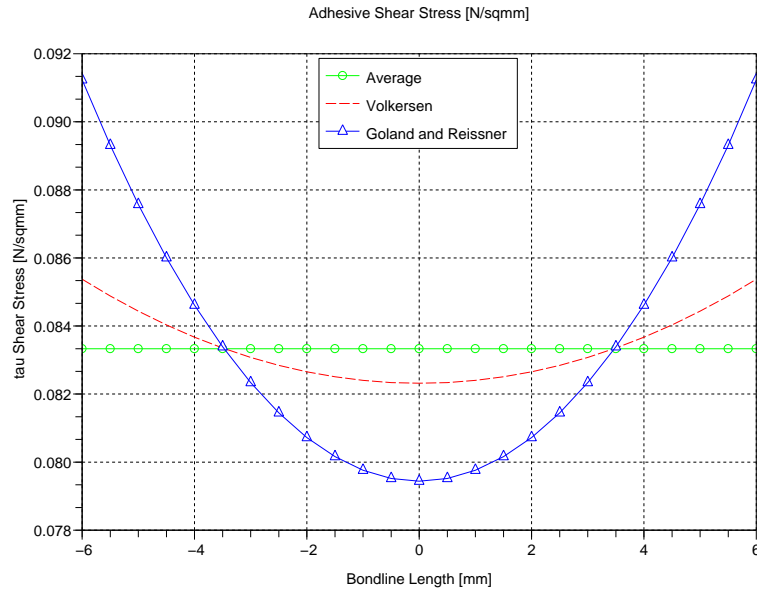


Figure 3.4: Shear Stress profile according to Goland and Reissner model.

Similarly, Goland and Reissner determined the Peel Stress (stress normal to the plane of the bond) as follows:

$$\sigma(x) = \frac{4Pt}{L^2 R_3} \cdot (A + B) \quad (3.12)$$

where:

$$\gamma = \sqrt[4]{\frac{6 \cdot E_a \cdot t}{Et_a}}$$

$$\lambda_p = \frac{\gamma L}{2t}$$

$$k' = k \cdot \frac{L}{2t} \cdot \sqrt{3(1 - \nu^2) \cdot \frac{P}{E}} = k \cdot \phi \cdot \sqrt{2}$$

$$R_1 = \cosh(\lambda_p) \cdot \sin(\lambda_p) + \sinh(\lambda_p) \cdot \cos(\lambda_p)$$

$$R_2 = \sinh(\lambda_p) \cdot \cos(\lambda_p) - \cosh(\lambda_p) \cdot \sin(\lambda_p)$$

$$R_3 = 0.5 \cdot (\sinh(2\lambda_p) + \sin(2\lambda_p))$$

$$A = \left(R_2 \lambda_p^2 \frac{k}{2} + \lambda_p k' \cosh(\lambda_p) \cos \lambda_p \right) \cdot \cosh\left(\frac{\lambda_p 2x}{L}\right) \cdot \cos\left(\frac{\lambda_p 2x}{L}\right)$$

$$B = \left(R_1 \lambda_p^2 \frac{k}{2} + \lambda_p k' \sinh(\lambda_p) \sin \lambda_p \right) \cdot \sinh\left(\frac{\lambda_p 2x}{L}\right) \cdot \sin\left(\frac{\lambda_p 2x}{L}\right)$$

or, using a non-dimensional expression:

$$\frac{\sigma(x)}{\sigma_{av}} = \frac{4t^3}{LR_3} \cdot (A + B) \quad (3.13)$$

Plotting the peel stress profile along the bondline (see Fig. 3.5), one can remark that also at the end of the joint the peel stress is at its maximum and a compressive stress is found in some of the parts of the adhesive layer.

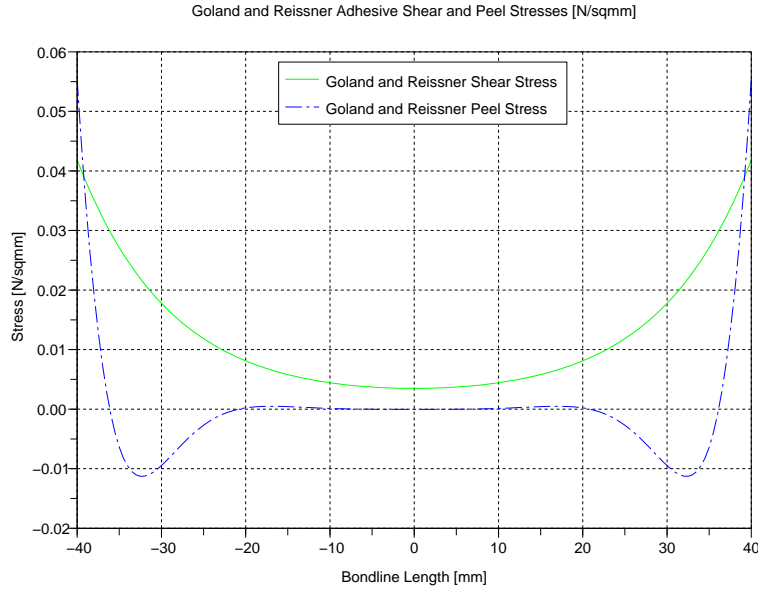


Figure 3.5: Peel Stress along the bondline according to Goland-Reissner model.

It has to be noted that the range of validity of the solution is given by:

$$\frac{t_1 G_a}{t_a G_1} \leq 0.1$$

and

$$\frac{t_1 E_a}{t_a E_1} \leq 0.1$$

3.1.4 Cooper and Sawyer Model

An improvement of the Goland and Reissner solution (in order to count for the non-linear effects) is presented by Cooper and Sawyer ([11]) where the shear stress distribution τ and the peel stress σ in the adhesive along the bond line, is given by:

$$\frac{\tau}{\tau_{av}} = \frac{1}{4 + 3\zeta} \left[(1 + 3k) \frac{\beta}{\sinh \beta} \cosh \left(\frac{2\beta x}{L} \right) + 3(1 - k + \zeta) \right]. \quad (3.14)$$

and

$$\frac{\sigma}{\sigma_{app}} = \frac{4t^2}{L^2 R_3} \cdot (A + B) \quad (3.15)$$

where

$$\zeta = \frac{ta}{t}$$

$$\tau_{av} = \frac{T_0}{L}$$

$$\beta = \sqrt{\frac{8G_a(1-\nu^2)}{t_a \cdot E \cdot t} \left(1 + \frac{3\zeta}{4}\right) c^2}$$

where k is

$$k = \frac{2M_0}{tT_0}$$

and

$$\sigma_{app} = \frac{T_0}{t}$$

$$\lambda_p = c \sqrt[4]{\frac{E_a}{2ta \cdot D}}$$

where D is the flexural stiffness of the adherend and is given by:

$$D = \frac{Et^3}{12(1-\nu^2)}$$

$$k' = \frac{cV_0}{tT_0}$$

$$R_1 = \cosh(\lambda_p) \cdot \sin(\lambda_p) + \sinh(\lambda_p) \cdot \cos(\lambda_p)$$

$$R_2 = \sinh(\lambda_p) \cdot \cos(\lambda_p) - \cosh(\lambda_p) \cdot \sin(\lambda_p)$$

$$R_3 = 0.5 \cdot (\sinh(2\lambda_p) + \sin(2\lambda_p))$$

$$A = \left(R_2 \lambda_p^2 \frac{k}{2} + \lambda_p k' \cosh(\lambda_p) \cos \lambda_p \right) \cdot \cosh\left(\frac{\lambda_p 2x}{L}\right) \cdot \cos\left(\frac{\lambda_p 2x}{L}\right)$$

$$B = \left(R_1 \lambda_p^2 \frac{k}{2} + \lambda_p k' \sinh(\lambda_p) \sin \lambda_p \right) \cdot \sinh\left(\frac{\lambda_p 2x}{L}\right) \cdot \sin\left(\frac{\lambda_p 2x}{L}\right)$$

where T_0 , V_0 , M_0 are adherend forces and the moment resultant at the edge of overlap, and are given by:

$$T_0 = P \cos \theta$$

$$M_0 = P \left(\frac{t + t_a}{2} \right) \cos \theta \frac{u_2 \cosh\left(\frac{u_2 L}{2}\right) \sinh(u_1 \cdot l)}{u_2 \sinh(u_1 \cdot l) \cosh\left(\frac{u_2 L}{2}\right) + u_1 \cosh(u_1 l) \sinh\left(\frac{u_2 L}{2}\right)}$$

$$V_0 = P \left(\frac{t + t_a}{2} \right) \cos \theta \frac{u_1 u_2 \cosh\left(\frac{u_2 L}{2}\right) \cosh(u_1 \cdot l)}{u_2 \sinh(u_1 \cdot l) \cosh\left(\frac{u_2 L}{2}\right) + u_1 \cosh(u_1 l) \sinh\left(\frac{u_2 L}{2}\right)}$$

where

$$\cos \theta = \frac{l + \frac{L}{2}}{\sqrt{\left(l + \frac{L}{2}\right)^2 + \left(\frac{t+t_a}{2}\right)^2}}$$

$$u_1 = \sqrt{\frac{P \cos \theta}{D}}$$

$$u_2 = \sqrt{\frac{P \cos \theta}{8D}}$$

For $\cos \theta = 1$, the resultants T_0 , V_0 , M_0 are reduced to the values predicted by Goland and Reissner.

It is interesting to note that this model takes into account the free length of the adherend from the supports (or the point of load application) to the beginning of the overlap (in other words the length of the adherend from its edge to grips is $l + L$). The shear stress distribution along the bondline is plotted in Fig. 3.6.

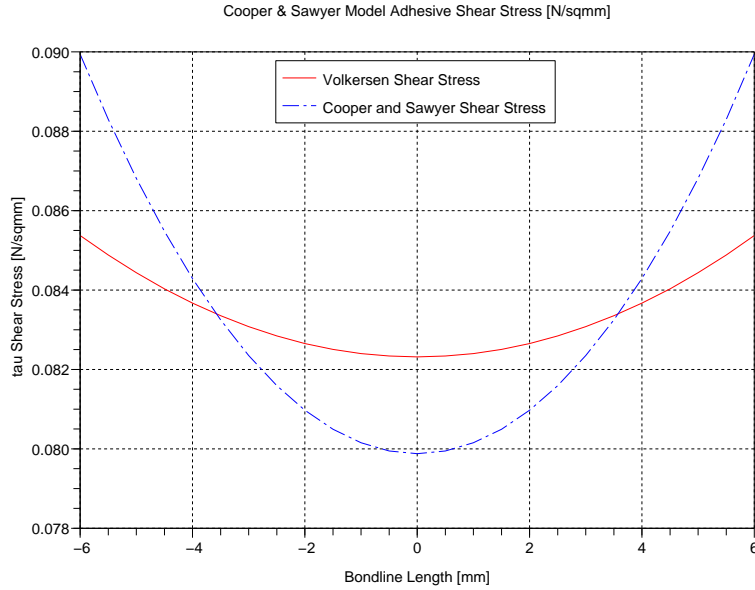


Figure 3.6: Shear Stress in Cooper and Sawyer Model

3.1.5 Bigwood and Crocombe Analysis

Starting with Goland and Reissner analysis, and using a adherend-adhesive sandwich model, Bigwood and Crocombe developed a general analysis of the bonded joints. According to this model a number of adhesive joints, such as single-lap joints, L- and T-joints as well as double-lap joints can be analysed, presuming some restrictions are taken into account.

A full elastic analysis is produced by considering that the adherends are subjected to a general state of tensile, shear and moment loading. The adhesive layer transfers the loading to the adherends through transverse tension and shear (Fig. 3.7).

The differential equations describing the shear and transverse stress distribution in the adhesive layer are simplified in order to obtain easy to use design formula. By considering each type of loading separately (T, V, M per unit width), the following equations can be deducted:

- Maximum transverse shear due to V:

$$\sigma_V = \frac{-\sqrt{2} \cdot \beta_1 V}{\sqrt[4]{(\beta_1 + \beta_2)^3}} \quad (3.16)$$

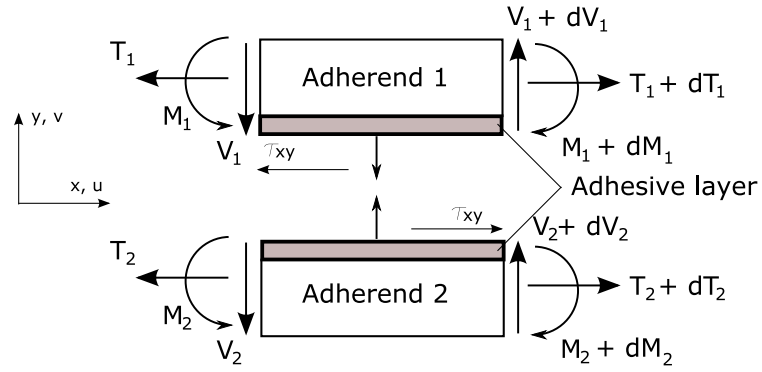


Figure 3.7: The general adherend-adhesive sandwich according with Bigwood and Crocombe

- Maximum transverse stress due to M:

$$\sigma_M = \frac{-\beta_1 M}{\sqrt{\beta_1 + \beta_2}} \quad (3.17)$$

- Maximum shear stress due to T:

$$\tau_T = \frac{-\alpha_1 T}{2\sqrt{\alpha_1 + \alpha_2}} \quad (3.18)$$

- Maximum shear stress due to V:

$$\tau_V = \frac{3V}{4t_1} \quad (3.19)$$

- Maximum shear stress due to M:

$$\tau_M = \frac{3\alpha_1 M}{t_1 \sqrt{\alpha_1 + \alpha_2}} \quad (3.20)$$

where

- β_1 and β_2 are peel compliance factors, a measure of relative stiffness of the adherends and adhesive and are defined as:

$$\beta_1 = \frac{12E_a(1 - \nu_1^2)}{E_1 t_1^3 t_a} [mm^{-4}] \quad (3.21)$$

and

$$\beta_2 = \frac{12E_a(1 - \nu_2^2)}{E_2 t_2^3 t_a} [mm^{-4}] \quad (3.22)$$

- α_1 and α_2 are shear compliance factors, a measure of relative shear stiffness of the adherends and adhesive and are defined as:

$$\alpha_1 = \frac{G_a (1 - \nu_1^2)}{E_1 t_1 t_a} [mm^{-2}] \quad (3.23)$$

and

$$\alpha_2 = \frac{G_a (1 - \nu_2^2)}{E_2 t_2 t_a} [mm^{-2}] \quad (3.24)$$

The equations are valid assuming the following conditions:

- The longitudinal direct stress in the adhesive is negligible compared with the similar stress in the adherends. Similar to the Goland and Reissner model, the adherend strains are negligibly small compared with adhesive strains.
- The adherends are isotropic and constant in thickness but can be of different materials and thicknesses. They are analysed as flat plates under bending and the normal stresses (σ_y) through the thickness are neglected.

The use of the simplified model is limited because of the inaccuracies introduced. For practical purposes, the formulas are valid in the following conditions:

$$\frac{\alpha_1}{\alpha_2} \geq 0.6$$

$$\frac{\beta_1}{\beta_2} \leq 2 \quad (3.25)$$

$$(\alpha_1 + \alpha_2) L^2 \geq 9$$

$$(\beta_1 + \beta_2) L^4 \leq 4.6^4$$

Later on, Bigwood and Crocombe, following the same sandwich model, developed a non-linear analysis presented in [5].

3.1.6 L.J. Hart-Smith Model - Elastic Analysis

An important milestone was set up by L.J. Hart-Smith in a series of NASA sponsored contract published in 1973 and 1974. His considerable amount of work has focused on the single-lap, double-lap, stepped and scarf joints and incorporates thermic effects and effects due to unbalanced stiffness of adherends. His approach was based on Volkersen and Goland and Reissner analysis. In order to characterize the adhesive, Hart-Smith has adopted an elastic-plastic model as shown in fig 3.8, the geometry and nomenclature is shown in Fig. 3.9 [18].

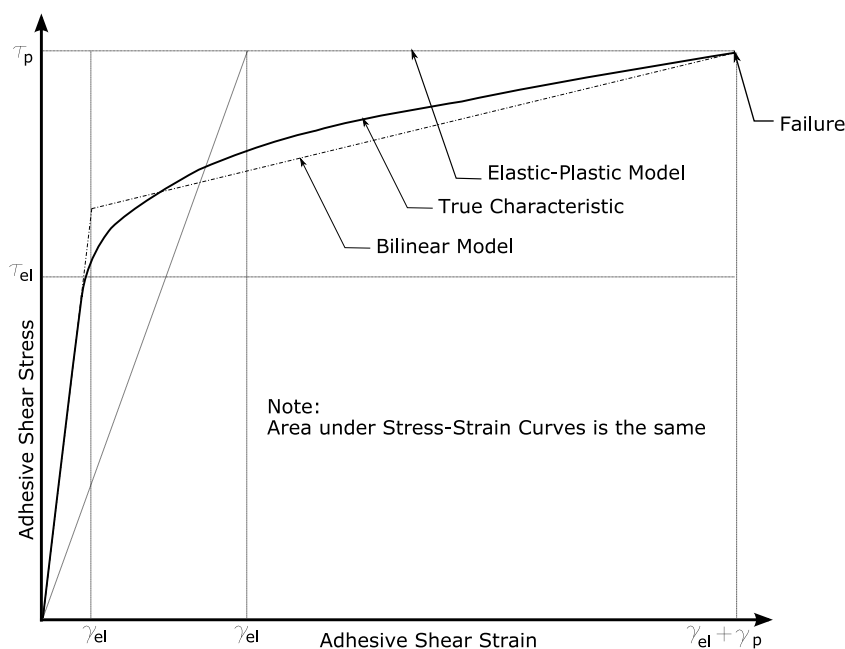


Figure 3.8: Adhesive shear stress-strain curves and mathematical models.

Hart-Smith obtained the following distribution of the shear stress in the adhesive along the bond line for a balanced single-lap joint (in the elastic region):

$$\tau(s) = A_2 \cosh(2\lambda's) + B_2 \sinh(2\lambda's) + C_2 \quad (3.26)$$

where:

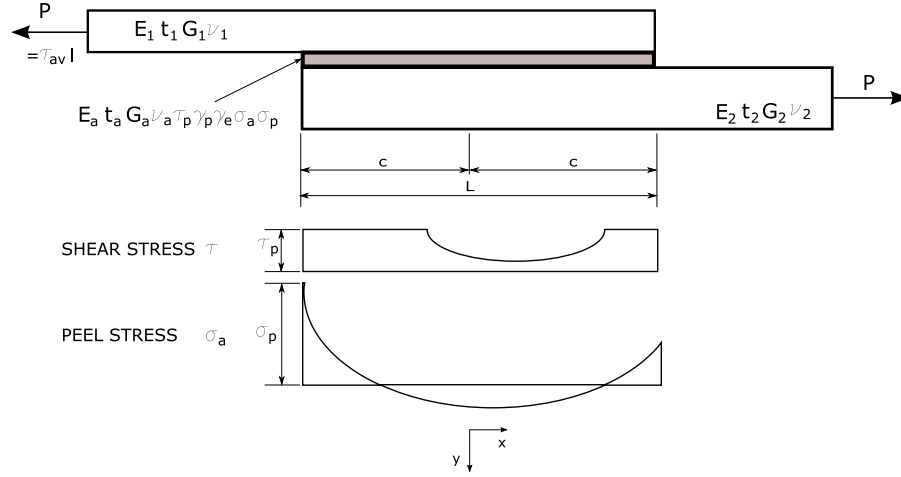


Figure 3.9: Geometry, Nomenclature and Mathematical model for analysis of unbalanced single-lap joints, [18].

$$s = x - \frac{L}{2} \quad (3.27)$$

The constant B_2 can be considered zero because of the anti-symmetry of the joint.

Resolving the above equation for the given boundary conditions, the A_2 and C_2 coefficients have the following form (where λ' is given in the Eq. 3.32):

$$C_2 = \frac{P}{L} - \frac{A_2}{\lambda' L} \sinh(\lambda' L) \quad (3.28)$$

$$A_2 = \frac{1}{2\lambda' \sinh(\lambda' L)} \frac{G}{E \cdot t \cdot t_a} \left[P + \frac{6(1-\nu^2) M_0}{k_b t} \right] \quad (3.29)$$

Here M_0 is the bending moment per unit width in the continuous adherend at the end of the joint and has the approximate form (here $\xi = \sqrt{P/D}$):

$$M_0 \cong P \left(\frac{t + t_a}{2} \right) \frac{1}{1 + \xi c + \frac{\xi^2 c^2}{6}} \cong k_{HS} P \frac{t}{2} \left(1 + \frac{t_a}{t} \right) \quad (3.30)$$

This form differs from the result obtained by Goland and Reissner (eq. 3.8) which due to the simplifications made, it leads to a slightly conservative

solution. Other forms of the bending factors have been shown in the previous section. In the above equation the bending stiffness parameter k_b is:

$$k_b = \frac{D}{\left[\frac{Et^3}{12(1-\nu^2)} \right]} \quad (3.31)$$

This factor serves to uncouple the bending and extensional stiffness for filamentary composites ($k_b = 1$ for metals). In the same manner, the notation λ' is introduced:

$$(\lambda')^2 = \left[\frac{1 + \frac{3(1-\nu^2)}{k_b}}{4} \right] \cdot \lambda^2 \quad (3.32)$$

where:

$$\lambda^2 = \frac{2G}{E \cdot t \cdot t_a} \quad (3.33)$$

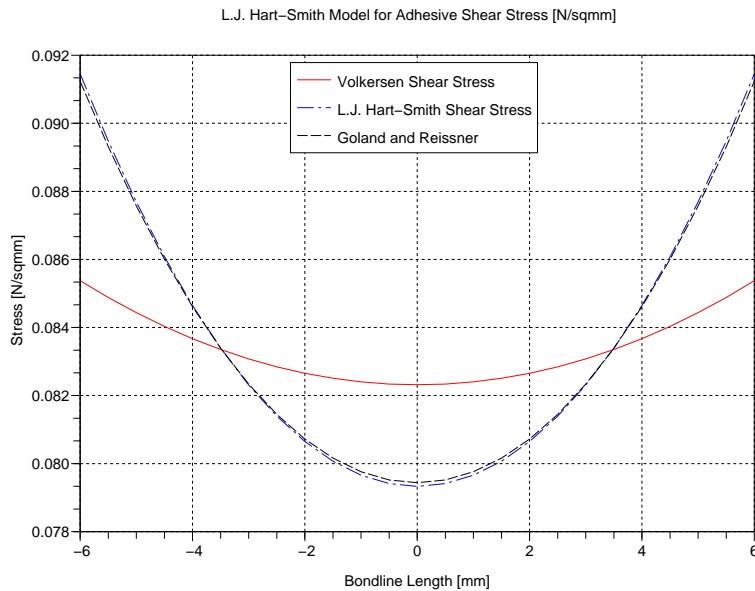


Figure 3.10: Shear Stress distribution - L.J.Hart-Smith

In Hart-Smith's model, this latest parameter characterizes the adhesive shear stress distribution. It is found that:

$$\frac{\tau_{av}}{\tau_{max}} = \frac{1}{1 + \left[1 + \frac{3k(1-\nu^2)}{k_b} \left(1 + \frac{t_a}{t} \right) \right] \left[\frac{\lambda^2}{4(\lambda')^2} \right] \left[\frac{2\lambda'c}{\tanh(2\lambda'c)} - 1 \right]} \quad (3.34)$$

which, for isotropic adherends, is reduced to the result of Goland and Reissner. A comparison between Volkersen, Goland and Reissner and L.J.Hart-Smith models is shown in Fig. 3.10.

Hart-Smith obtained the following distribution of the peel stress in the adhesive along the bond line for balanced adherends (in elastic region, see Fig. 3.11):

$$\sigma_a = A \cos(\varphi s) \cosh(\varphi s) + B \sin(\varphi s) \sinh(\varphi s) \quad (3.35)$$

where:

$$\varphi^4 = \frac{E_a}{2t_a D} = \frac{6E_a(1-\nu^2)}{Et^3 t_a k_b} \quad (3.36)$$

and φ has the same role as the parameter λ but for peel stress distribution. In the above equation the constants A and B have the following approximate form:

$$B = \frac{A [\cos(\varphi) + \sin(\varphi)]}{\cos(\varphi) - \sin(\varphi)} \quad (3.37)$$

and

$$A = [\cos(\varphi) - \sin(\varphi)] \cdot \frac{E_a M_o}{t_a D \varphi^2 e^{(\varphi)}} \quad (3.38)$$

It is found that (same as for shear stresses):

$$\frac{\sigma_{amax}}{\sigma_{av}} = k \left(1 + \frac{t_a}{t} \right) \sqrt{\frac{3E_a(1-\nu^2)t}{2k_b E t_a}} \quad (3.39)$$

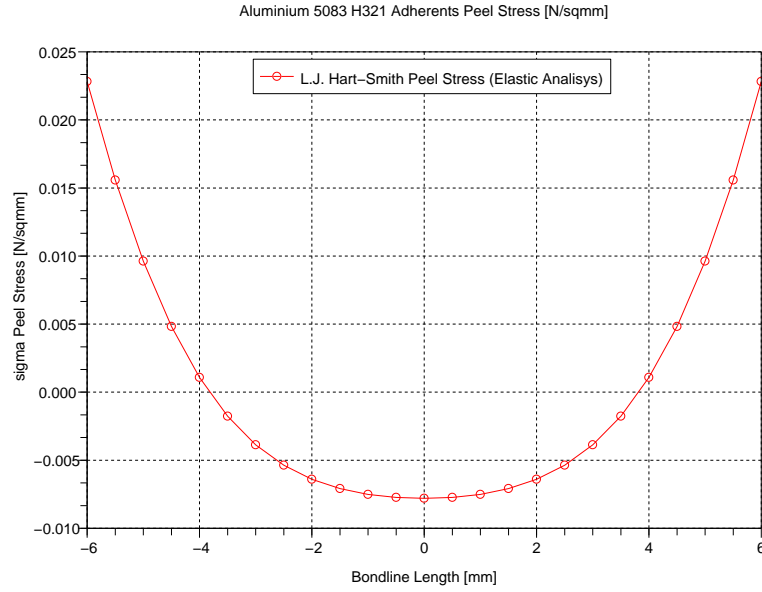


Figure 3.11: Peel Stress in Elastic Analysis along bondline - L.J.Hart-Smith

Hart-Smith obtains the adherend (substrate) stress distribution also, maximum stress adjacent to the bond line at the end of the overlap is given by:

$$\sigma_{smax} = \frac{P}{t} + \frac{Mc}{I} = \sigma_{sav} \left[1 + 3k \left(1 + \frac{t_a}{t} \right) \right] \quad (3.40)$$

and

$$\xi^2 = \frac{P}{D} = \frac{\sigma_{sav}}{\sigma_{smax}} \left[\frac{12(1-\nu^2)\sigma_{smax}}{k_b E t^2} \right] \quad (3.41)$$

For a given allowable stress $\sigma_{sa} = \sigma_{smax}$, the associated average stress is determined by iterations.

3.1.7 Wiedemann Analysis

Wiedemann [33] and [32], for his model, relies on Volkersen's stress analysis in order to estimate geometrical parameter - the overlap length. Plotting (see Fig. 3.12) the ratio of the maximum shear stress (eq. 3.4 for $x = L/2$), to the applied tensile tension in the adherend 1 ($\sigma_{10} = P/t_1$), it can be seen that for $\lambda L \geq 5$ the ratio become almost constant.

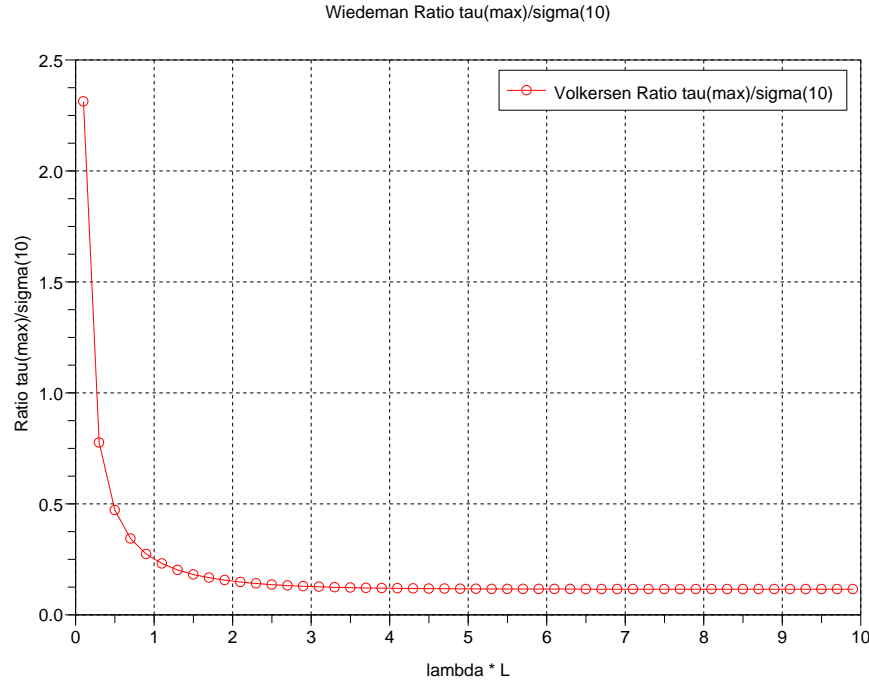


Figure 3.12: Volkersen τ_{max}/σ_{10} as a function of the product $\lambda * L$

So, for practical use we can consider $\lambda \cdot L = 5$ and we can estimate a minimum overlap length L_* as:

$$L_* \geq 5 \cdot \sqrt{\frac{E_1 \cdot t_1 \cdot t_a}{Ga \cdot (1 + \delta)}} \quad (3.42)$$

where δ is the adherend stiffness ratio:

$$\delta = \frac{E_1 \cdot t_1}{E_2 \cdot t_2} \quad (3.43)$$

The design value of L_{min} in Wiedemann analysis become:

$$L_{min} = 2 \cdot L_* \quad (3.44)$$

In Equation 3.44, '2' represents a factor of safety introduced by Wiedemann to account for the effects of peel and other moment induced stresses. All the time the indices of the adherends have to be selected in such a way that $\delta \leq 1$.

Using Equation 3.44, with the above findings ($\lambda * L = 5$) and considering the worst case scenario $\coth(\lambda L/2) \longrightarrow 1$, $\tanh(\lambda L/2) \longrightarrow 1$, Wiedemann estimates the maximum shear stress at the end of the overlap as a factor applied to the mean shear stress ($\tau_m = P/L$):

$$\tau_{max} = \frac{5}{1 + \delta} \cdot \tau_m \quad (3.45)$$

In these conditions, the joint designer only has to ensure that the shear strength of the adhesive τ_u (which is obtained by suitable tests) is larger than the maximum shear stress τ_{max} . It has to be noted that the above analysis is suitable for rigid adhesives where the adherends have a major importance in the quality of the joint.

As it can be seen, in his analysis, Wiedemann offers some easy-to-use formula for pre-dimensioning the capacity of the joint. The designer of the joint can quickly and easily get an idea whether the adhesives chosen in the preliminary stage are mechanically suitable for the job.

3.1.8 Chamis-Murthy Preliminary Analysis

C.C. Chamis and P.L.N. Murthy [10] developed simplified procedures for the adhesively bonded composite joints as part of the NASA aerospace programs. Their allowables (minimum length L_{min} , maximum shear stress in the adhesive $\sigma_{as.max}$, maximum normal stress (peel-off stress) in the adhesive $\sigma_{an.max}$) were obtained from the single-lap theory.

The general steps for designing adhesive joints, according to [10] are:

1. Establish design requirements: the loads, the adhesive, safety factors and environmental factors.
2. Obtain laminate dimensions and properties for the adherends using composite mechanics or tests.
3. Obtain the shear strength and the peel-off strength of the adhesive.

4. Degrade the adhesive properties for moisture, temperature and cyclic loads using the following equations:

$$\frac{\sigma_a}{\sigma_{a0}} = \sqrt{\frac{T_{gw} - T}{T_{gd} - T_0}} - 0.1 \cdot \log(N) \quad (3.46)$$

where:

σ_a = expected adhesive strength being calculated; σ_{a0} = the corresponding strength at reference conditions, usually taken as room temperature dry; T_{gw} = the wet adhesive glass transition temperature expressed as:

$$T_{gw} = (0.005 \cdot M^2 - 0.1 \cdot M + 1.0) \cdot T_{gd} \quad (3.47)$$

where:

M = moisture in the adhesive in percent by weight; T_{gd} = adhesive dry glass transition temperature, usually provided by the adhesive supplier; T = the temperature of the joint at service conditions; T_0 = the reference temperature at which σ_{a0} was determined, usually taken as room temperature; N = the number of cycles which the joint must endure under the design stress.

5. Select the design allowables (that are either set by the design criteria or are chosen). A safety factor of 1.5 of the degraded adhesive strength σ_a is recommended.
6. The length of the joint is calculated as following:

$$L = \frac{P}{\sigma_{as}} \quad (3.48)$$

where:

P = tensile/compressive/shear load per unit width; σ_{as} = design allowable shear stress in the adhesive;

7. Check the minimum length and the maximum shear and normal stresses in the adhesive (using the shear-lag theory equations).
8. Calculate the margin of safety (MOS) for all calculated stresses.

$$MOS = \frac{AllowableStress}{CalculatedStress} - 1$$

9. Calculate the joint efficiency.

$$JE = \frac{JointForceTransferredP}{AdherendFractureLoad(\sigma_1 t_1)} \cdot 100$$

The authors recommend that the preliminary design must be backed up by a finite element analysis and by carefully selected experiments. In the case of composite adherends two other important conclusions are drawn:

- The joints with induced bending should be avoided (inefficient with respect to load transfer).
- The environmental and cyclic load effects degrade the joint substantially, resulting in joint lengths several times those without these effects.

3.1.9 Failure Criteria

3.1.9.1 Adhesive Failure

The failure criterion of the adhesive can be expressed as a single characteristic value like $\tau_{max} \leq \tau_{allow}$ for shear, $\sigma_{max} \leq \sigma_{allow}$ for peel or/and $\gamma \leq \gamma_{allow}$ for strain (specially for flexible adhesives).

The test program of full scale joints can provide three variants of failure criteria [32]: $\gamma_{fc}/\gamma_m > \gamma_{max}$ (shear strain), $\tau_{fc}/\gamma_m > \tau_{max}$ (shear stress), $P_{fc}/\gamma_m > P_{max}$ (fracture load), where fc index is the characteristic value measured at fracture. γ_m is the overall safety factor (from eq. 3.49) and is recommended to be considered as a product of four partial safety factors [7] (its maximum value is 6.75).

$$\gamma_m = \gamma_{m1} \cdot \gamma_{m2} \cdot \gamma_{m3} \cdot \gamma_{m4} \quad (3.49)$$

Some proposed values for the partial safety factors are presented in Table 3.1 [7]:

Source of Adhesive Properties γ_{m1}	
Typical or textbook values	1.5
Values obtained by testing	1.25
Method of Adhesive application γ_{m2}	
Manual application, no adhesive thickness control	1.5
Manual application, adhesive thickness control	1.25
Established procedure with controlled parameters	1.0
Type of Loading γ_{m3}	
Long term loading	1.5
Short term loading	1.0
Environmental Conditions γ_{m4}	
Service conditions outside the adhesive test conditions	2.0
Adhesive properties determined for service conditions	1.0

Table 3.1: Partial Safety Factors for Adhesively Bonded Joints [7].

Alternatively, one needs to avoid any yielding of the adhesive, specially for some rigid adhesives that shows a relatively brittle nature. In this case, a failure criterion based on the yield stress is applicable and von Mises criterion is usually preferred. Although von Mises criterion is based on all stress components, a simplified version of it (3.50) can be applied, keeping in mind that the single-lap joint is dominated, in critical parts, by the peel and the shear stresses.

$$\sigma_{vonMises} = \sqrt{(\sigma_{peel})^2 + 3\tau^2} \quad (3.50)$$

This criterion is readily implemented in the finite element codes available on the market.

A more accurate criterion for polymeric adhesives was introduced by Raghava et.al. (eq. 3.51), but is usually left to be implemented by the user in the FE software code (where this option is available).

$$\sigma_V = \frac{(R - 1) + \sqrt{(R - 1)^2 + 4R(\sigma^2 + 3\tau^2)}}{2R} \quad (3.51)$$

where:

$$R = \frac{\sigma_{compression}^{yield}}{\sigma_{tension}^{yield}}$$

σ_V is the equivalent stress;

σ is the sum of the maximum applied normal stresses;

τ is the sum of the maximum applied shear stresses;

3.1.9.2 Adherend Failure

For adherends, a failure criterion will also depend on the nature of materials and usually the strength of the substrates are much higher than the adhesive strength. Where for metals von Mises criterion is an obvious choice, for composite adherends there are maybe tens of failure criteria. Failure can occur, for example, due to peel stresses at the edge of the overlap. These can lead to delamination of the adherend, hence an interlaminar failure criterion is needed. Tsai criterion takes into account shear and longitudinal stresses and is given by eq. 3.52:

$$\frac{\sigma_x^2 - \sigma_x \sigma_z}{X^2} + \frac{\sigma_z^2}{Z^2} + \frac{\tau_{xz}^2}{R^2} = 1 \quad (3.52)$$

where

X is the ultimate tensile strength, σ_x is the longitudinal stress in the top ply, σ_z is the peel stress in the top ply, τ_{xz} is the shear stress in the top ply, Z

is the interlaminar tensile strength and R is the through-the-thickness shear strength.

3.1.10 Summary of analytical models

A significant amount of research regarding the single lap joint has been accumulated over the years, each model with its different simplifications and assumptions. In summary, the designer of this type of joint has to choose between the following:

1. At a preliminary stage, the Wiedemann model can be used to determine the minimum length of the joint, and to ensure that the tensile stress in the adhesive is less than its ultimate strength.
2. Where moisture, temperature or cyclic loads are to be expected, the designer can follow the Chamis-Murthy model, degrading the adhesive properties accordingly.
3. A more comprehensive analysis would follow, using either Volkersen, Goland and Reissner, Cooper and Sawyer, Bigwood and Crocombe or L.J.Hart-Smith models, checking if the range of validity of each solution is fulfilled.
4. A suitable failure criterion is to be chosen and a suitable safety factor has to be calculated or chosen.

In order to have a meaningful comparison, the following have been considered as a benchmark for single-lap joints:

1. For adherends, marine grade Aluminium - 5083-H32 with the properties described at section 2.13.6 and EU460/Vinyl ester with the properties described at section 2.13.2 have been considered as a substrate. The aluminium specimen has a thickness of 3mm.

2. The adhesive chosen (Plexus MA550) has the shear modulus $G_a = 106$ N/sqmm, and the thickness $t_a = 0.5$ mm.
3. The overlap length of the single lap joint was chosen as $L = 12$ mm and $L = 50$ mm, with the width of $w = 25$ mm, and the applied force $T = 25$ N. For Cooper and Sawyer Model, the value for adherend length 'l' is 63mm and 25mm respectively, corresponding with the value 'L'. The joint represents a typical specimen used in ASTM D1002 standard test (see Fig. 3.22).

A table with the maximum shear stresses for each theoretical model and combination of adherends have been compiled and presented in Table 3.2 and Table 3.3. The values obtained (in MN/m^2) are then compared with Volkersen results for the respective case. Where [N/A] was used, it means that the results are outside the range of validity or dissimilar materials cannot be analyzed with this model. The following abbreviations have been used: Volk = Volkersen, GoRe = Goland/Reissner, CoSa = Cooper/Sawyer, LJHS = L.J. Hart-Smith. Bigwood and Crocombe model cannot be applied for these configurations.

Adherends	Average	Volk	GoRe	CoSa	LJHS
Al-Al	0.083333	0.085374	0.091234	0.090708	0.091450
Al-Al	-2.4%	-	+6.7%	+6.2%	+7.1%
Al-Comp	0.083333	0.089	[N/A]	[N/A]	0.118010
Al-Comp	-6.4%	-	[N/A]	[N/A]	+32.6%
Comp-Comp	0.083333	0.092564	[N/A]	0.115092	0.118010
Comp-Comp	-10.0%	-	[N/A]	+24.3%	+27.5%

Table 3.2: Maximum shear stress for benchmark cases using overlap length of 12mm.

A graph comparing the distribution of the shear stress along the bond line is presented in Fig. 3.13 and 3.14.

Adherends	Average	Volk	GoRe	CoSa	LJHS
Al-Al	0.02	0.027894	0.044434	0.035865	0.046096
Al-Al	-28.3%	-	+59.3%	+28.6%	+65.3%
Al-Comp	0.02	0.039648	[N/A]	[N/A]	0.094233
Al-Comp	-49.6%	-	[N/A]	[N/A]	+137.7%
Comp-Comp	0.02	0.049334	[N/A]	0.066573	0.094233
Comp-Comp	-59.5%	-	[N/A]	+34.9%	+91.0%

Table 3.3: Maximum shear stress for benchmark cases using overlap length of 50mm.

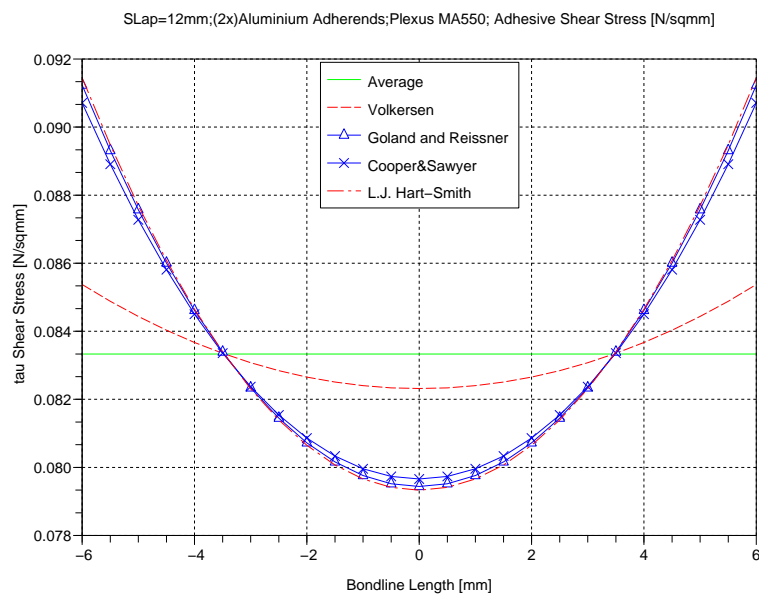


Figure 3.13: Shear Stress Distribution 12mm overlap.

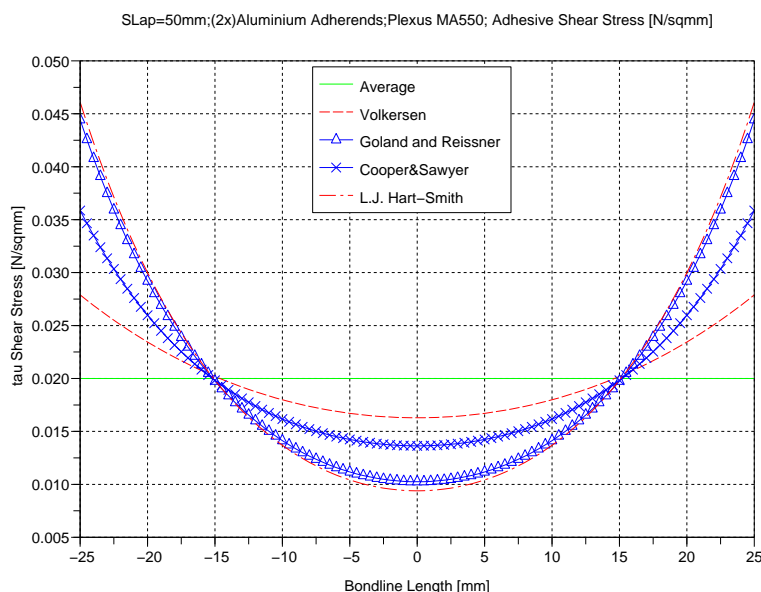


Figure 3.14: Shear Stress Distribution 50mm overlap.

3.2 Finite Element Analysis

For detailed analysis of complex geometries, the Finite Element Method (FE) has become the method of choice. Nowadays a personal computer is powerful enough to carry out the calculations required by the method. The commercial FE programs are usually cheap enough to be afforded by a small to mid size boatbuilding yard or by a design office. The open-source FE programs equivalents are available and are making ground. Many of these programs can handle both elastic and elastic-plastic models, several of them have coded in creep or fatigue capabilities. For this thesis, only the FE elastic model has been considered.

The greatest problem in the FE method analysis is the interpretation of the results. Again, the adhesive layer thickness to adherend size ratio is the culprit as will be shown below. Also, a number of unknowns related to the components for which the model is created influence the results of the analysis. For example, for adhesives, manufacturers' data sheets usually offer only rudimentary information and much of these represents the bulk data of the adhesive not the joint properties. Further, the materials used are highly sensitive

to the cure conditions, moisture or temperature. The geometry of the joint can vary due to the manufacturing tolerances (the thickness of the bonding layer and the spew dimensions are usually not easy to control). Also, the joints can be incompletely filled with adhesive or the adhesive contains voids from the cure process.

In these conditions, the designer of the joint (or the boatbuilder for this matter) has the option to build a database of successful models, compare them with the analytical models available and apply sensible safety factors.

3.2.1 FE Models

Four 2D and 3D types of models have been analysed and compared with the analytical models. All models represent a simplified model of the single lap joint without taking into consideration the end effects (spew or changes in the ends geometry), with aluminium adherends and Plexus MA550 adhesive with the same characteristics as the benchmark specimens from section 3.1.10. The level of mesh refinement required is also investigated.

The commercial software package MSC Nastran for Windows 4.0, with FEMAP 6.0 as IDE, has been used for this analysis.

The four models considered are [9]:

1. Model A: A mixed elements 1D and 2D configuration where the adherends are represented as beam elements and the adhesive is a plane element.
2. Model B: A mixed elements 1D and 2D configuration where the adherends are represented as beam elements and rigid elements, and the adhesive is a plane element.
3. Model C: A 2D configuration where the adherents and the adhesive are represented as plane elements.
4. Model D: A 3D configuration where the adherents and the adhesive are represented as 3D brick elements.

Several other models can be imagined for different applications. One can use 2D plate elements (plane strain, axisymmetric etc), for example modelling the sails and the bond between different panels. In this case the joint can be represented as two shell plates with a local thickening and an offset. In any of these cases, the results from the model has to be compared with results from known and detailed FE of the entire model and tests.

3.2.2 FE Model A

A mixed elements (1D and 2D) configuration has been tested, the geometry is shown in Fig. 3.15. The adherends are represented as 1D beam elements and are drawn as passing through the axis of the adherends. The adhesive is represented as 2D plane elements and, in order to compensate for the lack of thickness of the adherends, the actual thickness is increased with $(t_1 + t_2) / 2 = 3mm$ for a total of 3.5mm.

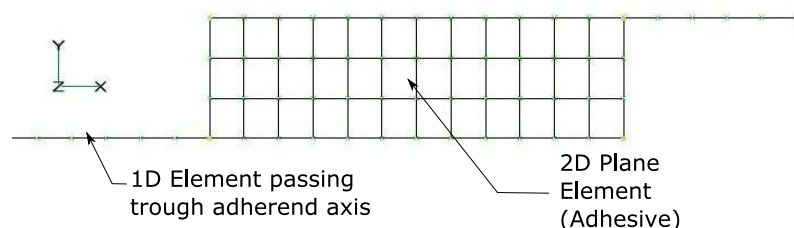


Figure 3.15: FE Model A - a mix between 1D elements (beam) and 2D elements (plane).

In order to compensate for the change in thickness, the G_a modulus of the adhesive has been proportionally increased $G'_a = G_a * ta'/ta$. The mesh size was 1.0, resulting in 12 elements along the interface. The maximum shear stress obtained in the adhesive layer is $0.11764MN/m^2$ (a nodal/corner un-averaged value) which represents +37.8% compared with Volkersen predicted value. An average value (at the centroid of the element) of the same element gives $0.087727MN/m^2$ shear stress, which represents +2.8% compared with the Volkersen analysis.

The main disadvantage of using this model is the fact that one has to change the properties of the material that represents the adhesive, which could be undesirable for other more complicated geometries and loading cases. One way to deal with this change in thickness would be to represent the 1D beam elements as being drawn passing through the top and bottom surfaces of the two adherends. The cross section of the beam would have to be offset accordingly.

3.2.3 FE Model B

A similar mixed elements (1D and 2D) configuration has been tested in the Model B, where the geometry is shown in Fig. 3.16. Like in model A, the adherends are represented as beam elements that pass through the axis of the adherends and the adhesive is represented as a plane element. In this case, in order to account for the thickness of the adherend, rigid elements have been used with the length equal to half thickness of the adherend $t_1/2$ and $t_2/2$.

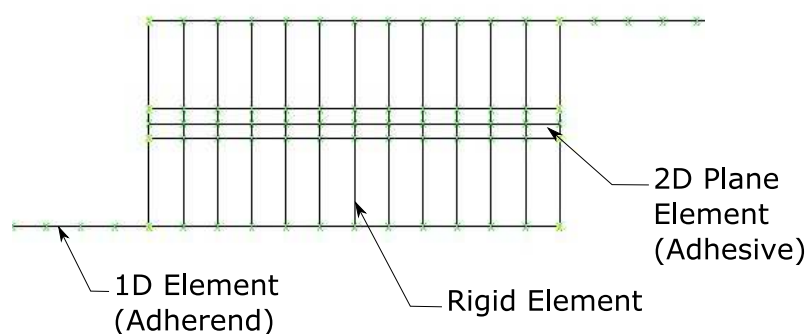


Figure 3.16: FE Model B - a mix between 1D elements (beam) and 2D elements (plane) using rigid elements to compensate for thickness.

The mesh size was 1.0, resulting in 12 elements along the interface. The maximum shear stress obtained in the adhesive layer is $0.098096 MN/m^2$ (a nodal/corner true value - not averaged) which represents +14.9% compared with Volkersen predicted value. An average value (at the centroid of the element) of the same element gives $0.093358 MN/m^2$ shear stress, which represents +9.4% compared with the Volkersen analysis.

The main disadvantage of using this model is the fact that one has to generate the rigid elements by hand (unless the process is automatized), which is undesirable for more complicated geometries.

Both Model A and Model B results show a fairly good correlation with the theory.

3.2.4 FE Model C

Model C is a 2D configuration where the adherends and the adhesive are represented as plane elements, its geometry is shown in Fig. 3.17. This model represents the most popular configuration used for the study of single lap joints, it appears in various shapes in industrial applications and is adopted as a reference and benchmark by the researchers.

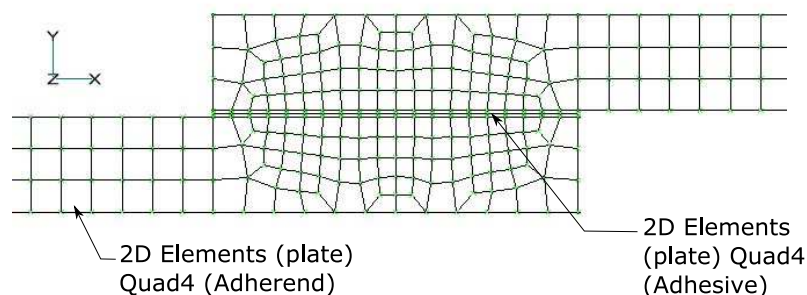


Figure 3.17: Model C: 2D plane elements have been used to represent the adhesive and the adherends

In order to analyse the influence of the mesh density, a parametric model has been created using FEMAP Basic Scripting Language (which provides an easy access to FEMAP Database Engine [13]). The program is easy to understand by an average user who has minimum knowledge of programming and can be modified and extended as desired.

Varying the parameters that define the mesh density, a picture of the stresses involved in the joint can be drawn. The difficulty here consists in the interpretation of the results because of the existence of the singularity points in the positions A, B, C, D as seen in Fig. 3.18. These singularities are

due to the presence of sharp corners at the end of the adhesive layer,.

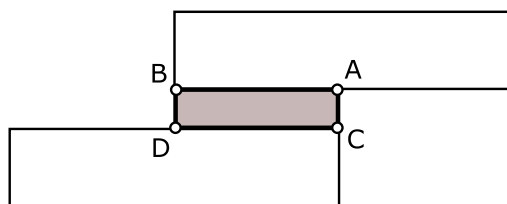


Figure 3.18: Single-Lap Singularities Points.

It can be seen (Fig. 3.19), that when the mesh density in that area is increased, it increases the value of the stresses in the adhesive. One way to deal with this problem is to consider stresses in the centre-line of the bondline. In this condition one has to consider the stresses obtained more like as average stresses (specially for a very thin layer). Suitable safety factors have to be used.

Another way to approach the problem, is to consider that the maximum stresses appear at a predetermined number of nodes away from the edge of the joint. This method is obviously dependent on the mesh density in that area.

BONDSHIP [32] generalized the idea and advice that the maximum stress is to be measured at a point at a distance t_a from the edge of the adhesive layer and at a height $t_a/10$ from the adherend, where t_a is the adhesive thickness.

Using Aluminium 5083-H32 adherends and Plexus MA550 adhesive, having the geometry and load conditions described in chapter 3.1.10, Goland and Reissner analysis give a maximum shear stress of $0.091234MN/m^2$, Hart-Smith elastic analysis give a maximum shear stress of $0.091450MN/m^2$. Maximum shear stress obtained by FE is plotted in Fig. 3.19 against the mesh density at the interface between the adherend and the adhesive. One curve represents an average value of the shear stress (close to the centroid of the element adjacent to points A and D), the other is a corner value obtained in A and D points. For this exercise, the interface lines were split equally into elements, the other mesh size parameters have been adapted each time in order to ensure a good element aspect ratio (which explains the sudden jump around the value of

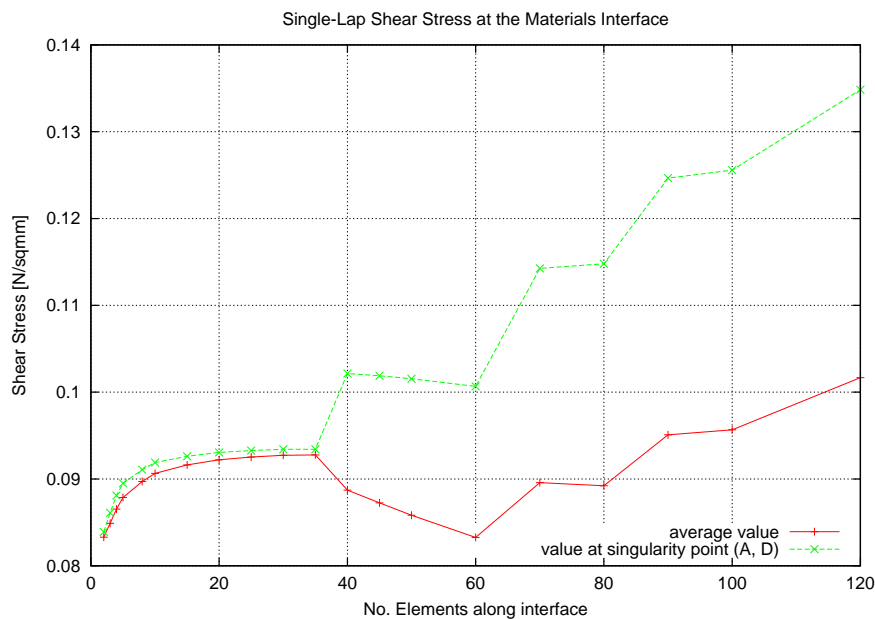


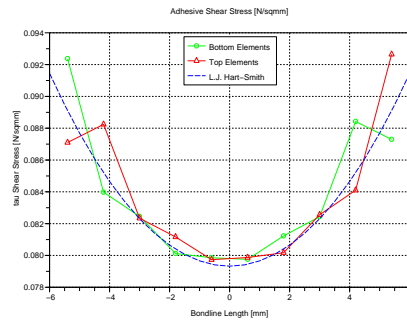
Figure 3.19: Single-Lap Maximum Shear Stress function of Mesh Density along interface between adherend and adhesive.

40 elements/12mm overlap - approximative 0.3mm/element width at 0.5 ratio when some elements were badly deformed and a redistribution of elements was need it). It can be seen that the corner values of the shear stress tend to grow with the number of elements.

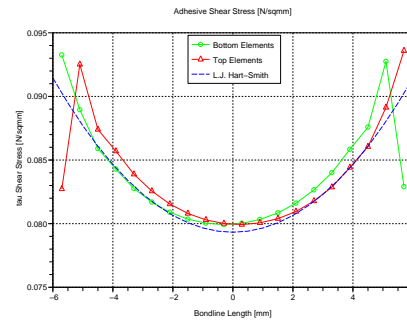
In the next step, for comparison, several models (with identical characteristics as above) have been analysed varying the number of elements generated along the interface (vertical division has been maintained to 2). The FE elements used to describe the adhesive are QUAD4, a four-nodes quadrilateral element. Each time a graph have been generated showing the through-thickness shear stress distribution compared with the shear stress obtained using L.J.Hart-Smith analysis (see Fig. 3.20).

It can be seen that the through-thickness distribution of the shear stresses obtained using finite element method is close to the distribution obtained using L.J. Hart-Smith analysis.

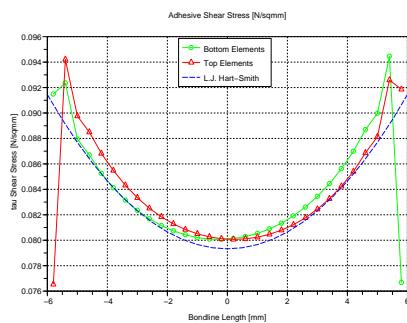
These examples show the importance of having a parametric benchmark model before deciding to use the FE analysis to represent the joint. Using this benchmark a similar level of discretization has to be applied to the final



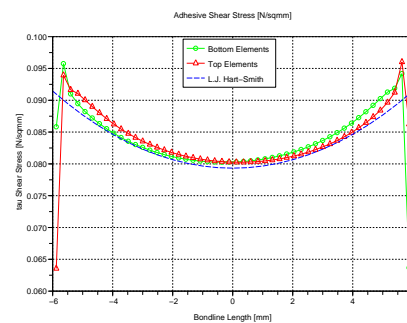
(a) 10x2 elements



(b) 20x2 elements



(c) 30x2 elements



(d) 50x2 elements

Figure 3.20: Through-thickness distribution of the shear stress.

model.

3.2.5 FE Model D

Model D is a 3D configuration where the adherends and the adhesive are represented as 3D brick elements (Brick8 a eight-nodes brick - hexahedron), the model is shown in Fig. 3.21.

The maximum shear stress obtained in the adhesive layer is $0.089436 MN/m^2$ (a nodal/corner true value - not averaged) which represents +4.8% compared with Volkersen predicted value. An average value (at the centroid) of the same element gives $0.088745 MN/m^2$ shear stress, which represents +3.9% compared with Volkersen analysis.

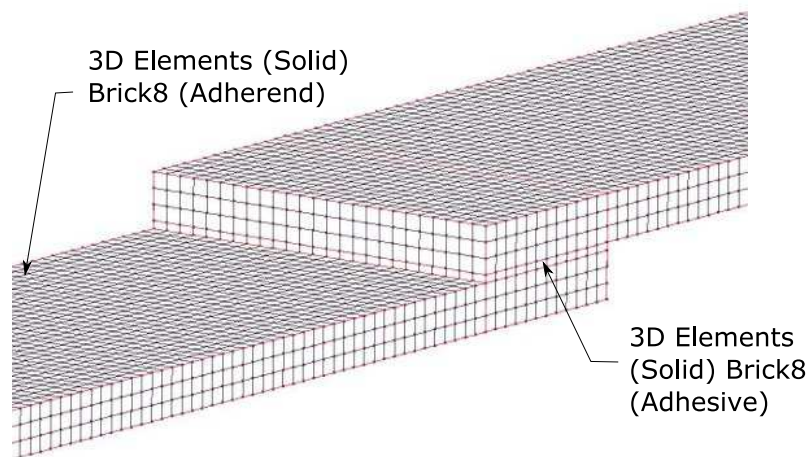


Figure 3.21: Model D: a 3D elements (bricks) are used to represent both the adherend and the adhesive.

3.3 FE Analysis Summary

All four models show a fairly good correlation with the analytical methods. In all cases, the maximum shear stress was obtained at the singularity points, the biggest value has been recorded in the model A, possibly due to the flexibility of the beam element representing the adherend. A closer result with the analytical models has been found by taking an average value of the corners of the element adjacent with the singularity point.

3.4 Single Lap Tests

Before an adhesive is used in a structure, especially where the bond failure can have important consequences, a detailed analysis needs to be conducted.

Experimental verification of the theories presented in the previous chapters is very difficult mainly because of the adhesive layer dimensions. Between the experimental stress tests available today (strain measurement with strain gauges, photo elastic methods [10] etc.), Moiré interferometry seems to be the one which can get the closest results to reality but its accuracy remains unclear.

In order to evaluate the adhesives presented in chapter 2.13.5 and 2.13.4

several samples have been prepared according to ASTM D1002 - *Standard Test Method for Apparent Shear Strength of Single-Lap-Joint Adhesively Bonded Metal Specimens by Tension Loading (Metal-to-Metal)*. Although the standard is based on for metal-to-metal joints, it can be used for composite materials or combinations also. This standard has its advantages, the specimen are economical, practical, and easy to make; the machine used for testing can be a standard tensile testing machine. This is the most widely used test for development and comparative studies involving adhesives and bonded joints, including manufacturing quality control. The main disadvantage is that the reported shear stress is not an intrinsic adhesive property and should not be used as a design-allowable stress. Other test methods have been developed in order to get more accurate estimates of the true shear strength of adhesives, but lack the simplicity of ASTM D1002. A discussion about the terms and results from ASTM D1002 tests is presented in ASTM D4896 standard - *Standard Guide of Adhesive-Bonded Single Lap-Joint Specimen Test Results*.

Three types of samples were built representing the three combinations of materials proposed for examination, aluminium-aluminium, aluminium-FRP and FRP-FRP. The tests involving composite materials and Sikaflex have been omitted due to the absence of a proper primer for the adherend (Sika Group - the adhesive manufacturer - strongly advice using adequate primer and solvent).

Although the standard recommends that at least 30 specimen shall be tested representing at least four different joints, only three samples were made using the three adhesives previously mentioned Plexus MA550, Sikaflex 252 and the in-house made vinyl ester based adhesive. This can be considered as a preliminary procedure conducted in order to rank the adhesives and to check the treatments given to the surfaces of the adherends. The standard dimensions for ASTM D1002 samples are presented in Fig. 3.22.

The adherends' dimensions were kept constant (3mm thickness for aluminium and 3.2mm for composites); shims of 0.5mm thickness have been used

the two parts of the joint (using the shims to control the layer thickness), the edges of the adhesive layer were cleaned of any spew. This configuration can be considered as the lowest common denominator of all single-lap joints and is intended to be used as a benchmark. Spew is usually unavoidable and it will increase the strength of the joint, but its geometry is not easy to control. The adhesive was left to cure for more than a week before tests.

3.4.0.1 Single Lap with Aluminium Adherends

Plexus MA550 Adhesive.

The results of the ASTM D1002 test using aluminium adherends are presented in Fig. 3.23 and summarized in the Table 3.4. The strain recorded is the shear strain where the apparent shear stress is at a maximum, 'C' represents the encountered mode of failure (cohesive failure in this case, which was seen for all specimen - see Fig. 2.2 /c). Average values obtained are: maximum apparent shear stress $\tau_{D1002} = 11.77MN/m^2$, maximum strain $\epsilon_{D1002} = 2.47$.

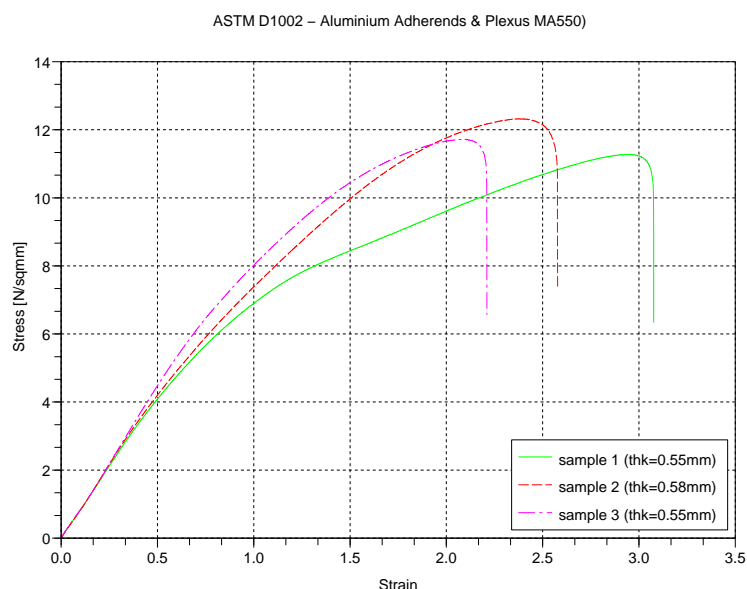


Figure 3.23: ASTM D1002 - Single lap joint test of aluminium adherends and Plexus MA550 adhesive.

Sikaflex 252 Adhesive.

In this case, the adherends were prepared according with adhesive's manu-

Sample	Adhesive Thk. [mm]	Max. apparent shear stress [MN/m^2]	Strain at max. stress [–]	Failure Mode
A1	0.55	11.28	2.94	C
A2	0.58	12.32	2.37	C
A3	0.55	11.72	2.09	C

Table 3.4: ASTM D1002 - Test results of aluminium adherends and Plexus MA550 adhesive.

facturer advice: after abrasion, the surface was clean using SIKA Cleaner 205, then SIKA Primer 210 was applied. The samples were left to cure for more than 7 days. The results of the ASTM D1002 test are presented in the graphs in Fig. 3.24 and summarized in the Table 3.5. Failure occurred through cohesive failure. Average values obtained are: maximum apparent shear stress $\tau_{D1002} = 1.01MN/m^2$, maximum strain $\epsilon_{D1002} = 4.54$.

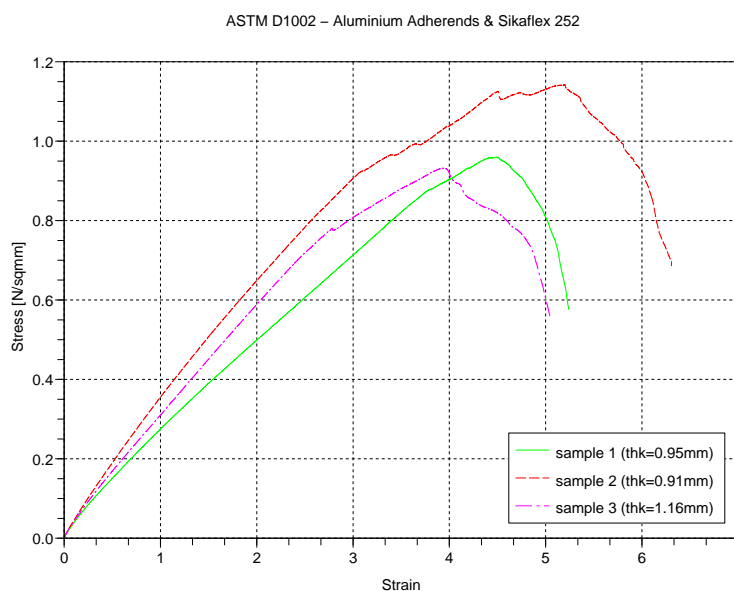


Figure 3.24: ASTM D1002 - Single lap joint test of aluminium adherends and Sikaflex 252 adhesive.

Vinyl ester/Epiglass HT120 Mix Adhesive

The results of the ASTM D1002 test are presented in the graphs in Fig.

Sample	Adhesive Thk. [mm]	Max. apparent shear stress [MN/m^2]	Strain at max. stress [-]	Failure Mode
SIKA1	0.95	0.96	4.50	C
SIKA2	0.91	1.14	5.19	C
SIKA3	1.16	0.93	3.94	C

Table 3.5: ASTM D1002 - Test results of aluminium adherends and Sikaflex 252 adhesive.

3.25 and summarized in the Table 3.6. Failure occurred through adhesive failure, all specimen failed at the interface with aluminium adherends - see Fig. 2.2 /e). Average values obtained are: for maximum apparent shear stress $\tau_{D1002} = 4.35 MN/m^2$, maximum strain $\epsilon_{D1002} = 0.33$.

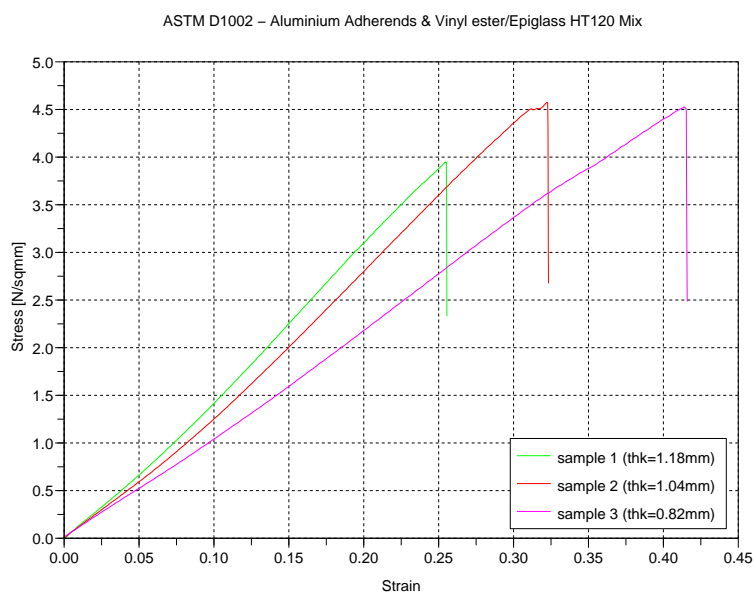


Figure 3.25: ASTM D1002 - Single lap joint test of aluminium adherends and vinyl ester/Epiglass HT120 mix adhesive.

Using aluminium substrates, in average, the best result in strength is obtained using Plexus MA550 followed by the Vinyl ester/Epiglass mixture, where the Sikaflex is the most flexible adhesive, but the weakest in strength.

Sample	Adhesive Thk. [mm]	Max. apparent shear stress [MN/m^2]	Strain at max. stress [-]	Failure Mode
V1	1.18	3.95	0.25	A
V2	1.04	4.57	0.32	A
V3	0.82	4.52	0.41	A

Table 3.6: ASTM D1002 - Test results of aluminium adherends and vinyl ester/Epiglass HT120 mix adhesive.

3.4.0.2 Single Lap Joint with Composite Adherends

Plexus MA550 Adhesive.

The results of the ASTM D1002 test are presented in the graphs in Fig. 3.26 and summarized in Table 3.7. Failure occurred through adhesive failure (see Fig. 2.2 /e). Average values obtained are: maximum apparent shear stress $\tau_{D1002} = 11.22MN/m^2$, maximum strain $\epsilon_{D1002} = 3.05$.

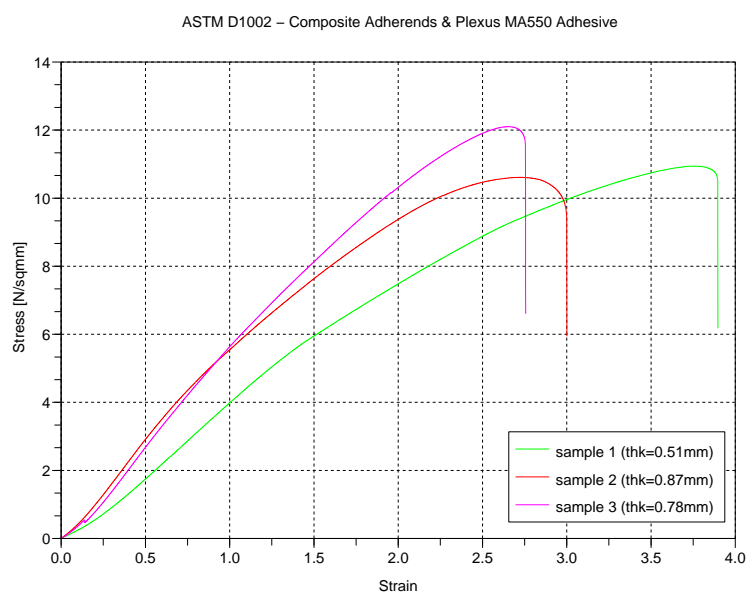


Figure 3.26: ASTM D1002 - Single lap joint test of composite adherends and Plexus MA550 adhesive.

Vinyl ester/Epiglass HT120 Mix Adhesive

Only 2 specimens were tested this time; the results are presented in the

Sample	Adhesive Thk. [mm]	Max. apparent shear stress [MN/m^2]	Strain at max. stress [-]	Failure Mode
C1	0.51	10.94	3.76	A
C2	0.87	10.61	2.72	A
C3	0.78	12.10	2.66	A

Table 3.7: ASTM D1002 - Test results of composite adherends and Plexus MA550 adhesive.

graphs in Fig. 3.27 and summarized in Table 3.8. Failure occurred through composite interlaminar failure (see Fig. 2.2 /b). Average values obtained are: for maximum apparent shear stress $\tau_{D1002} = 10.88MN/m^2$, maximum strain $\epsilon_{D1002} = 1.44$.

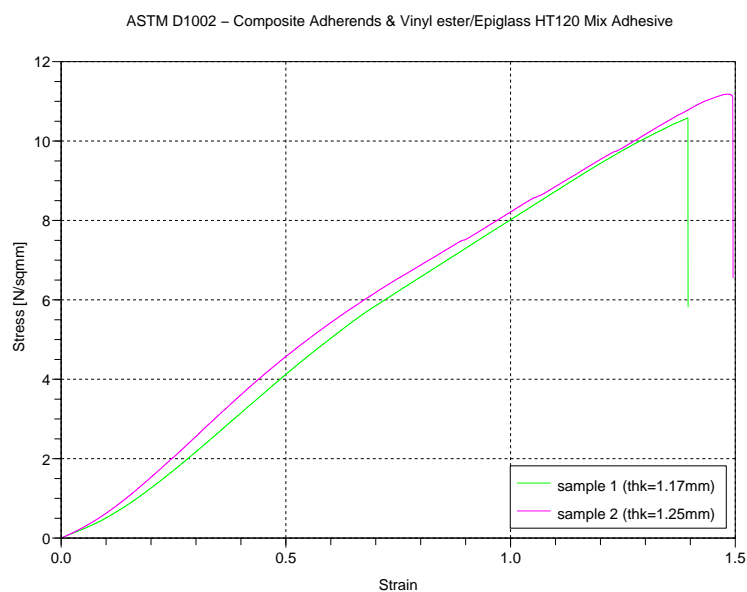


Figure 3.27: ASTM D1002 - Single lap joint test of composite adherends and vinyl ester/Epiglass HT120 mix adhesive.

Using only composite adherends, in average, Plexus MA550 is the strongest adhesive but very closely followed by the mixture and with Plexus MA550 being more flexible than the mix.

Sample	Adhesive Thk. [mm]	Max. apparent shear stress [MN/m^2]	Strain at max. stress [–]	Failure Mode
Vc1	1.17	10.50	1.39	I
Vc2	1.25	11.18	1.48	I

Table 3.8: ASTM D1002 - Test results of composite adherends and vinyl ester/Epiglass HT120 mix adhesive.

3.4.0.3 Single Lap Joint with Hybrid (Aluminium and Composite) Adherends

Plexus MA550 Adhesive.

The results of the ASTM D1002 test are presented in Fig. 3.28 and summarized in Table 3.9. Failure occurred through adhesive failure (see Fig. 2.2 /e). Average values obtained are: maximum apparent shear stress $\tau_{D1002} = 8.66MN/m^2$, maximum strain $\epsilon_{D1002} = 1.42$.

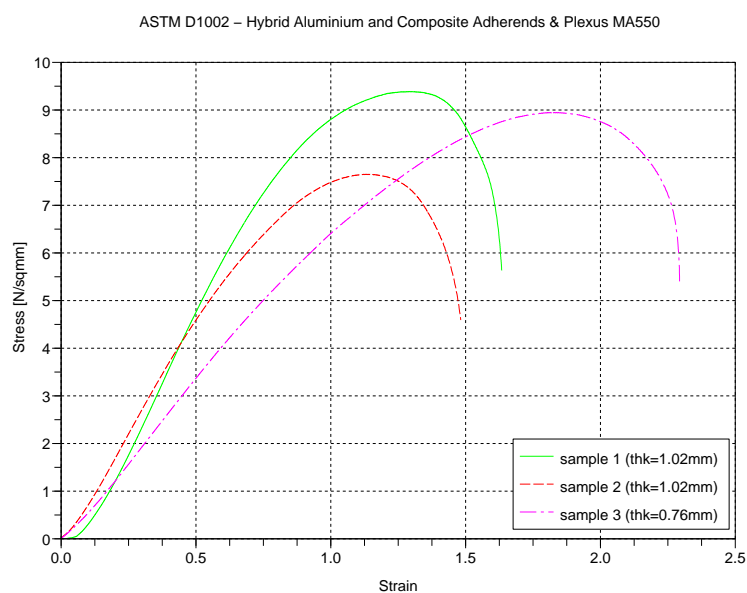


Figure 3.28: ASTM D1002 - Single lap joint test of hybrid (aluminium and composite) adherends and Plexus MA550 adhesive.

Vinyl ester/Epiglass HT120 Mix Adhesive

The results of the ASTM D1002 test the results are presented in Fig. 3.29

Sample	Adhesive Thk. [mm]	Max. apparent shear stress [MN/m^2]	Strain at max. stress [-]	Failure Mode
AC1	1.02	9.39	1.30	A
AC2	1.02	7.65	1.13	A
AC3	0.76	8.95	1.83	A

Table 3.9: ASTM D1002 - Test results of hybrid aluminium and composite adherends and Plexus MA550 adhesive.

and summarized in the Table 3.10. Failure occurred through composite interlaminar failure (see Fig. 2.2 /b). Average values obtained are: maximum apparent shear stress $\tau_{D1002} = 3.95 MN/m^2$, maximum strain $\epsilon_{D1002} = 0.42$.

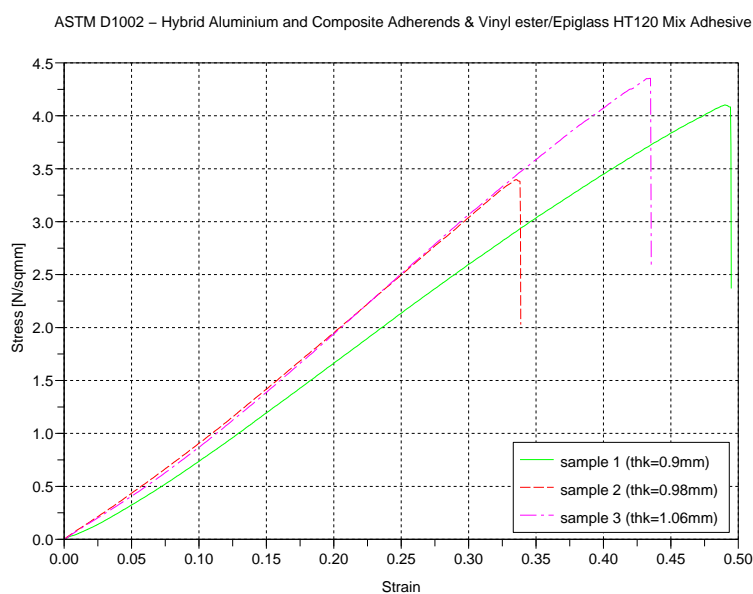


Figure 3.29: ASTM D1002 - Single lap joint test of hybrid (aluminium and composite) adherends and vinyl ester/Epiglass HT120 mix adhesive.

Using both aluminium and composite adherends (a hybrid joint), in average, Plexus MA550 is by far the strongest and most flexible adhesive.

Sample	Adhesive Thk. [mm]	Max. apparent shear stress [MN/m^2]	Strain at max. stress [–]	Failure Mode
ACV1	0.90	4.10	0.49	I
ACV2	0.98	3.40	0.34	I
ACV3	1.06	4.35	0.43	I

Table 3.10: ASTM D1002 - Test results of hybrid (aluminium and composite) adherends and vinyl ester/Epiglass HT120 mix adhesive.

3.4.0.4 Single Lap Joint with Composite Adherends and Carrier Fabric

Vinyl ester and EU460 as Carrier Fabric

The results of the ASTM D1002 test the results are presented in the graphs in Fig. 3.30 and summarized in Table 3.11. Failure occurred through composite interlaminar failure (see Fig. 2.2 /b). Average values obtained are: maximum apparent shear stress $\tau_{D1002} = 14.05 MN/m^2$, maximum strain $\epsilon_{D1002} = 3.01$.

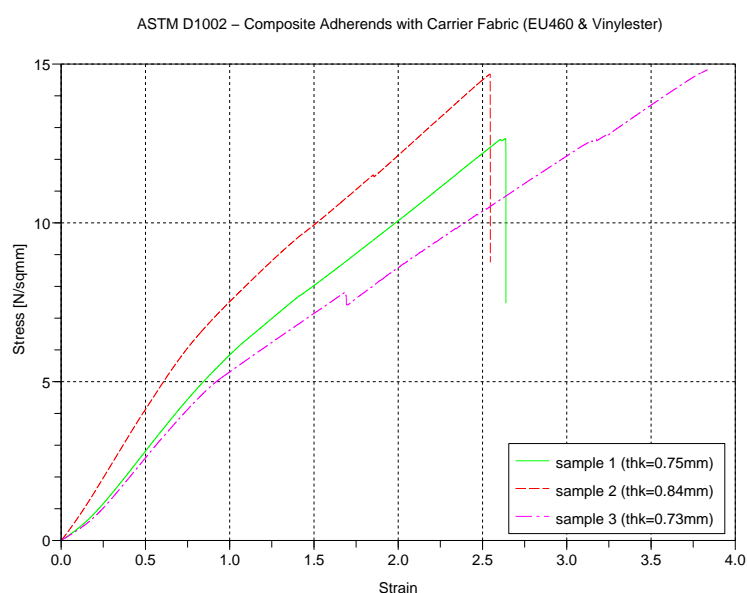


Figure 3.30: ASTM D1002 - Single lap joint test of composite adherends and vinyl ester/EU460 as carrier fabric.

Sample	Adhesive Thk. [mm]	Max. apparent shear stress [MN/m ²]	Strain at max. stress [-]	Failure Mode
CCLA1	0.75	12.66	2.64	A
CCLA2	0.84	14.68	2.54	A
CCLA3	0.73	14.82	3.84	A

Table 3.11: ASTM D1002 - Test results of composite adherends and vinyl ester/EU460 as carrier fabric.

Unfortunately, the load applied to last specimen exceeded the maximum allowable for the load cell used (5KN), so the test has been automatically stopped. In the average figures calculated, the last reading has been considered. A fair amount of bending of the adherends have been noted during the tests (more that in any other single lap joints).

3.4.0.5 Single Lap Joint with Hybrid (Composite and Aluminium) Adherends and Carrier Fabric

Vinyl ester and EU460 as Carrier Fabric

The aluminium specimen was treated differently this time: the adhesion area was isolated with tape, a layer of vinyl ester was applied onto marked area and the abrasion of the substrate was done through this wet layer. A similar solution was used successfully for the beam (aluminium) to hull's bulk-head (composite) join of the 63 feet VSD racing catamaran designed by Derek Kelsall - the wet layer used then was polyester resin. The results of the ASTM D1002 test the results are presented in the graphs in Fig. 3.31 and summarized in Table 3.12. Failure occurred through adhesive failure along the aluminium specimen's interface (see Fig. 2.2 /e). Average values obtained are: maximum apparent shear stress $\tau_{D1002} = 5.72MN/m^2$, maximum strain $\epsilon_{D1002} = 0.95$.

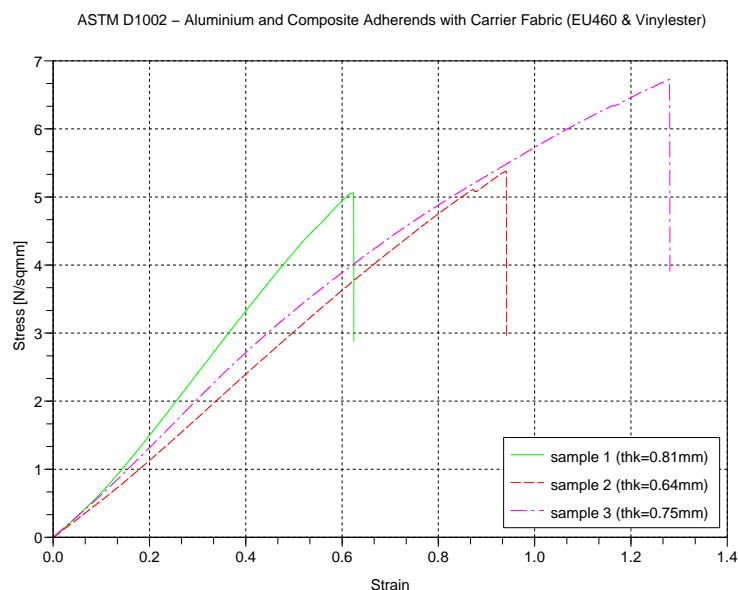


Figure 3.31: ASTM D1002 - Single lap joint test of hybrid (aluminium and composite) adherends and vinyl ester/EU460 as carrier fabric.

3.5 Summary of single lap tests (ASTM D1002)

Although a direct comparison between the adhesive systems presented cannot be made (for the reasons already presented), a summary of average values of maximum apparent shear stresses are presented in the Table 3.13. A discussion regarding these results is presented in Chapter 5 of the thesis. All values in Table 3.13 are given in $[MN/m^2]$, in parenthesis are given the mode of failure of the samples.

Sample	Adhesive Thk. [mm]	Max. apparent shear stress $[MN/m^2]$	Strain at max. stress [-]	Failure Mode
ACLA1	0.81	5.06	0.62	A
ACLA2	0.64	5.38	0.94	A
ACLA3	0.75	6.73	1.28	A

Table 3.12: ASTM D1002 - Test results of hybrid (aluminium and composite) adherends and vinyl ester/EU460 as carrier fabric.

Adhesive	Substrate	Aluminium	Composite
Plexus MA550	Aluminium	11.77(<i>C</i>)	8.66(<i>A</i>)
	Composite	8.66(<i>A</i>)	11.22(<i>A</i>)
Sikaflex 252	Aluminium	1.01(<i>C</i>)	[<i>N/A</i>]
	Composite	[<i>N/A</i>]	[<i>N/A</i>]
Vinyl ester/filler mixture	Aluminium	4.35(<i>A</i>)	3.95(<i>I</i>)
	Composite	3.95(<i>I</i>)	10.88(<i>I</i>)
Vinyl ester/filler mixture and carrier fabric	Aluminium	[<i>N/A</i>]	5.72(<i>A</i>)
	Composite	5.72(<i>A</i>)	14.05(<i>A</i>)*

Table 3.13: ASTM D1002 - Summary of Results.

Note: * the figure represents the last reading, load applied exceeded the maximum allowable for the load cell used.

3.6 Computer Code

The analytical models presented in this chapter have been implemented in Scilab [1] (an open-source scientific software package for numerical computations similar with Matlab) and attached in Appendix A.

Chapter 4

T-joints

4.1 Quasi-Static Analysis of T-joints

In a small marine craft, hundreds of meters of T-joint can be found, mostly in the form of bulkhead-to-hull, bulkhead-to-deck, bulkhead-to-cabin sides or cabin-top joints. For these joints, large panels are brought into contact and the probability of introducing manufacturing errors is great. Different materials with very different characteristics come into contact and are expected to work together towards a safe structure. These kinds of connections naturally introduce concentrated loads into panels and joining material.

4.1.1 Design Rules for joints

As for many other fields of engineering, in the early days of boat building, progress occurred only by trial and error. Information was sparse and mainly viewed as a trade secret. In recent years, more attention has been given to theoretical analysis and methodical testing of joints.

The earliest approaches to GRP structure design are outlined in Gibbs and Cox's manual which recommends arrangements of various joints and simple design examples ([21]). Moments of inertia and other parameters of stiffeners and joints are given in tables, as resulting from experience, but no specific procedures about designing them were provided.

Later Gougeon Brothers Company, a famous boatbuilding and wind turbine building company from the USA, published a manual [14] focused on constructing boats using wood and the WEST System^R epoxy-based resin as primary engineering materials. Recognizing that a boatbuilder has to take engineering decisions without consulting the design office, they offer some simple tests to be done to check the strength and stiffness of the joints that are produced.

According to Gougeon Brothers the main way of connecting an out-of-plane joint is by means of a fillet. The materials chosen were WEST System^R epoxy-based resin and, according to the purpose, 406 Coloidal Silica or 409 Microsheres fillers. For structural joints 406 Coloidal Silica was recommended, resulting in a smaller fillet as is seen in Fig. 4.1.

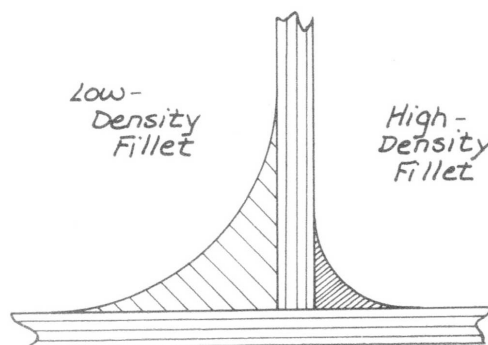
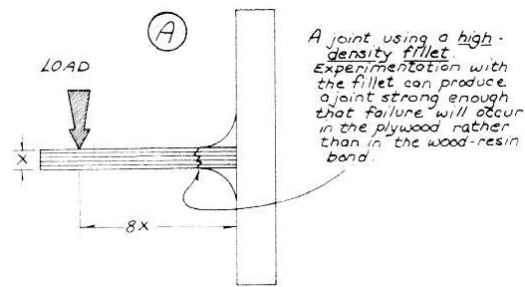


Figure 4.1: Low and High Density Fillet in the Wood and WEST^R epoxy (from [14])

A recommendation of the test to be performed, the materials and the radius of the fillet used are shown in Fig. 4.2. Here a force is applied until the destruction of the joint, at a distance equal with eight times the thickness of the material being joined. If the breaks occur in the piece being joined, it was assumed that a sufficient joint strength has been achieved. If the break occurs at the interface between the fillet and the part, or inside the fillet, it was advised to increase the radius of the fillet or to change the properties of the filling material. No recommendations were made about the way the sample was to be supported.



	Plywood thickness	Fillet radius
High-density Fillets (100% 406 mixture)	5/32"	5/8"
	3/16"	3/4"
	1/4"	7/8"
	Radii above represent fillets large enough to produce failure in plywood as in detail A	
Low-density Fillets (90% 409 10% 406 mixture)	5/32"	1 3/4"
	3/16"	1 3/4"
	1/4"	1 3/4"
	Fillet radii up to and including 1 3/4" failed as in detail B.	

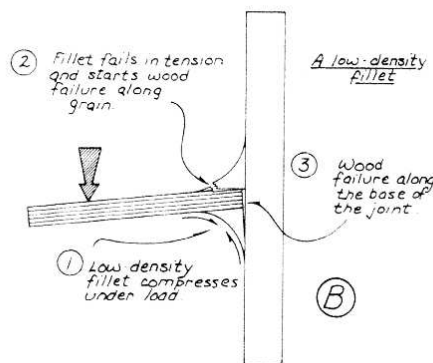


Figure 4.2: Test results and failure modes for samples using low- and high-density fillets (from [14])

This kind of testing has the advantage that is easy to perform and will give a quick indication of the abilities and limitations of the materials used and can also give an idea of the skills of the manufacturer of the joint.

In the early sixties, Royal Dutch Navy built several 47' Landing Craft Assault boats using Airex foam and FRP sandwich construction. The Navy undertook a series of tests to evaluate the impact, bending, fatigue and bond strength of the joints ([20]) and the connection between parts was evaluated on the ability to withstand the landing loads. The goal was to create a connection between bulkheads and hulls that "allows the movement of the hull within the

elastic range of its materials". No explanation of what this means was given and although some recommendations were made (like using foam inserts and the dimensions of the fillet), no other details were given.

Naval Engineering Standards cited by [21] stated that the T-joints are made using glass fibres tapes and the thickness of both boundary angles shall be $k(t - n)$ mm of CSM + n plies of WR, where t is the thickness of the leg, n is a coefficient taken as 4 for machinery spaces and 2 elsewhere and k is a parameter inbetween 0.5 and 0.67. The extend of the boundary angle along both the leg and the top of the tee should be 100mm (better 150mm) and 75mm for minor structures.

The same authors [21] cite *Lloyd's Register of Shipping Rules*, which states that the weight of the laminate forming each angle is to be at least 50% the weight of the lighter member connected and the length of the extention over the adjacent parts should be 50mm + 25mm per 600g/sqm of reinforcement.

The same recommendations are given by Germanicher LLoyd, a sketch of the laminated corner is shown in Fig. 4.3. In the case of using other methods of making out-of-plane joints, like using adhesives fillets, these methods are subjected to special examination by the Society [12].

Simple and elegant rules for laminating T-joints were provided by the ABS (American Bureau of Shipping) in their 1978 version of the standard. The Rules differentiate between single skin joints and sandwich made T-joints. It is stated that the thickness of each tabbing angle is not to be less than:

- for single-skin to single-skin - 1.5 times the thickness of the two laminates being joined.
- for sandwich to sandwich - the thickness of one skin of the thinner of the panels joined.
- for sandwich to single skin - either 1.5 times the thickness of the single skin laminate or the thickness of one skin of the sandwich, whichever is less.

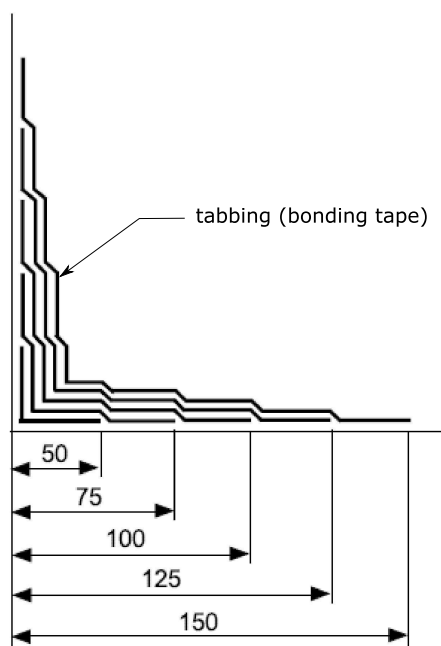


Figure 4.3: Typical bulkhead connections (from [12])

The width of each flange must be 15 times more the thickness obtained above.

ISO Standard 12215-6 (2008) Small craft - Hull Construction and Scantlings - Part 6 - Structural arrangements and details [16] recognize that it is difficult to prescribe a standard design for out-of-plane joints as they are highly dependent of the skill of the manufacturer, the materials involved and the prescribed design conditions. It advises boat builders to test thoroughly the joints or to use the ones that have been validated by practice. Some good-practice examples (only for plywood connections) are presented in Fig. 4.4.

If the member connected is a sandwich laminate, the thickness of the tabbing need not exceed the thickness of the sandwich skin being connected. The value t_{BHD} is considered to be the combined thickness of the skins (for plywood sandwich) or thickness of plywood bulkhead. The values b_{w1} and b_{w2} need not to be greater than 75mm or have a value of $3 \cdot t_{BHD}$ (for plywood bulkheads). Also the mass of the reinforcement is required to be $0.06 \cdot t_{BHD}$ kg/sqm. In the case of bonding only, the connection is required to be able to transmit the shear load designed using a safety factor of 4.

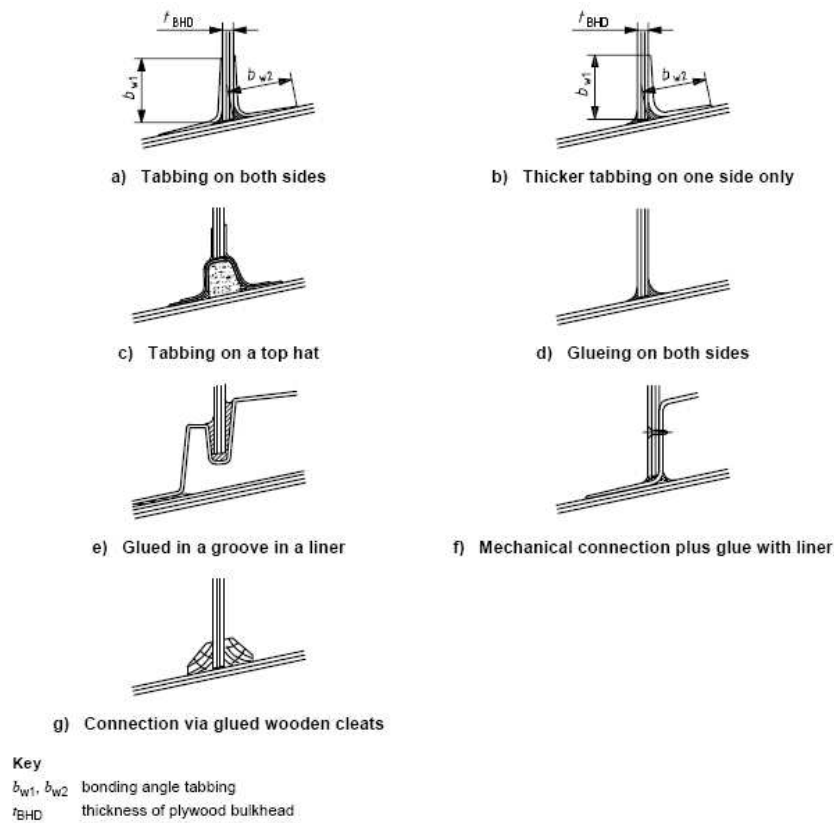


Figure 4.4: Typical bulkhead connections (from ISO 12215-6).

4.1.2 R.A. Sheno and F.L.M. Violette Study of T-joint

As early as 1990, R.A. Sheno and F.L.M. Violette ([28]) from the University of Southampton have studied sandwich T-joints used as hull bulkheads in a typical small craft. They considered five different joints, three having a radiused filler fillet ($R=10, 25$ and 40mm) made from microballoons mixed with resin and tabbing, one with a foam pad insert between the bulkhead and the hull, the last one having a couple triangular inserts each side of the joint and tabbing (see Fig. 4.5).

The scantlings of the bulkheads and the hulls panels were kept the same during the testing, a PVC core and epoxy laminated E-glass skins were used. As the study was oriented towards bulkhead-to-hull joints only, a symmetrical push-pull force was the only loading case considered. A panel with a span of 1000mm was considered, this geometry permits, in authors vision, to focus on local instability and wrinkling phenomena of the hull section.

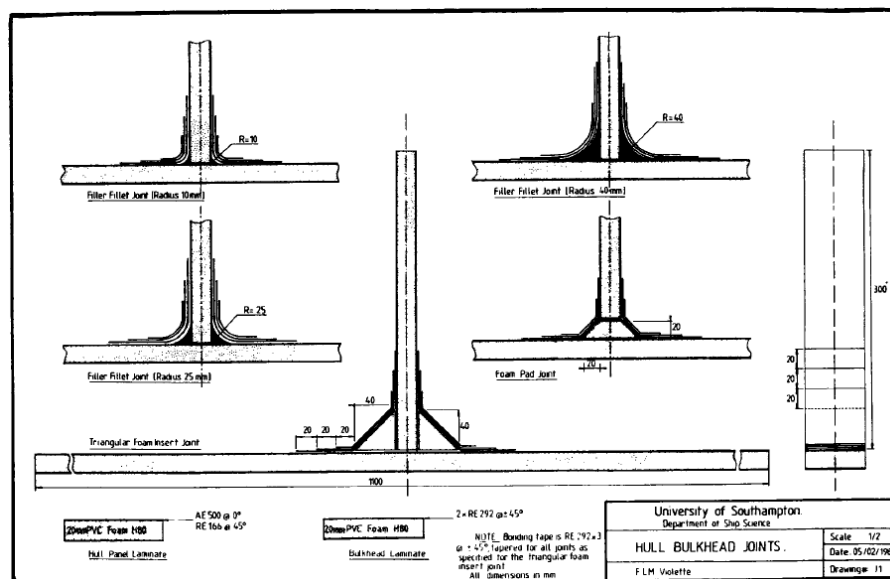


Figure 4.5: T-joints (Bulkhead-to-Hull) investigated by R.A. Sheno and F.L.M. Violette.

The results showed that the joint with a radiused filler fillet of 10mm has achieved the best strength. The authors concluded that, as a rule-of-thumb, the optimum fillet radius should match the thickness of the sandwich panel (also a rule previously developed by the wood/plywood boatbuilders).

The study focused also on the weight, cost and production efficiency of each of five joints. Again the 10mm radiused joint performed the best.

Later on, one of the authors (R.A. Sheno) together with Pei Junhou [21] have done a summary of work performed to date on out-of-plane joints (mainly T-joints and top-hat stiffeners). Among other things, they concluded that a purely theoretical estimates of joint strength is not acceptable as a basis for the design because of the uncertainty about imperfections, local stress concentrations and materials mode of failure. They advise that the new designs shall be thoroughly tested for evaluation of static, fatigue and impact strength.

4.1.3 Burchardt Analysis

Claus Burchardt [6] has investigated several types of T-joint used in marine applications, mainly the configurations used for boats expected to evolve in planning mode. The typical geometry of such a T-joint is shown in Fig. 4.6.

The following parameters were varied during the tests: the fillet material, the thickness and the Young's modulus for the bonded tape laminate, the stiffness of the hull panels inner laminate.

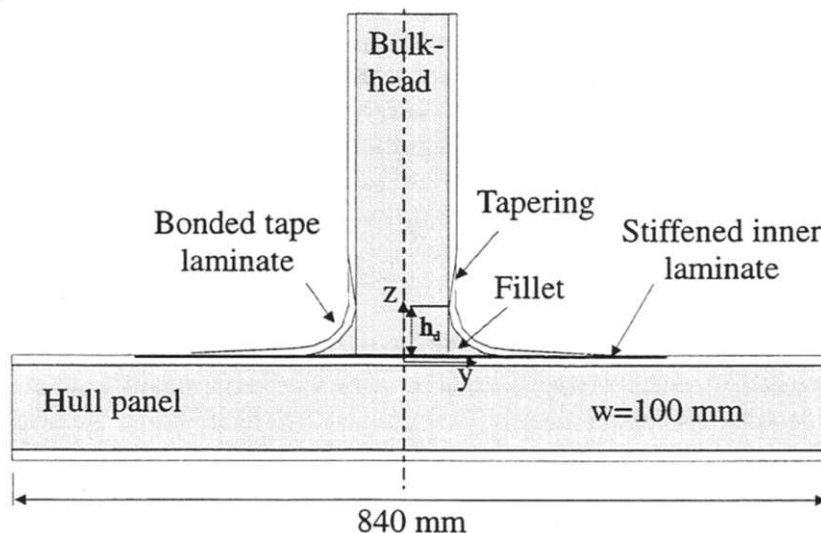


Figure 4.6: T-joint (Bulkhead-to-Hull) investigated by C. Burchardt.

The materials used were: E-glass (double bias and CSM) for hull and bulkhead panels, carbon fibres for the hull, bulkhead panels and for the reinforcement of the inner laminate. Vinyl ester was the resin of choice for both laminates. The foam material used was DivinycellTM for both the panels and for the fillet. CrestomerTM, an urethane modified styrenacrylate, was also used for radiused fillet. All materials were assumed to be linearly elastic and isotropic. The radius of the circular fillet was kept constant at 40mm (where the bonding laminate was used) and at 10mm without the bonded tape laminate.

Two load cases were considered, a symmetrical load (where the force acted along the bulkhead) and an anti-symmetrical one (where the force acted perpendicular to the bulkhead). The anti-symmetrical case was applied avoiding the high level of stresses on the face layers of the hull panels (no inner reinforcement and shorter span for the hull panel).

From the symmetrical test results, Burchardt concluded the following:

- The stiffness of the bonding tape has a small influence on the failure

load.

- The ultimate strength of the fillet material is important.
- The strain level in the inner laminate of the hull panel is important for the ultimate strength of the structural joint.

The failure modes in the case of symmetrical loads show that the initiation of the failure was located at the tip of the fillet against the hull panel (where the bonding tape laminate was used). The author concluded that the reasons of failure are the cracks introduced during the joining of the panels that seems to propagate and cause failure. For the case where only the fillet was used, the failure mode was initiated at the surface of the circular fillet.

From the anti-symmetrical test results, Burchardt concluded the following:

- The tapering of the bulkhead skins has an important role and it has to stop very close to the end of the connection.
- The stiffness of the bonding tape has a large influence on the failure load.
- The T-joint bonded only with a radiused fillet performed well.

It was concluded that when a bonding tape is used, the tabbing is required to be stiff enough in order to care for the anti-symmetric load and when a radius fillet only is used, the strength of the fillet material is important.

Further, Burchardt studied the fatigue of bonded T-joints, using only a symmetrical load. Different designs were investigated, manufacturing errors were introduced (similar with those found in real life). He concluded that the radiused fillet using CrestomerTM performed poorly, whereas the design that included a foam fillet performed 50% better in fatigue. Reducing the thickness of the bonding laminate has proved to be beneficial.

4.2 Experimental Conditions

The studies referred to above have taken into consideration only the geometry and loading of the bulkhead-to-hull type T-joints. In Burchardt's study, the span of the hull panel is 840mm in length (420mm each side of the bulkhead axis), whereas in the studies made by R.A. Shenoi and F.L.M. Violette, a span of 1000mm was considered. Shenoi et al. argued that this length reflects the current practice in small craft and the experiments were intended to achieve a skin compression failure rather than core shear failure.

These samples are expensive to make and require a big testing machine. One can argue that the loading case is much exaggerated, the deflections recorded by the authors are in the order of 85 to 101mm (Shenoi's test) and somewhat more realistic in the cases presented by the Burkhardt (of the order of 17 to 36.3mm), both in the symmetrical load case. In the Burkhardt study, due to the configuration of the experiment the deflection was not measured in the anti-symmetric loading case.

Due to the complexity of the state of stress in a composite T-joint, due to (literally) tens of materials formulations available to a boatbuilder/designer and thousands of combination of these materials that are possible, an all encompassing analytical design method is virtually impossible. In the absence of an expensive testing program, a better approach would be to analyse an existing proven solution, compare it with the proposed solutions and decide the pros and cons of each arrangement. In the present study, a standard T-joint was prepared in a traditional way (using a small radiused filler and tabbing - see Fig. 4.7), all other proposed methods of joining were compared with the witness (benchmark) specimen.

In this study, a simpler and cheaper T-joint is proposed and tested (see Fig. 4.8), using a simple testing jig (see Fig. 4.9) suitable for a small testing machine. The sample is fixed on the top support of the jig and simply supported by the lower one, in order to allow a free bending of the flange. If big deflections of the flange are encountered, shims can be placed between the

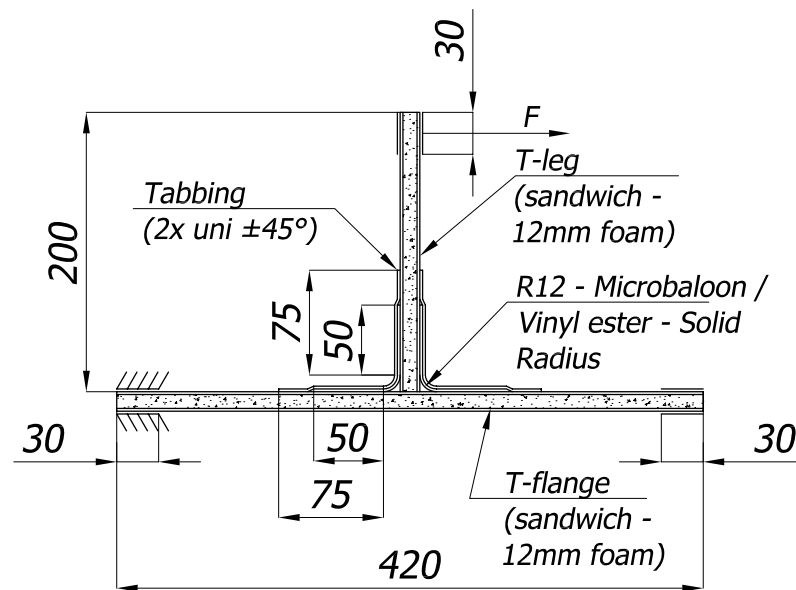


Figure 4.7: Common T-joint with tabbing - sample form and dimensions.

sample and the jig. The load is applied at the end of the T-leg, and, to allow a free rotation of the end, a hinge is used between the crosshead and the end support.

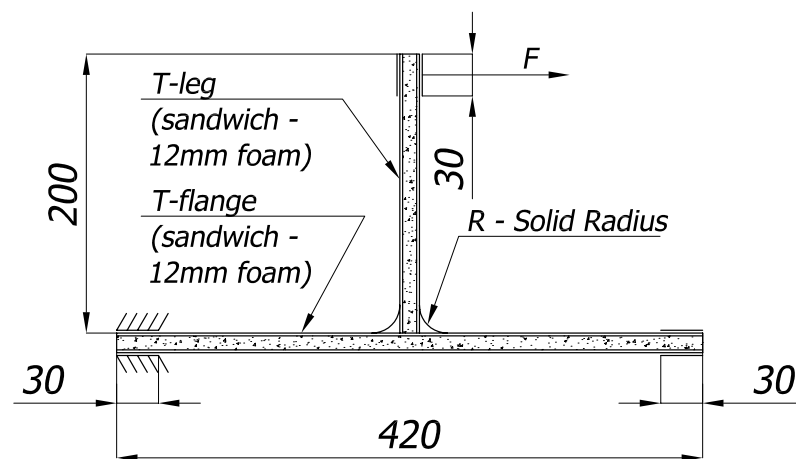


Figure 4.8: T-joint with adhesive solid radius - sample form and dimensions.

This arrangement is considered to represent the most unfavourable loading case (anti-symmetric) where the flange and the leg is loaded in bending and the fillet/tabbing is loaded in compression and tension. Due to the size of the specimen, any small or medium size boat yard can run these inexpensive tests, especially where the budget of the project prohibits a proper laboratory testing. One can simply modify the testing jig to allow weights to be used

instead of the controlled load.

In the experiments conducted, only the static loading case is considered, but the simplicity of the proposed test permits a future fatigue, creep and environmental degradation testing program (especially in the case when adhesives are used). Also, the geometry of the proposed specimen is intended to represent a larger category of T-joints - not only the bulkhead-to-hull joint - but also deck-to-hull topside (same for floors and soles), bulkhead-to-cabin top or cabin side, or some shorter span type of joints like the mastbox-to-deck, mastbox-to-bridgedeck joints.

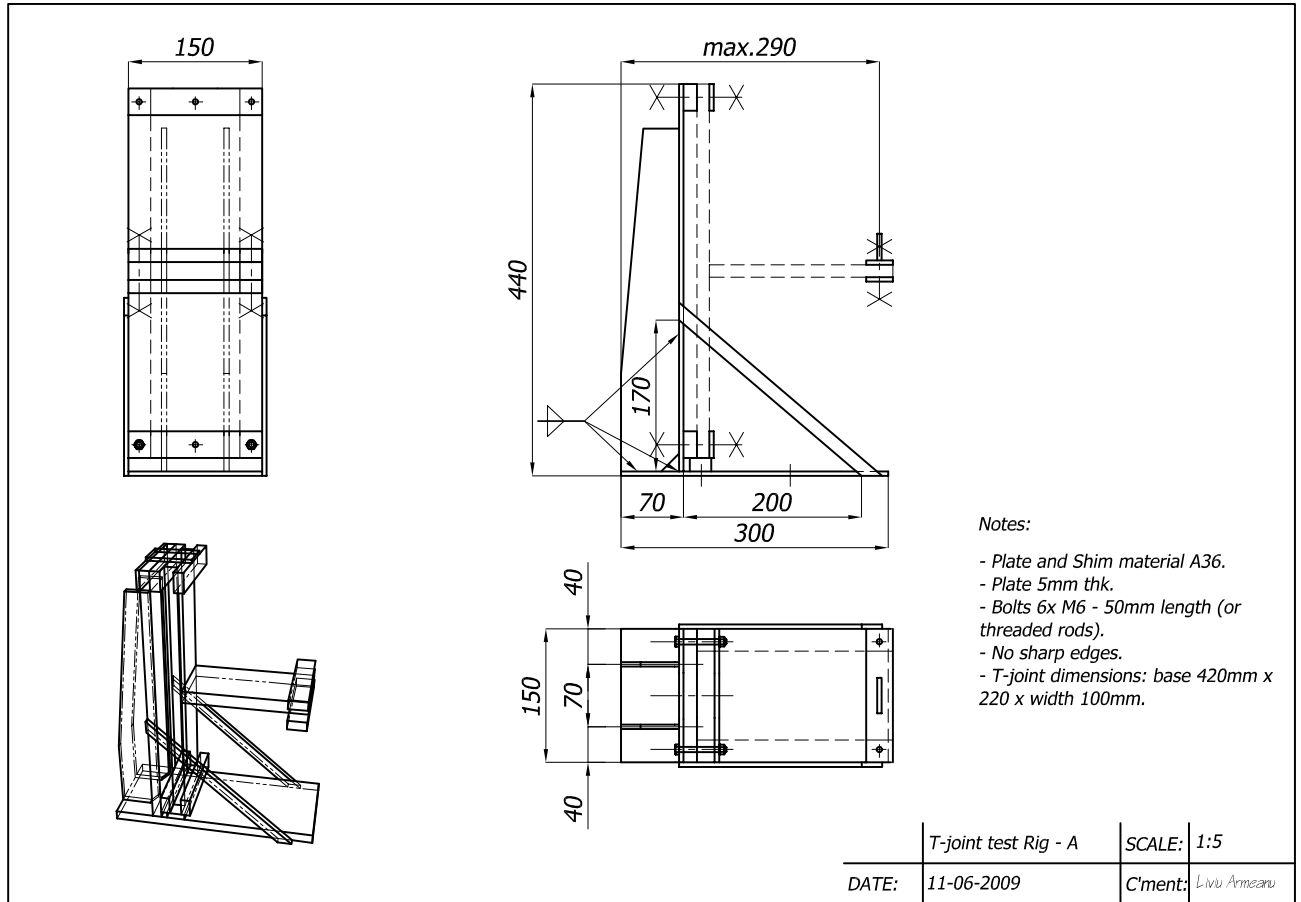


Figure 4.9: Testing jig for T-joint samples.

4.2.1 Specimen Construction and Experimental Details

Two oversized panels have been manufactured from the same materials as described in section 2.13.3, 2.13.2 and 2.13.1 of this study: Airex foam as core, E-glass EU460 as fibre reinforcement and vinyl ester as a matrix. The panels were made by hand-layup on a flat table with shiny surface (Formica) as the mould, and it is expected that the skins have the same glass content by mass as recorded in the samples obtained for the experiments described in the section 2.13.2. A mould release agent has been used to coat the table in order to facilitate the panel extraction after the cure. The two tabbing layers are made from the same E-glass, cut at $+/-45^\circ$, one with the width of 170mm and the other with the width of 120mm (length of radiused part plus overlaps).

The two panels have been thoroughly sanded in the joint area using 80 grit sand paper. The sanded surface was then dusted off and wiped using acetone. The panel representing the leg of the T-joint has been placed along the middle line of the panel representing the flange of the T. No other mechanical treatments were applied on the edge of the T-leg panel, so a gap of 1-2mm is noticeable in some parts of the interface (similar with manufacturing imperfections found in real life). The panels were held in place till bonded with the help of staples applied across joint at the end of panels. No pad layer or other material was inserted between the bulkhead and the flange panel. This is considered to be the standard practice in small craft building, where when two big panels are brought in contact, filling the gap resulted from misalignment is usually considered to be a time-consuming and not so effective operation.

In the case of tabbed T-joint (traditional joint), a R12mm radiused fillet of Q-Cel/vinyl ester filler (same composition as described in section 2.13.4) has been added with the help of a radiused spatula. Then the first layer of tabbing was added and wetted throughout with resin with a brush. Then the second layer was laid down with the fibres at 90° with the first one, in this way the tabbing runs at $+/-45^\circ$ across the joint. The joint was left to cure over night before it was carefully cut with a skill saw. Initially, the panels were designed

oversized (so the measurement for the three samples started from the middle of the panels) and the ends were discarded in order to eliminate any possible manufacturing imperfections at the end of the fillet.

In the vinyl ester/filler mix and Sikaflex 252 cases, a R40mm adhesive radius was applied, and in Plexus MA550 case a R20mm adhesive radius was applied using a radiused spatula. In the first case, the radius was chosen similar to common practice [22] and [14] (which represents a recommended solution for high density fillets), while in the Sikaflex 252 case, the radius was chosen similar to common practice [14] (for low density fillets). Due to the high price of the Plexus product, and due to the high mechanical properties of the adhesive, a smaller radius was chosen. The cutting procedure was the same as in the case of tabbed joints.

This joining procedure (or similar) is expected to be found in any composite boat building yard. There are some discussions among the professionals about the tabbing overlaps schedule, the sequence of the laminate layer drop-off. The testing conducted by the U.S. Navy and Owens-Corning and cited by "Professional Boatbuilder" magazine [27] did not show any noticeable difference between the two. It is accepted though that the probability of trapping air bubbles, inbetween the tabs is greater in the case when the narrower tabbing layer is laid first (in contrast with the method proposed by Germanicher LLoyd, see Fig. 4.3).

It is acknowledged that the joining method with the help of tabbing is simply a glue joint in which the skin of adherends is cured and chemically inactive [26]. In this case there is only a mechanical adhesion between the tabs and the substrate (a secondary bonding), opposite to a primary bonding where there is a chemical cross-link between the resin and the skin. It is expected that a secondary bonding to be structurally weaker than a primary one, hence a need to a good preparation of the substrate that comes in contact with the resin.

4.2.2 Static Tests

The test were conducted on a LLoyd LR 100K testing machine with a speed of a 10mm/min. A detail of the T-joint (with fillet and tabbing) is presented in Fig. 4.10 and a detail of a T-joint with radiused fillet only is presented in Fig. 4.11. The results are presented below.

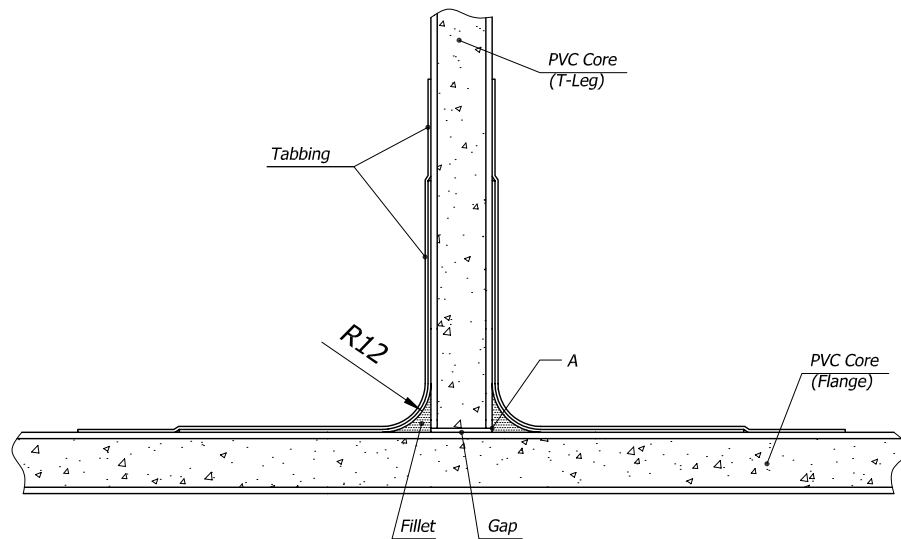


Figure 4.10: T-joint with fillet and tabbing.

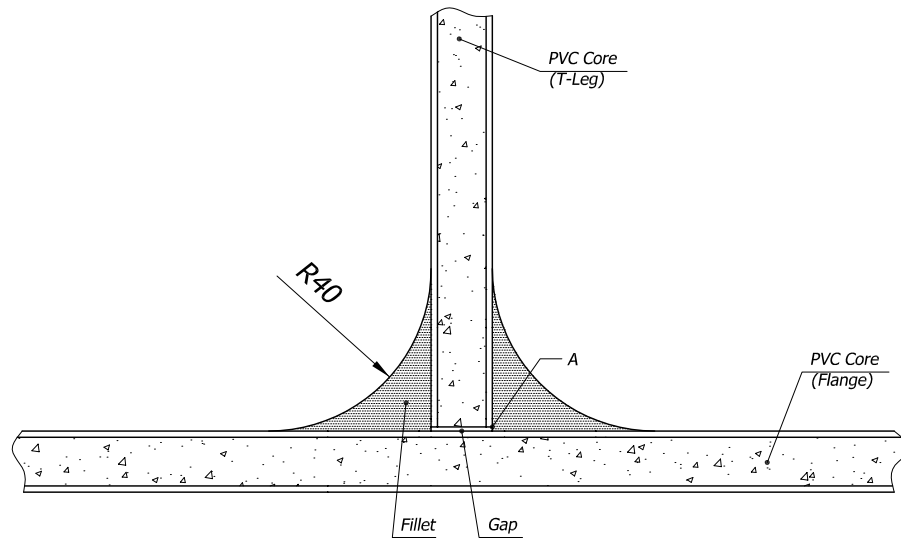


Figure 4.11: T-joint with radiused fillet (no tabbing).

4.2.2.1 T-joint with Tabbing

In the case of a T-joint with tabbing and QCel microballoons fillet R12mm, a graph was generated representing the load per unit width of joint (10mm) (see Fig. 4.12). The average maximum load recorded was $44.8N/10mm$, the average deflection recorded at peak load was $25.6mm$.

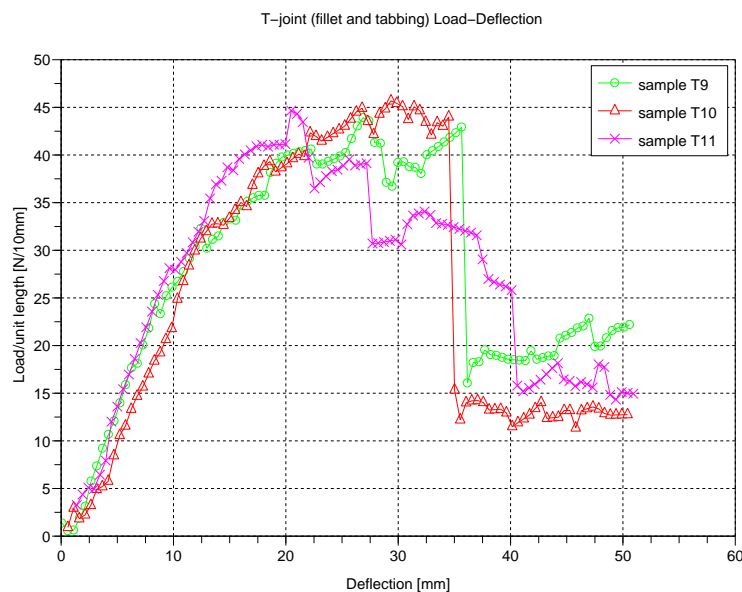


Figure 4.12: T-joint with fillet and tabbing.

Sample	Maximum Load [$N/10mm$]	Maximum deflection [mm]
T9	43.9	26.9
T10	45.3	29.4
T11	44.7	20.5
Average	44.8	25.6

Table 4.1: Test Results of T-joint with fillet and tabbing.

In all three samples, the failure was initiated in point A (at the end of the gap - see Fig. 4.10). It continued with delamination of the tabbing along the inside skin of the flange. By the time the experiment was stopped (at

around 50mm deflection), sample T9 had a crack developed across the core of the T-leg (a failure in shear) and samples T10 and T11 had a crack developed across the fillet in compression. It is important to observe that no damage was recorded in the flange panel, meaning that the joint would fail before the panels.

4.2.2.2 T-joint with vinyl ester/Epiglass HT120 fillet R40mm

In the case of a T-joint with vinyl ester/Epiglass HT120 fillet R40mm, the graph representing the load per unit width of joint (10mm) is presented below (see Fig. 4.13). The average maximum load recorded was $57.5N/10mm$, the average deflection recorded at peak load was $29.1mm$.

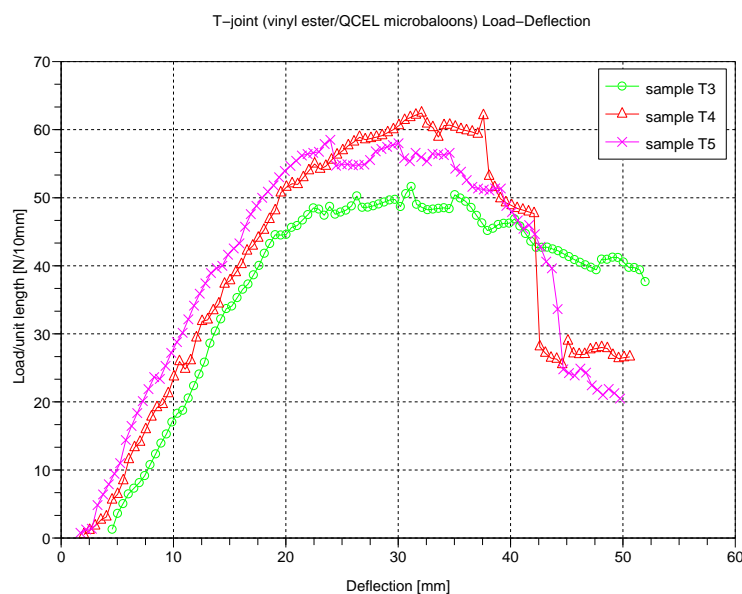


Figure 4.13: T-joint and vinyl ester/Epiglass HT120 fillet R40mm.

In two of three samples (T3, T5), failure initiated at point A (at the end of the gap - see Fig. 4.11). It continued with delamination of the fillet along the skin of the T-leg. By the time the experiment was stopped (at around 50mm deflection), sample T3 had a crack developed across the core of the T-leg (a failure in shear) at around 30mm from the end. No damage was observed in the flange panel in these cases. In the case of sample T4, the flange panel also failed in shear in the core.

Sample	Maximum Load [$N/10mm$]	Maximum deflection [mm]
T3	51.7	31.2
T4	62.5	32.1
T5	58.5	24.0
Average	57.5	29.1

Table 4.2: Test Results of T-joint with vinyl ester/Epiglass HT120 fillet R40mm.

This kind of joint shows approximate +28.6% increase in strength and +13.7% increase in deflection compared with the tabbed design (the benchmark solution). It is possible that a reduction in the radius of the fillet (meaning also a reduction in the overall weight of the samples) could provide the same performances as the previous samples.

4.2.2.3 T-joint with SikaFlex 252 Fillet R40mm

In the case of a T-joint with SikaFlex 252 Fillet R40mm, the graph representing the load per unit width of joint (10mm) is presented in Fig. 4.14.

The test was stopped when the deflection recorded was around 70mm. No damage in the plates or in the adhesive fillet have been recorded, the joint recovered with no signs of damages from the deformed position. The joint using Sikaflex 252 shows a great flexibility and tolerance. It is expected that a small reduction of the fillet radius could provide comparable performance to benchmark joint.

4.2.2.4 T-joint with Plexus MA550 fillet R20mm

In the case of a T-joint with Plexus MA550 fillet R20mm, the graph representing the load per unit width of joint (10mm) is presented in Fig. 4.15. The average maximum load recorded was $37.45N/10mm$, the average deflection

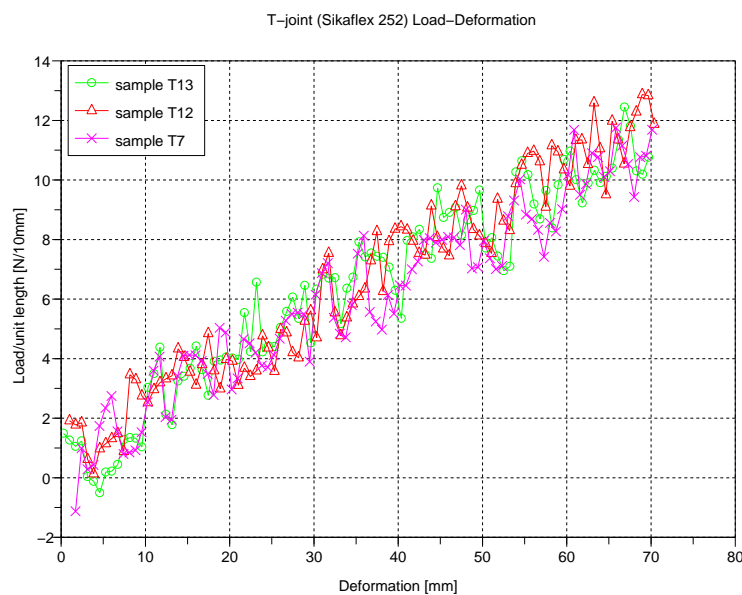


Figure 4.14: T-joint and SikaFlex 252 Fillet R40mm

recorded at peak load was $32.47mm$.

Sample	Maximum Load [N/10mm]	Maximum deflection [mm]
T8	34.2	20.2
T14	37.3	29.2
T15	40.8	48.0
Average	37.5	32.5

Table 4.3: Test Results of T-joint and Plexus MA550 fillet R20mm.

In all three samples, the fracture mode was flange core shear failure. In addition, sample T15 showed interlaminar failure of the inside skin of the flange when the test was stopped. On average, samples built using Plexus MA550 are weaker in strength and are stiffer than the first two groups. Being rigid and having good adhesion to the substrates, MA550 adhesive transmitted most of the load into the panels being joined, and the core of the flange was the first to fail.

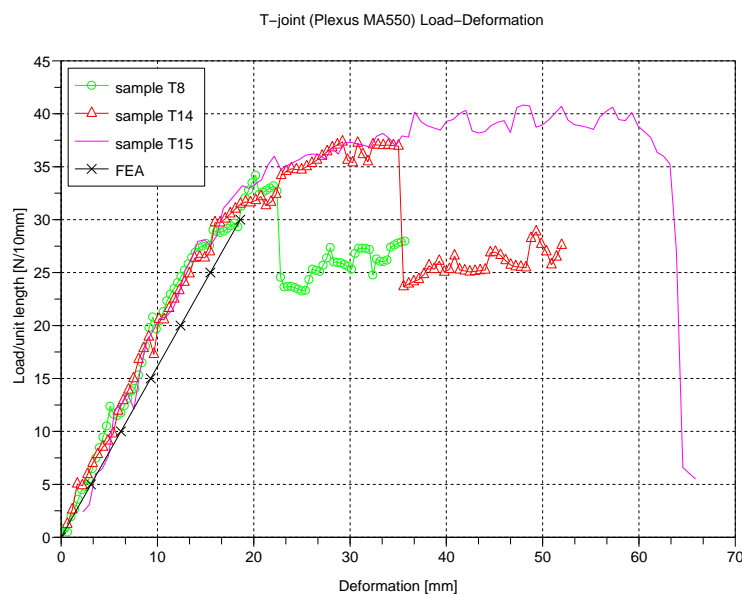


Figure 4.15: T-joint and Plexus MA550 fillet R20mm.

Pictures showing the experimental settings for T-joint with tabbing, for T-joint and SikaFlex 252 Fillet R40mm and for T-joint and Plexus MA550 fillet R20mm are shown Appendix B in Fig. B.1, B.2, and B.3 respectively.

4.3 Finite Element Analysis of T-joints

A parametric 2D model of the T-joint with Plexus MA550 fillet has been created and analysed in MSC/Nastran (joint detail in Fig. 4.16). The ends of the fillet have been cut back in order to avoid the distortion of the last elements, 1mm gap has been left between T-leg and T-flange. All materials are considered isotropic and their properties are defined in Chapter 2. One would expect that similar results are obtained using the other adhesives investigated.

Compared with test results (see Fig. 4.15), it shows that the model is slightly less stiff than in real life, due to the choice of FE elements used (QUAD4 - a fact easily checked by a benchmark beam model in flexure).

The von Mises stress for each zone in the model (adhesive, T-leg core, T-flange core etc) has been compiled in a graph (see Fig. 4.17). The stresses recorded in the T-leg's skins are almost identical, their graphs are overlapping.

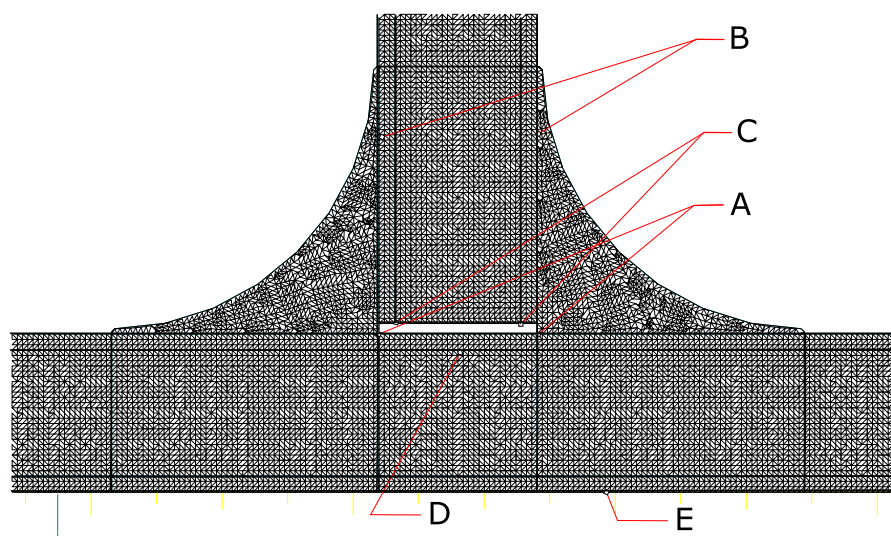


Figure 4.16: 2D Finite Element model of T-joint and Plexus MA550 fillet R20mm.

Maximum stress for adhesive and for the inside skin of the flange have been found at point A, for the leg's skins at point B, for the foam core for the T-leg and T-flange at the points C and D respectively. In point E has been recorded the highest stress in outside skin of the flange. The values are to be careful considered for the same reasons as the ones presented in the chapter regarding single-lap joints - the singularity points presented at sharp corners or at the interface between materials. The FE model presented here can offer only a qualitative view over the level of stresses in the joint. One can notice that all the time the highest stress is obtained at the inside skin of the flange (point A - a hard spot) followed closely by the T-leg's skins. In these conditions, as a first measure, adding a reinforcing layer on the inside of the flange in the area most stressed can improve the level of stress. During the tests, the principal mode of failure was by flange core shear failure. The path followed by the crack coincide with the direction DE - but the fact is not self evident when one analyses the von Mises stresses resulted from Finite Element model.

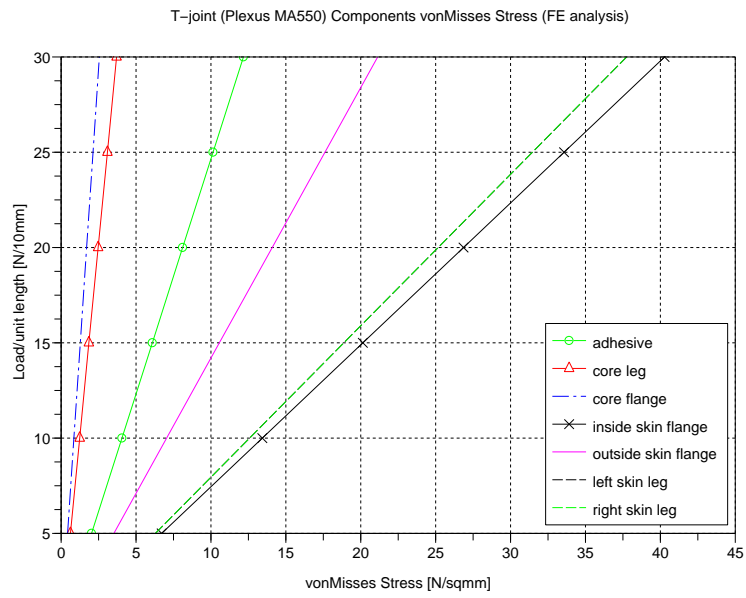


Figure 4.17: T-joint (Plexus MA550 R20mm) components von Mises stresses (FE analysis).

Chapter 5

Conclusions and future work

5.1 Conclusions from Chapter 2 - Adhesive Joints

Several different materials are commonly used in the boat building of a modern small craft. Aluminium, foam and glass reinforced plastic properties are well-known or are fairly easy to determine.

The matter becomes more complicated when adhesives are introduced. Although there are standard test methods developed to determine the mechanical properties of the adhesive, these data are to be carefully considered. The adhesives are known to have a high degree of sensitivity to rate of strain and to the environmental conditions so the data obtained by these tests can only help to create an incomplete image of the material.

This sensitivity necessitates testing the adhesive over a broad range of environments and load-time scales which make the development of new products based on adhesive joints an expensive exercise.

5.2 Conclusions from Chapter 3 - Single lap joints

There are literally hundreds of adhesive formulations that are commercially available. Although several of them are marketed specially to the marine applications, the designer of a bonded joint to be used in a small craft has to ensure that the resulted product is safe for the demanding marine environment.

The single-lap joint has been identified as being the simplest way to compare the multitude of combinations between the adhesives and adherends. At the beginning of this chapter, several analytical models have been analysed and compared in order to determine in what degree these models can be used as a tool in the preliminary phase of the design. All the models are easy to implement in an open-source software package for numerical computations. The designer can, using these methods, evaluate the length of the overlap, calculate the maximum shear and peel stresses, calculate the joint efficiency etc. There have been identified methods of taking into account the degradation of the adhesive due to the expected moisture, temperature and cyclic loading.

The preliminary design has to be backed up by a finite element analysis. Several common FE models have been analysed, including a 2D parametric model, the results are found to be close with the results from the analytical methods. It has been observed that in FE models, the maximum shear stresses recorded are bigger than the one resulted from analytical models. More over, the results are influenced by the underlying mesh. This is due to the nature of the numerical method used in FE, where a "singularity" point is developed at the corner of the adhesive layer. For preliminary purposes, results closer to those obtained using the analytical methods are obtained (for shear stresses) considering an average value of the maximum shear stress calculated using the corner values of the element adjacent to the critical point. The same level of discretization should be applied in the analyses of the joint to be designed.

In order to evaluate and compare the adhesives and the substrates, several

ASTM D1002 tests have been carried out. The samples were made in conditions resembling closely with working environment found on a boatyard (e.g. no climate control) and a simple surface treatment was chosen (abrasion and cleaning). It was found that Plexus MA550 adhesive gave the best adhesion to both substrates tested (aluminium and composite) and is largely independent of the interface treatment. The Sikaflex 252 adhesive is the most flexible of all and in spite of the surface treatment applied, it tends to fail in adhesion (only aluminium substrates were tested). The mixed vinyl ester/Epiglass HT120 adhesive shows the characteristics of a brittle adhesive. The best results are obtained using composite substrates (what was expected due to the compatibility between adhesive and adherend), for which its strength is comparable with the industrial made one (Plexus).

An interesting result has been obtained using the mixed vinyl ester/Epiglass HT120 and the carrier fabric. Using composite adherends, the loading cell maximum allowable force was exceeded and the test was stopped. In this case, the role of the carrier fabric is presumed not only to keep the adhesive layer constant in thickness, but also to delay the eventual cracks that can develop in the adhesive layer.

In general, the overlap length was found to be too small, the probability of introducing manufacturing defects is substantial. More over, it is rare that this kind of short joints will be found anywhere on a boat. It will be more appropriate to use a bigger length of the overlap, a minimum 50mm is desirable. Also, it was found that the thickness of the adhesive is very hard to control. It is desirable to make and test more than 3 samples and the results are to be compared according to the thickness of the layer.

5.2.0.5 Future Work

For this study, only the elastic behaviour of the adhesives has been investigated. Experimental testing carried out by different researchers has shown that the majority of adhesives behave non-linearly. For highly loaded joints,

these non-linear effects have to be investigated using hyperelastic models for flexible adhesives (like for Sikaflex 252 adhesive) and elastic-plastic models for rigid adhesives (like for Plexus MA550 and vinyl ester/filler based one). LJ Hart-Smith and Bigwood and Crocombe have developed elastic-plastic analytical models that can be used for single lap joints or other simple geometries. For more complicated configuration, FE analysis is required; most FE commercial packages nowadays have ready implemented elastic-plastic material models and non-linear analysis.

No ageing effects, like temperature and moisture, have been taken into consideration during the testing program, as well as long term effects like fatigue and creep. For a full characterization of the adhesive-adherend system these effects have to be studied and there are standard tests based on simple single-lap joint that can be used (like ASTM 1002 or ISO 4587).

Adhesives usually behave differently in tension than in compression, a program of tests to determine the compressive properties are required in order to complement the tensile properties.

In the light of the results of the testing program carried out for this thesis, it will be interesting to test the behaviour of a combination between Plexus MA550 (with its good adhesion characteristics over different substrates) and a carrier fabric (a light weight EU glass or CSM) as an adhesive solution.

5.3 Conclusions from Chapter 4 - T joints

As shown, a purely theoretical estimate of joint strength is not possible or acceptable as a basis for the design because of the uncertainty about imperfections, local stress concentrations and materials modes of failure. Without an expensive testing program, one can only approximate the stresses between the parts involved in the connection.

In the testing program carried out for this thesis, the results obtained from static tests using a R40mm fillet of vinyl ester/Epiglass HT120 fillet are

the closest to the benchmark joint (R12mm fillet made from vinyl ester/QCel microballoons). Showing almost +30% reserve strength (compared with the benchmark), a decreased fillet radius (say R30mm) would be the next step to be tested. It seems to be the best candidate to replace the traditional joint, given the results, the price and the availability. The joint using R40mm Sikaflex 252 radiused fillet have shown the most interesting results. The tests have been stopped at around 70mm deflection, none of the materials forming the joint suffered any visible damages, the whole system returned to the initial position intact. It is the decision of the joint designer if such a flexibility is desired in the structure. It would be interesting to find the results of tests using a smaller fillet radius.

The joint using R20mm Plexus MA550 radiused fillet have proved the rigid nature and the good adhesion characteristics of the adhesive. In all the tests the flange was damaged (core shear) earlier than the benchmark samples. Again, it would be interesting to know the results of tests using a smaller fillet radius.

In the light of the results from these tests, at the beginning, a builder/designer can choose to replace, say, only one side of a bulkhead joint with a radiused adhesive fillet, leaving the other one done in a traditional manner. The joint will need to be supervised and inspected regularly over time. When it is considered that enough data have been collected over time, and the connection is considered successful, than the other side of connections can be replaced with the new arrangement.

5.3.0.6 Future Work

No attempts were made to calculate manufacturing prices, but it is expected that the execution time will be shortened in the case of adhesives fillet. The perspective of automatisisation will make the joining process cheaper.

No testing program was carried out using dissimilar materials in T-joints. One can see the advantages of using, say, composite superstructures over metal-

lic (aluminium) frame, where the use of adhesives would be a great advantage by reducing and eliminating the bolting or rivets. Plexus MA550 would be a good candidate in this case.

No ageing effects or fatigue and creep effects have been taken into consideration during the testing program. For a full characterization of the adhesive-adherend T-joint system these effects have to be studied. The experimental conditions (the jig and the sample's dimensions) are easy to adapt to a new testing program.

Appendix A

Scilab Program for Adhesive Stress Calculation

```
/// Initialize Data
/// This function has to be called first.
/// User can overwrite any variable initialized here.
///-----
/// T = applied Force [N]
T = 25;
/// L = bondline length [mm]
L = 12;
c = L/2;
/// w = width of bondline
w = 25;
P = T/w;
/// E = Young's modulus of the adherend [MN/m2]
E1 = 68918; //Aluminium 5083
E2 = 68918; //Aluminium 5083
/// nu = Poisson's ratio of the adherend
nu = 0.35;
//E1 = 14400; //composite
//E2 = 14400; //composite
/// t = thickness of the adherend [mm]
```

```

t1 = 3;
t2 = 3;
/// ta = Adhesive thickness [mm]
ta = 0.5;
/// Ga = Shear Modulus of the adhesive [MN/m2]
Ga = 106;
/// niua = Poisson's ratio of the adhesive
niua = 0.3;
Ea = 2*(1+niua)*Ga;
///endfunction

/// Average Shear Stress Analysis
function Tau1=AvShearStress()
    Tau1 = P/(2*c);
endfunction

/// Volkersen Shear Stress Analysis
function Tau2 = VolkersenShearStress(x)
    lambda = sqrt(Ga/ta*(E2*t2 + E1*t1)/(E2*t2*E1*t1));
    Tau2 = P*lambda*cosh(lambda*x)/(2*sinh(lambda*L/2))
    +P*lambda*sinh(lambda*x)/(2*cosh(lambda*L/2))
    *(E2*t2 - E1*t1)/(E2*t2*E1*t1);
endfunction

/// Volkersen Joint Strength]
/// Usage: Valid only for identical adherends
/// Declare first E=E1=E2, t=t1=t2
function Pmax = PJSVolkersen(tauadh, E, t, ta)
    lambda = sqrt(Ga/ta*2/(E*t));
    Pmax = 2*tauadh/lambda*tanh(lambda*L/2);
endfunction

```

```

/// Goland and Reissner Shear Stress
/// Usage: Valid only for identical adherends
/// Declare first E=E1=E2, t=t1=t2
function Tau3=GoReShearStress(x)
    bbeta = sqrt(8*Ga*t/(E*ta));
    llambdas = bbeta*L/(2*t);
    phi = L/(2*t)*sqrt((P/E)*(3*(1-niu^2)/2));
    k = cosh(phi)/(cosh(phi) + 2 * sqrt(2) * sinh (phi));
    Tau3 = (1/4)*(P/L)*(llambdas*(1+3*k)*cosh(llambdas*2*x/L)
    /sinh(llambdas)+3*(1-k));
endfunction

/// Goland and Reissner Peel Stress (transverse normal)
/// Usage: Valid only for identical adherends
/// Declare first E=E1=E2, t=t1=t2
function Sigma3=GoRePeelStress(x)
    ggamma = (6*Ea*t/(E*ta))^0.25;
    llambdap = ggamma*L/(2*t);
    phi = L/(2*t)*sqrt((P/E)*(3*(1-niu^2)/2));
    K = cosh(phi)/(cosh(phi) + 2 * sqrt(2) * sinh (phi));
    Kprim = K*phi*sqrt(2);
    R1 = cosh(llambdap)*sin(llambdap) + sinh(llambdap)*cos(llambdap);
    R2 = sinh(llambdap)*cos(llambdap) - cosh(llambdap)*sin(llambdap);
    R3 = 0.5*(sinh(2*llambdap) + sin(2*llambdap));
    A = (R2*llambdap^2*K/2 + llambdap*Kprim*cosh(llambdap)
    *cos(llambdap))*cosh(llambdap*2*x/L)*cos(llambdap*2*x/L);
    B = (R1*llambdap^2*K/2 + llambdap*Kprim*sinh(llambdap)
    *sin(llambdap))*sinh(llambdap*2*x/L)*sin(llambdap*2*x/L);
    Sigma3 = 4*P*t/(L^2*R3)*(A + B);
endfunction

/// L.J. Hart-Smith Shear Stress (Elastic Analysis)

```

```

/// Usage: Valid only for identical metallic adherends
/// Declare first E=E1=E2, t=t1=t2
function Tau4=LJHSShearStressElastic(x)

    kb = 1; ///metals

    llambda = sqrt(2*Ga/(E*t*ta));

    llambdaprim = llambda*sqrt((1+3*(1-niu^2))/(4*kb));

    D = E*t^3/(12*(1-niu^2));

    phi = L/2*sqrt(P/D);

    kHS = 1/(1+phi+phi^2/6);

    Mo = kHS*P*t/2*(1+ta/t);

    A2 = 1/(2*llambdaprim*sinh(llambdaprim*L))

    *Ga/(E*t*ta)*(P+6*(1-niu^2)*Mo/(kb*t));

    C2 = P/L - A2/(llambdaprim*L)*sinh(llambdaprim*L);

    Tau4 = A2*cosh(2*llambdaprim*x)+C2;

endfunction

```

```

/// L.J. Hart-Smith Peel Stress (Elastic Analysis)
/// Usage: Valid only for identical metallic adherends
/// Declare first E=E1=E2, t=t1=t2
function Sigma4=LJHSPeelStressElastic(x)

    kb = 1; ///metals

    llambda = ((6*Ea*(1-niu^2))/(E*t*ta*kb))^0.25;

    D = E*t^3/(12*(1-niu^2));

    phi = L/2*sqrt(P/D);

    kHS = 1/(1+phi+phi^2/6);

    Mo = kHS*P*t/2*(1+ta/t);

    A = (cos(llambda*L/2)-sin(llambda*L/2))

    *Ea*Mo/(ta*D*llambda^2*exp(llambda*L/2));

    B = A*(cos(llambda*L/2)+sin(llambda*L/2))/(cos(llambda*L/2)-sin(llambda*L/2));

    Sigma4 = A*cos(llambda*x)*cosh(llambda*x)

    +B*sin(llambda*x)*sinh(llambda*x);

endfunction

```

```

/// Wiedemann Ratio
/// Usage: Valid only for identical metallic adherends
/// Declare first E=E1=E2, t=t1=t2
/// x represents variable "lambda" (say 0.1 to 10)
function R=WRatio(x)
    R=x/2*coth(x/2);
endfunction

/// Cooper and Sawyer Model for Peel Stress
/// Usage: Valid only for identical metallic adherends
/// Declare first E=E1=E2, t=t1=t2
/// x represents variable "lambda (say 0.1 to 10)
/// this model requires the length of the adherends (l+ta)
function Sigma5=CooperSawyerPeelStress(x)
    teta = acos((l+L/2)/(sqrt((l+L/2)^2+((t+ta)/2)^2)));
    D = E*t^3/(12*(1-niu^2));
    u2=sqrt(P*cos(teta)/(8*D));
    u1=sqrt(P*cos(teta)/D);
    X=u2*sinh(u1*l)*cosh(u2*L/2);
    Y=u1*cosh(u1*l)*sinh(u2*L/2);
    Mo=P*(t+ta)/2*cos(teta)*u1*u2*cosh(u2*L/2)*sinh(u1*l)/(X+Y);
    Vo=P*(t+ta)/2*cos(teta)*u2*cosh(u2*L/2)*sinh(u1*l)/(X+Y);
    To=P*cos(teta);
    K=2*Mo/(t*To);
    Kprim=c*Vo/(t*To);
    llambdap = c^4*sqrt(Ea/(2*ta*D));
    R1 = cosh(llambdap)*sin(llambdap) + sinh(llambdap)*cos(llambdap);
    R2 = sinh(llambdap)*cos(llambdap) - cosh(llambdap)*sin(llambdap);
    R3 = 0.5*(sinh(2*llambdap) + sin(2*llambdap));
    A = (R2*llambdap^2*K/2 + llambdap*Kprim*cosh(llambdap)
    *cos(llambdap))*cosh(llambdap*2*x/L)*cos(llambdap*2*x/L);

```

```

B = (R1*llabdap^2*K/2 + llabdap*Kprim*sinh(llabdap)
*sin(llabdap))*sinh(llabdap*2*x/L)*sin(llabdap*2*x/L);
sigmaapp=To/t;
Sigma5=sigmaapp*4*t^2/(L^2*R3)*(A+B);
endfunction

/// Cooper and Sawyer Model for Shear Stress
/// Usage: Valid only for identical metallic adherends
/// Declare first E=E1=E2, t=t1=t2
/// x represents variable "lambda (say 0.1 to 10)
/// this model requires the length of the adherends (l+ta)
function Tau5=CooperSawyerShearStress(x)
    teta = acos((l+L/2)/(sqrt((l+L/2)^2+((t+ta)/2)^2)));
    D = E*t^3/(12*(1-niu^2));
    u2=sqrt(P*cos(teta)/(8*D));
    u1=sqrt(P*cos(teta)/D);
    X=u2*sinh(u1*l)*cosh(u2*L/2);
    Y=u1*cosh(u1*l)*sinh(u2*L/2);
    Mo=P*(t+ta)/2*cos(teta)*u2*cosh(u2*L/2)*sinh(u1*l)/(X+Y);
    To=P*cos(teta);
    K=2*Mo/(t*To);
    Tauav=To/L;
    Xi=ta/t;
    bbeta = sqrt((8*Ga*(1-niu^2))*(1+3*Xi/4)*c^2/(E*ta*t));
    Tau5=Tauav/(4+3*Xi)*((1+3*K)*bbeta/sinh(bbeta)
*cosh(2*bbeta*x/L)+3*(1-K*Xi));
endfunction

```

Appendix B

T-Joint Experimental settings

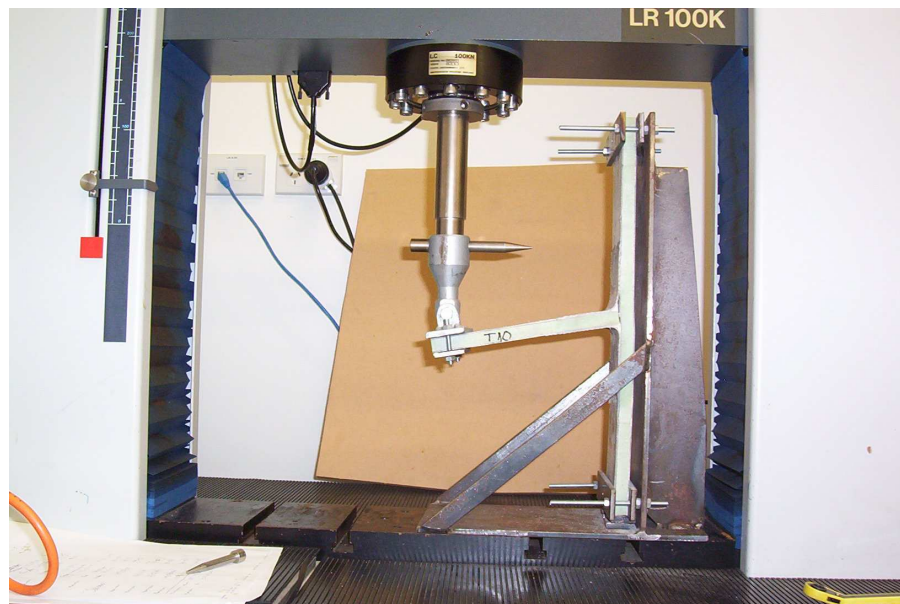


Figure B.1: The experimental setting for T-joint with tabbing.

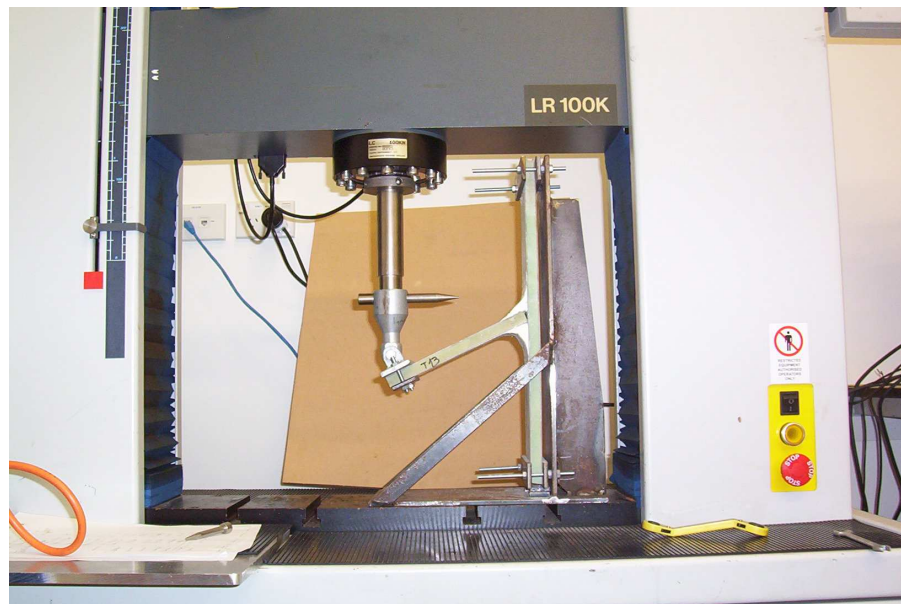


Figure B.2: The experimental setting for T-joint and SikaFlex 252 Fillet R40mm.

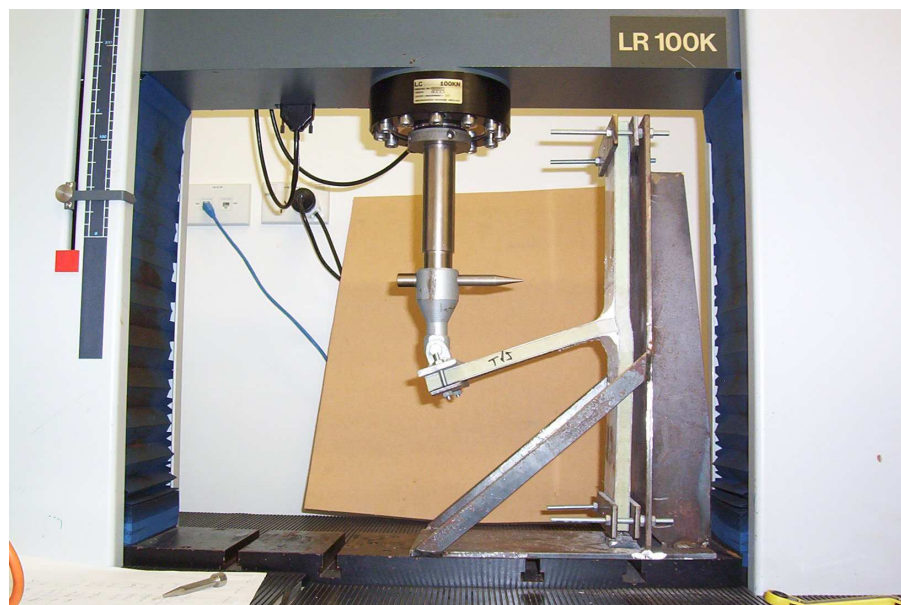


Figure B.3: The experimental setting for T-joint and Plexus MA550 fillet R20mm.

List of Tables

2.1	ASTM & ISO Testing standards for Adhesives and Bonded Joints [34]	18
2.2	Relevant ASTM standards for characterize the unidirectional laminate.	22
2.3	EU460/Vinyl ester mechanical properties.	31
2.4	EU460/Vinyl ester 0°, 90° laminate properties.	32
2.5	EU460/Vinyl ester 0°, 90°, 90°, 0° laminate properties.	32
3.1	Partial Safety Factors for Adhesively Bonded Joints [7].	55
3.2	Maximum shear stress for benchmark cases using overlap length of 12mm.	58
3.3	Maximum shear stress for benchmark cases using overlap length of 50mm.	59
3.4	ASTM D1002 - Test results of aluminium adherends and Plexus MA550 adhesive.	72
3.5	ASTM D1002 - Test results of aluminium adherends and Sikaflex 252 adhesive.	73
3.6	ASTM D1002 - Test results of aluminium adherends and vinyl ester/Epiglass HT120 mix adhesive.	74
3.7	ASTM D1002 - Test results of composite adherends and Plexus MA550 adhesive.	75
3.8	ASTM D1002 - Test results of composite adherends and vinyl ester/Epiglass HT120 mix adhesive.	76

3.9	ASTM D1002 - Test results of hybrid aluminium and composite adherends and Plexus MA550 adhesive.	77
3.10	ASTM D1002 - Test results of hybrid (aluminium and composite) adherends and vinyl ester/Epiglass HT120 mix adhesive.	78
3.11	ASTM D1002 - Test results of composite adherends and vinyl ester/EU460 as carrier fabric.	79
3.12	ASTM D1002 - Test results of hybrid (aluminium and composite) adherends and vinyl ester/EU460 as carrier fabric.	80
3.13	ASTM D1002 - Summary of Results.	81
4.1	Test Results of T-joint with fillet and tabbing.	98
4.2	Test Results of T-joint with vinyl ester/Epiglass HT120 fillet R40mm.	100
4.3	Test Results of T-joint and Plexus MA550 fillet R20mm.	101

List of Figures

2.1	Basic Joint Geometries (from [34]).	11
2.2	Failure Modes in Single-Lap joint (from [30]).	12
2.3	E-glass fibre mechanical properties function of fibre content by mass ψ according with ISO 12215-5.	22
2.4	ASTM D638-3 - Test Specimen form and dimensions.	27
2.5	ASTM 638-3 - Tensile properties of Epiglass HT120/Vinyl ester ratio 1.5:1.	28
2.6	ASTM 638-3 - Tensile properties of QCel/Vinyl ester ratio 2.3:1.	29
2.7	ASTM D3039/D 3039M-00 - Specimen form and dimensions.	30
3.1	Single-Lap Geometry and Notations.	34
3.2	Shear Stress along bondline according to Volkersen	36
3.3	Joint Strength as function of the adhesive thickness according to Volkersen.	37
3.4	Shear Stress profile according to Goland and Reissner model.	38
3.5	Peel Stress along the bondline according to Goland-Reissner model.	40
3.6	Shear Stress in Cooper and Sawyer Model	43
3.7	The general adherend-adhesive sandwich according with Bigwood and Crocombe	44
3.8	Adhesive shear stress-strain curves and mathematical models.	46
3.9	Geometry, Nomenclature and Mathematical model for analysis of unbalanced single-lap joints, [18].	47
3.10	Shear Stress distribution - L.J.Hart-Smith	48

3.11 Peel Stress in Elastic Analysis along bondline - L.J.Hart-Smith	50
3.12 Volkersen τ_{max}/σ_{10} as a function of the product $\lambda * L$	51
3.13 Shear Stress Distribution 12mm overlap.	59
3.14 Shear Stress Distribution 50mm overlap.	60
3.15 FE Model A - a mix between 1D elements (beam) and 2D elements (plane).	62
3.16 FE Model B - a mix between 1D elements (beam) and 2D elements (plane) using rigid elements to compensate for thickness.	63
3.17 Model C: 2D plane elements have been used to represent the adhesive and the adherends	64
3.18 Single-Lap Singularities Points.	65
3.19 Single-Lap Maximum Shear Stress function of Mesh Density along interface between adherend and adhesive.	66
3.20 Through-thickness distribution of the shear stress	67
3.21 Model D: a 3D elements (bricks) are used to represent both the adherend and the adhesive.	68
3.22 ASTM D1002 - Single Lap Joint Form and Dimensions of Test Specimen.	70
3.23 ASTM D1002 - Single lap joint test of aluminium adherends and Plexus MA550 adhesive.	71
3.24 ASTM D1002 - Single lap joint test of aluminium adherends and Sikaflex 252 adhesive.	72
3.25 ASTM D1002 - Single lap joint test of aluminium adherends and vinyl ester/Epiglass HT120 mix adhesive.	73
3.26 ASTM D1002 - Single lap joint test of composite adherends and Plexus MA550 adhesive.	74
3.27 ASTM D1002 - Single lap joint test of composite adherends and vinyl ester/Epiglass HT120 mix adhesive.	75
3.28 ASTM D1002 - Single lap joint test of hybrid (aluminium and composite) adherends and Plexus MA550 adhesive.	76

3.29	ASTM D1002 - Single lap joint test of hybrid (aluminium and composite) adherends and vinyl ester/Epiglass HT120 mix adhesive.	77
3.30	ASTM D1002 - Single lap joint test of composite adherends and vinyl ester/EU460 as carrier fabric.	78
3.31	ASTM D1002 - Single lap joint test of hybrid (aluminium and composite) adherends and vinyl ester/EU460 as carrier fabric.	80
4.1	Low and High Density Fillet in the Wood and WEST ^R epoxy (from [14])	83
4.2	Test results and failure modes for samples using low- and high-density fillets (from [14])	84
4.3	Typical bulkhead connections (from [12])	86
4.4	Typical bulkhead connections (from ISO 12215-6).	87
4.5	T-joints (Bulkhead-to-Hull) investigated by R.A. Shenoj and F.L.M. Violette.	88
4.6	T-joint (Bulkhead-to-Hull) investigated by C. Burchardt.	89
4.7	Common T-joint with tabbing - sample form and dimensions.	92
4.8	T-joint with adhesive solid radius - sample form and dimensions.	92
4.9	Testing jig for T-joint samples.	94
4.10	T-joint with fillet and tabbing.	97
4.11	T-joint with radiused fillet (no tabbing).	97
4.12	T-joint with fillet and tabbing.	98
4.13	T-joint and vinyl ester/Epiglass HT120 fillet R40mm.	99
4.14	T-joint and SikaFlex 252 Fillet R40mm	101
4.15	T-joint and Plexus MA550 fillet R20mm.	102
4.16	2D Finite Element model of T-joint and Plexus MA550 fillet R20mm.	103
4.17	T-joint (Plexus MA550 R20mm) components von Mises stresses (FE analysis).	104

<i>Chapter 5 - Conclusions and future work</i>	124
B.1 The experimental setting for T-joint with tabbing.	117
B.2 The experimental setting for T-joint and SikaFlex 252 Fillet R40mm.	118
B.3 The experimental setting for T-joint and Plexus MA550 fillet R20mm.	118

References

- [1] <http://www.scilab.org>.
- [2] R.D. Adams, J. Comyn, and W.C.Wake, *Structural adhesive joints in engineering*, second ed., Chapman & Hall, 1997.
- [3] K.B. Armstrong, *Selection of adhesives and composite matrix resin for aircraft repairs*, Ph.D Thesis - City University, London (1990).
- [4] Keith B. Armstrong, L. Graham Bevan, and William F. Cole II, *Care and repair of advanced composites*, second ed., SAE International, 2005.
- [5] DA. Bigwood and AD. Crocombe, *Non-linear adhesive bonded joint design analysis*, International journal of adhesion and adhesives **10**.
- [6] Claus Burchardt, *Bonded sandwich t-joint for maritime applications - ph.d. dissertation*, Institute of Mechanical Engineering - Aalborg University, 1996.
- [7] Edited by John L. Clarkey, *Structural design of polymer composites: Eurocomp design code and background document*, European Structural Polymeric Composites Group, 1996.
- [8] Edited by Leonard Hollaway, *Hanbook of polymer composites for engineers*, Woodhead publishing limited - Cambridge England, 1994.
- [9] D. Castagnettia and E. Dragoni, *Efficient stress analysis of adhesive bonded joints by finite element techniques*, XXXV Convegno Nazionale - 13-16 Settembre 2006, Universita Politecnica delle Marche (2006).
- [10] C.C. Chamis and P.L.N. Murthy, *Simplified procedures for designing adhesively bonded composite joints*, National Aeronautics and Space Administration Technical Memorandum 102120 (1989).
- [11] Paul A. Cooper and James Wayne Sawyer, *A critical examination of stresses in an elastic single lap joint*, NASA Technical Paper 1507 - Langley Research Center (1979).

- [12] Germanischer Lloyd *GL, Rules for the classification of high speed craft*, Germanischer Lloyd, 2002.
- [13] Inc. Enterprise Software Products, *Femap basic scripting language api reference*, (1996).
- [14] Meade Gougeon et al., *The gougeon brothers on boat construction: Wood an west system*, second ed., Pendell Printing Inc., 1980.
- [15] International Organization for Standardization *ISO, ISO12215-5 small craft - hull construction and scantlings - part 5: Design pressures for monohulls, design stresses, scantlings determination*, first ed., ISO, 2008.
- [16] ———, *ISO12215-6 small craft - hull construction and scantlings - part 6: Structural arrangements and details*, first ed., ISO, 2008.
- [17] M. Goland and E. Reissner, *The stresses in cemented joints*, J Appl Mech Trans ASME **66** (1944), A17–A27.
- [18] L.J. Hart-Smith, *Adhesive-bonded single-lap joints*, NASA CR 112236 - Langley Research Center (1973).
- [19] ASTM International, *Standard terminology of adhesives*.
- [20] Thomas S. Johannsen, *One-off airex fiberglass sandwich construction*, Chemacryl Inc., N.Y., 1973.
- [21] Pei Junhou and R.A. Shenoi, *Detailed research review of the performance characteristics of out-of-plane joints in frp marine structure*, Department of Ship Science, University of Southampton (1994).
- [22] Kelsall Catamarans Ltd., *Build instructions*, Kelsall Catamarans Ltd., 2007.
- [23] P.K. Mallick, *Particulate and short fiber reinforced polymer composites*, Comprehensive Composite Materials **2** (2000), 291–331.
- [24] Paul H. Miller, *Fatigue prediction verification of fibreglass hulls*, Marine Technology **38**.
- [25] Norman Nudelman, *Principles of fiberglass boat design and construction*, Westlawn Institute of Marine Technology, 1990.
- [26] Bruce Pfund, *Secondary bonding revisited*, Professional Boatbuilder - February/March (1996), 27–28.

- [27] ———, *Taping and tabbing*, Professional Boatbuilder - February/March (1996), 19–25.
- [28] R.A. Shenoi and F.L.M. Violette, *A study of structural composite tee joints in small boats*, Journal of Composite Materials **24** (1990), 644–666.
- [29] SP Systems, *Guide to composites*, SP Systems marine bussiness of Gurit, 1990.
- [30] John Tomblin, Waruna Seneviratne, Paulo Escobar, Yoon-Khian Yap, and Pierre Harter, *Adhesive behavior in aircraft applications*, Presentation at FAA Workshop on Key Characteristics for Advanced Material Control - September 1618 (2003).
- [31] O. Volkersen, *Rivet strength distribution in tensile-stressed rivet joints with constant cross-section*, Luftfahrtforschung **15**, no. 1.
- [32] Jan R. Weitzenbock and Dag McGeorge, *BONDSHIP project guidelines*, first ed., Det Norske Veritas DNV, 2005.
- [33] J. Wiedemann, *Leichtbau 2: Konstruktion*, Springer, 1996.
- [34] Aixi Zhouand and Jack Lesko, *Polymers adhesives for the infrastructure*, Presentation at Virginia Fiber-Reinforced Polymer Composites: Materials, Design and Construction - September 2021 (2006).